Performance Investigation of Solar Thermal Local Areke Production System Using Dish Concentrator

By

Seyoum Getachew Nigussie

Advisor: Dr. Addisu Bekele

A Thesis Submitted to Department of Thermal and Aerospace Engineering

School of Mechanical, Chemical and Materials Engineering

Office of Graduate Studies

Adama Science and Technology University

July, 2020

Adama, Ethiopia

DECLARATION

I hereby declare that this M.Sc. thesis entitled *"PERFORMANCE INVESTIGATION OF SOLAR THERMAL LOCAL AREKE PRODUCTION SYSTEM USING DISH CONCENTRATOR"* in partial fulfilment of the requirements for the award of the degree of Master of Science in Thermal Engineering is an authentic record of my own work under the supervision of Dr. Addisu Bekele, Assistant Professor of Thermal Engineering, Adama Science and Technology University.

The matter embedded in this thesis has not been submitted for the award of a degree or diploma in any other university. All relevant resource information used in this paper has been duly acknowledged.

Seyoum Getachew	______________	____________
Candidate	Signature	Date

This is to certify that the above statement made by the candidate is correct to the best of my knowledge and belief. This thesis has been submitted for examination with my approval.

Dr. Addisu Bekele	___________	__________
Advisor	Signature	Date

APPROVAL OF BOARD OF EXAMINERS

We, undersigned, members of the board of examiners of the final open defense by Seyoum Getachew Nigussie have read and evaluated his thesis entitled "*Performance Investigation of Solar Thermal Local Areke Production System Using Dish Concentrator*" and examined the candidate. This is, therefore, to certify that the thesis has been accepted in partial fulfilment of the requirements of the degree of Masters of Science in Thermal Engineering.

Name	Signature	Date
Name of student	Signature	Date
Advisor	Signature	Date
External Examiner	Signature	Date
Internal Examiner	Signature	Date
Chair Person	Signature	Date
Head of Department	Signature	Date
School Dean	Signature	Date
Post Graduate Dean	Signature	Date

ACKNOWLEDGMENT

First and foremost, I would like to thank the only almighty GOD, the embodiment of wisdom who provides health, strength and accurate insight into reality for his divine intervention during my thesis work.

Although this thesis work ultimately represents my accomplishments, I have benefited significantly from multiple peoples that I would like to acknowledge. First and foremost, I am grateful to my hard-working advisor: Dr. Addisu Bekele for his excellent supervision and scientific input in this research work. It is a great privilege and honor for me to be advised by him. His positive influence will always be a guide as I venture out on my own to tackle challenging scientific problems. I am lucky to be guided and advised by him and in general his friendly approach makes me a successful man. I would like to thank my sister Senait Getachew and my uncle Getachew Abebe who supported me financially and morally to achieve this master's program, I appreciate their positive attitude for this thesis work from the beginning to the end. I am thankful to Debre Birhan University, department of Chemical Engineering for supporting me to test the alcohol content of the product output.

Finally, I am always grateful to my mother Aberash Abebe, all my ways have been prosperous with her prayer and support.

ABSTRACT

Energy is indispensable for human development that strategies for reducing poverty, achieving an improved standard of living and civilization. Using solar energy for Areke production system is a quick acting solution to overcome the energy scarcity and an effective mitigation mechanism for concerning global climate changes, deforestations, and economic problems of Ethiopian's who base their life on Areke production. The main aim of this study is to design, develop and experimentally test the performance of solar thermal local Areke distillation process using indirect heating system under Debre Birhan weather condition as an alternate source of energy instead of burning biomass. An average solar radiation is calculated as maximum in Jan (7.2 kWh/m^2/day) and minimum in July (4.6 kWh/m^2/day) and Annual average daily solar radiation is 6.1 kWh/m^2/day. Based on minimum solar intensity, parabolic dish solar collector system with aperture diameter of 2 m, depth of 0.25 m and focal length of 1m, receiver diameter 0.15 m, length 0.27 m having truncated cone shape at the bottom side is designed in full scale. However, for the experimental test ratio of 2.22:1 is used. During absorber temperature testing improved truncated one cavity absorber has attained a maximum surface temperature of 300.3 ℃ in morning (9:45am – 12:25pm) and the thermal efficiency of the collector is obtained as 54.6% with low solar intensity. The input power required for solar thermal areke production is 0.211 kW, but input power required for traditional areke production for equal amount of input Difdif is 1.93 kW. Water started to evaporate at 90.2 ℃, ethanol evaporates at 71.4℃ this indicated boiling point is affected by altitude, if altitude increase boiling point temperature decrease. From 2 liters of difedif 0.2 liters of liquid Areke with an average alcohol content of 45% has been obtained with average time of 65 minutes. On average it takes 25 minutes to reach the boiling temperature of ethanol at atmospheric pressure of 0.722atm. Similarly, the condenser water temperature reaches 59.1 ℃ after ethanol vapor condensation.

Keywords: *performance investigation, Solar thermal, Parabolic dish, Solar concentrator, Truncated Cone, Cavity absorber, Local Areke.*

TABLE OF CONTENTS

CONTENTS PAGE

LIST OF FIGURES

FIGURE PAGE

LIST OF TABLES

TABLE PAGE

ABBREVIATIONS AND ACRONYMS

WDI	World Development Indicator
WHO	World Health Organization
MoWE	Ministry of Water and Energy
ERG	Ethio Resource Group
CSA	Central Statistics Authority
NASA	National Aeronautics and Space Administration
PM	Particulate matters
CO	Carbon monoxide
UCB	University of California, Berkley
HOMER	Hybrid Optimization Model for Electrical Renewable
CFD	Computational Fluid Mechanics
NMA	National Meteorology Agency
NTU	Number of Transfer Unit
HTF	Heat Transfer Fluid
DNI	Direct Normal Irradiation
PDSC	Parabolic Dish Solar Concentrator
LCS	Life Cycle Saving
LCC	Life Cycle Cost
CO2	Carbon dioxide
GTZ	Deutsche Gesellschaft fur Techniche Zusammenarbeit

GREEK SYMBOLS

ω	Hour angle, (°)
θ_z	Zenith angle, (°)
θ	Angle of incident, (°)
φ	Latitude angle, (°)
δ	Declination angle, (°)
γ	Intercept factor
τ	Transmittance
α	Absorptivity
ε	Emissivity
ρ	Density, $(\frac{\mathrm{kg}}{\mathrm{m}^3})$
Δ	Change
σ	Reflectivity
η_{th}	Thermal efficiency
η_{ex}	Exergy efficiency
σ	Stefan Boltzmann constant, $(\frac{\mathrm{W}}{\mathrm{m}^2\mathrm{K}^4})$

NOMENCLATURE

A	Area, (m^2)
h	Convective heat transfer coefficient, (W/m^2K)
R_e	Reynolds number
H	Global daily radiation, (W/m^2)
I	Global hourly radiation, (W/m^2)
D	Diameter, (m)
m	Mass, (kg)
V_d	Volume of Difdif, (m^3)
ΔP	Pressure drop, (N/m^2)
k	Thermal conductivity, (W/mK)
T_a	Ambient temperature, (K)
V	Velocity, (m/s)
N	Day time duration
$\dot{m}$	Mass flow rate, (kg/s)
L_p	Length of pipe, (m)
P_{loss}	Pipe loss
Q_u	Useful energy, (W)
C	Concertation ratio
L_c	Length of helical coil
C_{min}	Minimum fluid capacity rate

SUBSCRIPTS

amb	Ambient	avg	Average
abs	Absorber	a	Aperture
G	Global	conv	Convection
D	Diffuse	cond	Conduction
B	Beam		
rad	Radiation		
cav	Cavity		
min	Minimum		
u	Useful		
d	Difdif		
l	Loss		
o	Optical		
ex	Exergy		
sur	Surface		
c	Coil		
s	Shell		
g	Gesho		
w	Water		
b	Bikil		
c	Corn		

CHAPTER ONE

INTRODUCTION

1.1. Background of the Study

Energy is indispensable for human development that strategies for reducing poverty, civilization and achieving an improved standard of living. Now a day’s several researches have been conducting in energy affairs and it has been a pointed issue in the world. This is because the conventional energy sources have become in short supply to meet primary energy source demand; even though it is simple to get some conventional energy sources, but follow further problems (Pane, 2010). Conventional energy sources are decreasing from generation to generation; this shows us it is limited in amount. From the energy scenario information data, the maximum energy consumption is oil and the least energy consumption is recorded as nuclear energy (Alem, 2011).

In developing country biomass will continue to dominate national energy consumption for many years (Ramakrishna, 2015). Biomass, including wood, dung and crop residues, is the source for above 92.4% of Ethiopia’s total energy use, primarily in the household (Awash, 2014). About 80.1% of Ethiopian total population are living in rural areas and only 3.51 % of total people have access to clean fuels and technologies for cooking and heating purpose (WDI, 2016).

1.2. Traditional Areke production in Ethiopia

Areke is a traditional homemade alcohol drink which is widely consumed in most regions of Ethiopia including, Arsi Negelle, Dembecha and Debre Birhan. Areke produced from mixture of different ingredients such as, milled gesho (Rhamnus Prinoides), finely ground and cooked/baked cereals, and water called mash (local name difedif), by the process of distillation (Alem, 2011). Recent research findings reveal that around 3,500 households in Arsi Negelle produce the local alcoholic drink, which is sold at market in colorful jugs and transported across Ethiopia, as well as to neighboring Kenya and Djibouti (Araya, 2013). Each household produce 150 liters of Areke in six working days in traditional way on an average consuming of 450 kg of fuel wood (Shewangizaw, 2016). For this study the site of study area is Debre Birhan since maximum local areke production is takes place next to Arsi Negele. The study was conducted in Debre Birhan, based on the 2007 national census conducted by the Central Statistical Agency of Ethiopia (CSA), this town has a total population of 65,231, of whom 31,668 were men and 33,563 women. Moreover, maximum populations of the area are depending on traditional areke distillation. Random data taken from four kebele 96 households produce local areke by using biomass wood in open fire three stone stove (Solomon and Demel, 2018).

1.3. Draw Backs of Using Biomass as Energy Source

In many developing countries (particularly sub-Saharan Africa), the use of fire wood/biomass for energy source leading to significant negative impacts on human health and the environment (Stephen, 2004).

Figure 1.1: Women loaded with fire wood (https://www.alamy.com).

Shown in figure 1.1 is women collecting and carrying wood from outside far distance. Elder women are forced to carry the wood and travel long roots to their households.

Green house emission to the environment leading to varies diseases on human being due to burning the fuel/biomass during Areke distillation are the major challenges for women and children in rural areas of Ethiopia (Araya, 2013).

Figure 1.2: Traditional Areke production (https://www.google.com).

Figure 1.2 shows traditional areke production by using firewood in open three stove stone. The smoke from the open stove released to the indoor. Indoor air pollution due to burning solid fuels is the leading causes of child mortality in the world, accounting for up to 20% of fatalities among children under five, almost all of them in developing countries (WHO, 2009). Along with energy consumption CO_2 impacts has increased as the energy consumption mainly from the sources such as charcoal, firewood, cow dung etc.

Figure 1.3: Deforestation and forest degradation (https://www.worldwildlife.org).

Figure 1.3 shows wood has been stripped even protected forests of trees and rapidly escalating deforestation. Fuel wood, agricultural residues and animal dung all produce high emissions of carbon monoxide, hydrocarbons and particulate matter. The low temperature, low oxygen conditions found in cooking fires result in the formation of carbon monoxide, methane, nitrogen dioxide and other gases which are from 5 to 280 times more reactive than carbon dioxide (Funk, 1996). Recent research suggested that carbon dioxide emissions from deforestation and forest degradation contribute range from 6 to 17% of total anthropogenic (Alem, 2011). According to WHO indoor air pollution from inefficient traditional wood-fired cook stove is leading to serious health damage such as respiratory diseases including pneumonia, tuberculosis and chronic pulmonary disease, obstetrical problems, low birth weight, blindness and heart diseases (Yohannes *et al.*, 2014).

According to the ministry of water and energy of Ethiopia the energy policy of the country broadly aims at ensuring energy supply to the development of agriculture and industry at reasonable prices, shifting from traditional energy resources to the modern ones, attaining energy self-sufficiency, improving the energy use and its efficiency and ensure the development and utilization of environmentally friendly energy resources called renewable. Renewable energy is derived from natural resources such as sunlight, wind, tides and geothermal heat (Kulal *et al*., 2016).

No more substantial study has been conducted in Ethiopia towards improvement of traditional inefficient Areke distillation stoves by efficient modern stoves or use of alternative renewable energy sources, like solar energy. As a result, it was motivated to conduct different researches on the way of improving the process of local Areke distillation either by developing energy efficient distillation stoves or by designing the way to use naturally endowed renewable solar energy which is environment friendly and smoke free energy source using efficient solar collectors.

This study focuses on the performance of the use of solar thermal energy technology for local Areke production system using parabolic dish solar concentrator collector, by considering indirect heating system (circulating the working fluid). The working fluid is heated by the improved solar receiver (truncated conical shape on the bottom side).

1.4. Statement of the Problem

Debre Birhan is one of the town in which large amount of local areke production is takes place. In Debre Birhan all domestic energy need is achieve by biomass only. This follows so many problems such as related with health, Environment and other social problems. Traditional Areke production system takes place in an open fire three stone stove, that consume large amount of fire wood. A survey conducted by Shewangizaw (2016) indicated producing 150 liters of Areke consumed 450 kg of fire wood. This fire wood cultivated from the nearby forests, that causes deforestation. From this much kilogram of fire wood maximum pollutant gas emitted to the environment. The amount of pollutant gas emitted from 3500 households is 118,280.55 tones, this leads to climatic change on the environment (Araya 2013). In Ethiopia the daily fuel collection time ranges from three to four hours (Kebede, 2018), besides the negative effect of fuel wood gathering on nutrition, exposes women for risk of assault and natural hazards.

In every solar system, the system efficiency is highly dependent on the amount of collected solar energy relative to collector area, since the weather condition is cold compared to other towns of Ethiopia, so the concentration ratio must be greater this is done by improving the absorber geometry of the dish concentrator collector to trap maximum solar radiation.

Therefore, this study will deliver an improved and efficient solar thermal based local Areke distiller. Since solar energy is available everywhere in nature, free from charge and environmentally friendly, with improved solar receiver and as a part of remedy to those mentioned problems and to reduce women’s and children’s firewood collection task.

1.5. Objectives of the Study

1.5.1. General Objective

The general objective of this study is to investigate the performance of solar thermal local Areke production by using indirect heating system to substitute biomass stove in household under Debre Birhan weather condition.

1.5.2 Specific Objectives

The specific objectives of this study are to:

- Assess the solar potential of Debre Birhan.
- Design and fabricate solar receiver and distillation column.
- Specify the capacity of Difdif.
- Determine the energy and time taken required for one cycle of distillation process.

- Theoretically analyze the heat loss from the receiver and distillation pot.
- Analyze the temperature distribution inside the distillation column, condenser and solar receiver.
- Visualize the effect of wind flow over the dish-receiver system.
- Improve the thermal efficiency.
- Develop prototype on solar thermal Areke production system.
- Validating the result of the present work with studies in the literature.
- Test and compare the alcohol content of the product output.

1.6 Significance of the Study

The majority of people in Ethiopia depend on firewood as energy sources for Areke distillation, so use of solar distiller plays important role, economically improving their life and reduce energy consumption. Most people buy the firewood from market, which is additional expense, since solar energy is obtained free from charge, use of solar distiller for Areke distillation helps to save the money they spent on firewood. Specially women and children in rural areas of Ethiopia spent much of their time in gathering firewood and they are exposed for health problems due to smoke from burning firewood, using solar distiller helps to avoid health problems and reduce environmental pollution. And also improve awareness about the utilization of renewable energy resources.

Therefore, the use of solar as energy source for local Areke distillation benefit individuals, each households and those who prepare Areke for sale can improve their life socially and economically.

1.7 Scope and Limitation of the Study

This thesis focuses on performance analysis of solar thermal Areke production system. Includes, Analytical estimation of solar energy potential of the site of study, analytical design and selection of alcohol condenser, solar receiver, analyze temperature distribution inside the receiver and distillation column, numerically analysis of the effect wind over the solar receiver, determining the efficiency of the dish concentrator and developing prototype and conducting experiment for Areke production system. The experimental results helped to conduct the validation. The experimental results are time taken, energy loss and energy consumption of

Areke production system which are evaluated and compared with results of previous studies. Also, in order to develop confidence about the developed model, the result is compared with the traditional Areke production system. The study also includes analyzing of different input parameters followed by the design of each component of the system.

The limitations of this study are variation of the weather condition, lack of necessary instruments, experimental evaluation is not conducted on full scale dimension of the designed component due to shortage of economical income.

1.8 Research Questions

There are numerous questions that arise regarding the solar-assisted local Areke production system with an improvement of solar thermal systems. However, for this thesis the specific research questions are:

- How to analyze solar thermal potential of the site of study?
- How much heat is required to evaporate ethanol vapor from the input Difdif?
- How much liter of Areke is produced from one cycle of distillation process?
- How long to complete one cycle of distillation process?
- How to increase the heat transfer area of the receiver?
- How long it takes to boil the working fluid inside the receiver?
- What are the factors that influence the performance of the collector?
- What is the minimum temperature at which the mixture called Difdif starts to vaporize?
- How does the solar thermal distillation performance compare with the traditional distillation process?

1.9 Outline of the Thesis

This thesis is divided into eight chapters. Chapter one, introduces the importance of energy, harnessing solar energy, motivations and objective of the present work. Chapter two, involves a literature review covering previous theoretical, experimental and numerical work on solar energy potential assessment on local Areke production system. Chapter three, presents materials and methods of the study. Chapter four, presents the solar energy potential of the site of study. Chapter five, Presents the detail design of each component of solar thermal Areke production system, theoretical formulations and numerical simulations. Chapter six, presents the detail experimental setup and procedures. Chapter seven, presents the result and discussion of the experimental and numerical investigation of solar thermal local Areke production system. Chapter eight presents the conclusion and recommendation for future work.

CHAPTER TWO

LITERATURE REVIEW

This chapter presents the review of literature on solar thermal system and different local Areke production system, briefly description of solar energy and its application area. Effect of varies parameters on the parabolic dish concentrator collector, review about condenser heat exchanger, summary from the literature review and research gap.

2.1 Solar Energy Basics

The sun is a sphere of intensely hot gaseous matter with a diameter of 1.39×10^9 m and is, on the average, 1.5×10^{11} m from the earth (Dincer, 2011). Sun is considered as continuous fusion reactor the temperature of central interior region is estimated as 8×10^6 to 40×10^6 K (Beggs, 2009). The sun has effective blackbody surface temperature of 6000K (Petela, 2010). It is estimated that the total annually solar energy received by the earth is about 1.7×10^{17} W (Saperstein, 1975).

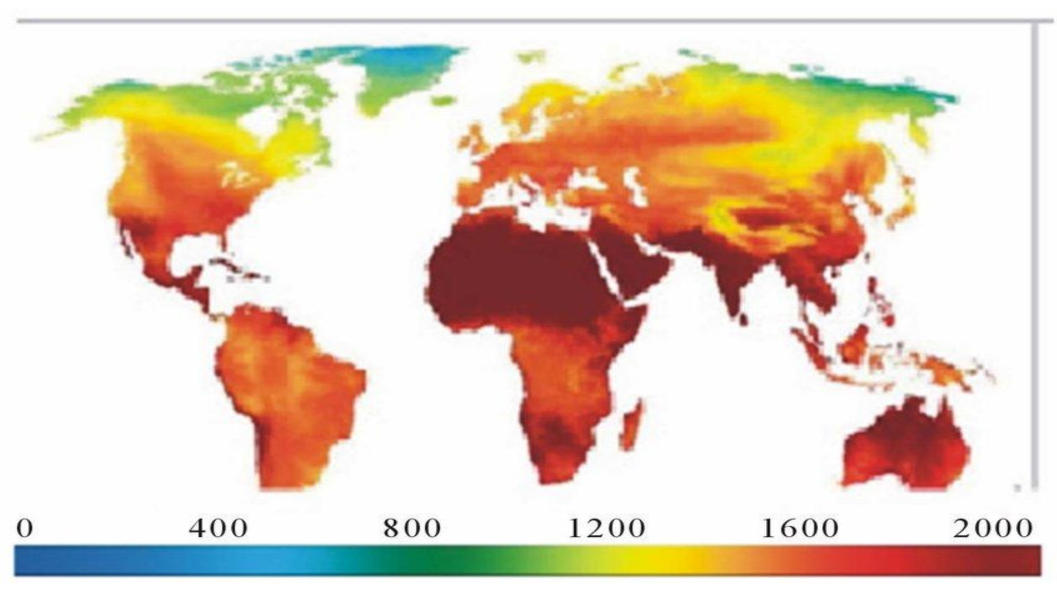

Figure 2.1: Map of world solar energy potential (NASA, 2013).

Figure 2.1 shows worlds solar energy potential, the solar potential at the equator is higher. Since Africa is located at the equator the solar energy potential is maximum. This is a large amount of energy that is estimated to be about 18 times that of the current primary energy demand. However, only 18% of the world's energy demand is supplied from renewable energy sources, one of which is solar power (Gilbert, 2004). In the U.S.A, the world's leading country in renewable energy production; only 7% of its energy demand is generated from renewable sources with the rest coming from petroleum, natural gas, coal, and nuclear power in the order of decreasing dependency (CSE, 2014). Ethiopia is located in the tropics and thus highly gifted with a wealth of solar energy that Received 5.5 to 6.5 kWh/m^2/day of solar insolation (ERG, 2009). According to ministry of water only less than 1% of solar energy potential in Ethiopia has been exploited so far.

2.2 Solar Collectors

Different types of renewable energy resources are available in nature such as solar, wind, geothermal, tidal...etc. from these available renewable energy sources, solar energy is the most used form of energy, as it's vital and abundant in nature (Raghurajsinh and Kedar, 2016). Solar collectors are a special kind of heat exchangers which transform solar radiation energy to internal energy of the transporting medium (Soteris, 2004). It is a device that absorbs incoming solar radiation, converts it into heat and transfers that heat to a fluid (usually air or water) that flow through the receiver. In all solar collectors, there are three characteristic energy processes: a collection of solar radiation, energy loss to the environment and the useful energy extracted from the collector (Zbysław, 2011).

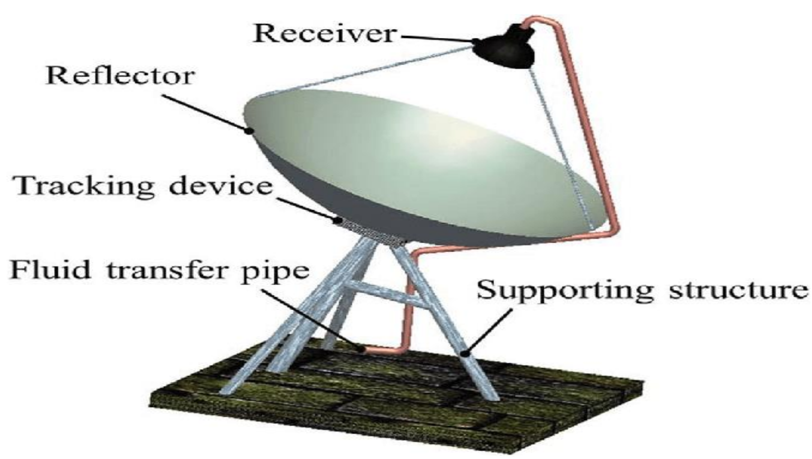

Figure 2.2: Parabolic dish collector (Pushkaraj *et al.*, 2017).

Shown in the Figure 2.2 is parabolic dish concentrator collector. As shown the figure the system consists of a reflector which is parabolic dish in shape and that concentrates the solar radiation to the receiver at the middle.

2.3 Factors Affecting the Performance of Parabolic Dish Concentrator

2.3.1 Effect of Receiver Position

The worst distribution of flux happened when the focal point was located inside the receiver;

the best however, when the geometry of the receiver was shifted away to allow the focal point to be located outside the geometry (Daabo *et al*., 2016).

2.3.2 Effect of Receiver Shape

It is clear that the geometrical shape of the receiver itself has a role in terms of the amount of energy received, absorbed, reflected and lost. After the rays hit the absorber wall, it has two different probabilities, either to be directly absorbed by the wall or reflected. The absorbed rays are considered as useful energy. However, the reflected rays also have two different possibilities. it either hit another part of the cavity surface area and by doing so those rays will have the chance to be absorbed by the internal cavity walls and counted as useful energy, or it might go directly outside the cavity geometry of the receiver through the aperture area and they will be considered as lost energy **(**Ahmed *et al.,* 2016).

Therefore, the shape of the receiver plays an important role in terms of reflected rays as well as the number of times that these rays are going to be reflected. As a result, the effect of the receiver’s geometry is examined in order to know which path each geometry has followed. Conical shape has received and absorbed the highest amount of energy compared to the other receivers’ configurations (Raja *et al.*, 2019).

2.3.3 Effect of Aperture Area of Concentrator

The aperture area of dish concentrator is defined as the total surface area of the solar concentrator upon which solar energy is incident. (Ghani, 2014) defined it as the area that receives the solar radiation. The size of the solar concentrator will affect the amount of solar thermal energy delivered to the receiver, large aperture diameter of the dish concentrator collects more radiation to the focal point (Kleih *et al*., 2009). Therefore, the concentrator needs to size to assure it can deliver enough of thermal energy to the receiver (Rosnani *et al*., 2015). Meanwhile, the quality of a concentrator is measured by its reflectance. In which, reflectance can be determined as the percentage of incident sunlight that reflected from the concentrator mirror surface.

2.3.4 Effects of Reflector Material

The reflectivity of the material of the concentrator affects greatly the percentage of the solar radiation to the receiver. Table 2.1 Shows the reflectivity of some materials that can be used in the design of the solar dish concentrator.

Table 2.1: Characteristics of solar reflector materials (Hafez *et al*., 2006).

Materials	Reflective (%)	Emissive (%)
Polymeric film, non-metal	98	2
Aluminum acrylic	98	2
Aluminum acrylic	97	3
Aluminum	86	14
Aluminum maylar	97	3
Glass/silver	95	5.4
Polished stainless	50	50

The material selected for this study is glass because it is easily available on local market and economically not expensive. The glass cut into small pieces and posted using postish on the surface of the dish.

2.3.5 Effect of Wind Speed

The convective heat loss from the surface of solar collector and receiver is known to be influenced by wind speed. With increase in wind speed over the surface of the collector result in an increase in heat loss thereby decrease in the thermal efficiency of the concentrator collector (Dawit, 2009).

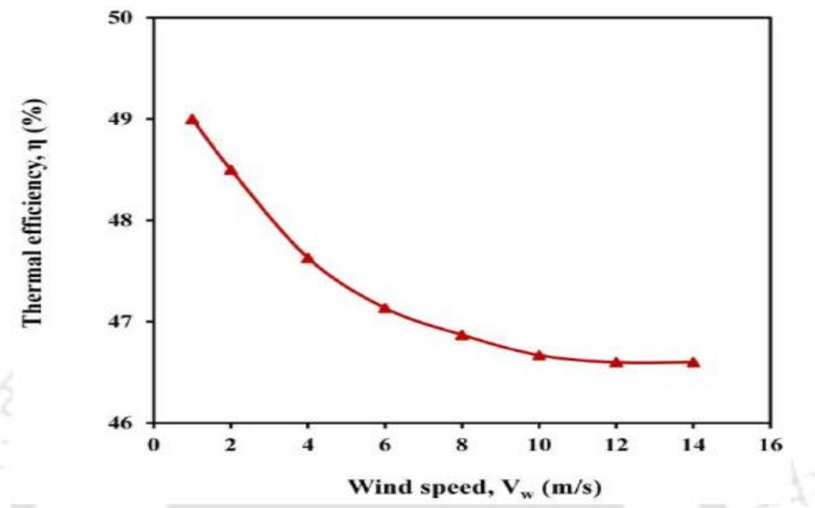

Figure 2.3: Effect of wind speed.

Shown in Figure indicates the thermal efficiency of the collector decrease with the increase in wind speed.

2.3.6 Effect of Ambient Temperature

Among the various climatic factors, it had been found that ambient temperature also has an effect on the thermal efficiency of the solar collector. Heat loss by conduction, convection and radiation decreases with increase in the ambient temperature (Dawit, 2009).

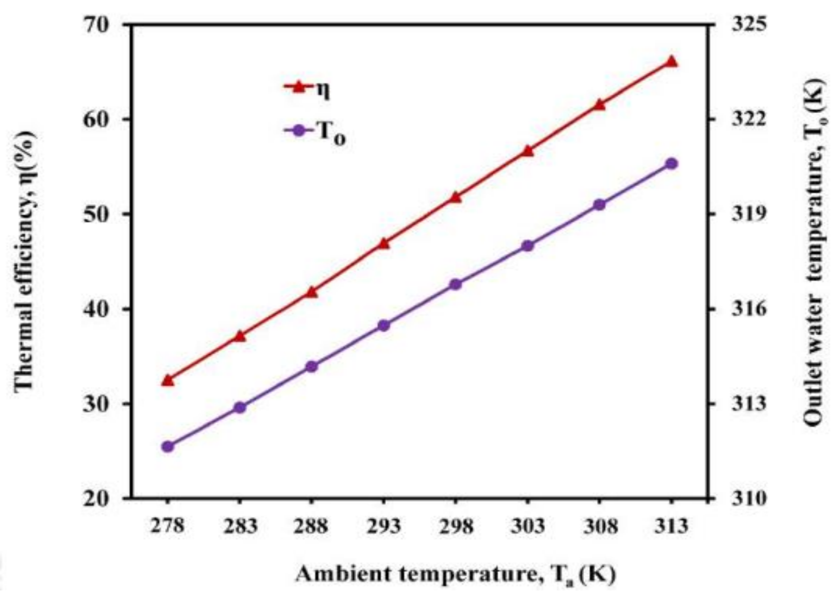

Figure 2.4: Effect of ambient temperature.

2.4 Solar Receiver

The main part in the dish concentrator is the absorber that functions as a connection link between the incoming energy (concentrated and reflected by the parabolic dish) and the fluid to be heated. Receivers for concentrating collectors should be designed in such a way to intercept as much reflected radiation from the concentrator as possible while at the same time ensuring that radiative heat losses from the receiver are minimized. Therefore, their size was determined by the compromise between intercepted radiation maximization, and heat loss from the receiver minimization to enable maximum power at sufficient temperatures for the intended application (Amos *et al*., 2015). The performance analysis of cylindrical, conical and spherical geometries of receiver were studied by (Daabo, 2019). The study considered with the objective of analyzing their optical and thermal behavior using the ray tracing method and Computational Fluid Dynamic (CFD) model. The results showed that the conical shape of the receiver gathered, as well as absorbed, a higher amount of reflected flux energy than the other shapes.

2.5 Types of Receiver

2.5.1 External Absorber

An external absorber is essentially a flat plate. The reflected radiation impinges on the plate and heats the surface. External absorbers are extremely simple and cheap but have many inefficiencies. External absorbers are directly exposed to ambient air and at high temperatures convection losses can be extreme. Temperature stratification will also occur inside the receiver. For an external absorber, if any radiation is reflected off the surface, it is reflected away from the absorber and lost (John, 2009).

2.5.2 Cavity Absorber

The absorber is recessed inside the receiver. Solar radiation is reflected by the concentrator through an opening, referred to as the receiver aperture, and collected on the absorber surface. Most modern receivers are of this type. Cavity absorbers are more expensive and complicated than external absorbers, but are much more efficient. If any radiation reflects off the absorber surface it was reflected onto another part of the absorber. In this way, the absorber has an increased chance of absorbing radiation each time light strikes its surface (John, 2009). For this study cavity type receiver is selected because it reduces radiation losses by recapturing radiated energy.

Seyed (2017) investigated the convective heat losses from a real scale cavity receiver with the nominal thermal power of 75 MW Results of this study showed that the convective heat loses in this scale and inclination level is highly related to forced convection induced by wind and can significantly affects the efficiency of the receiver.

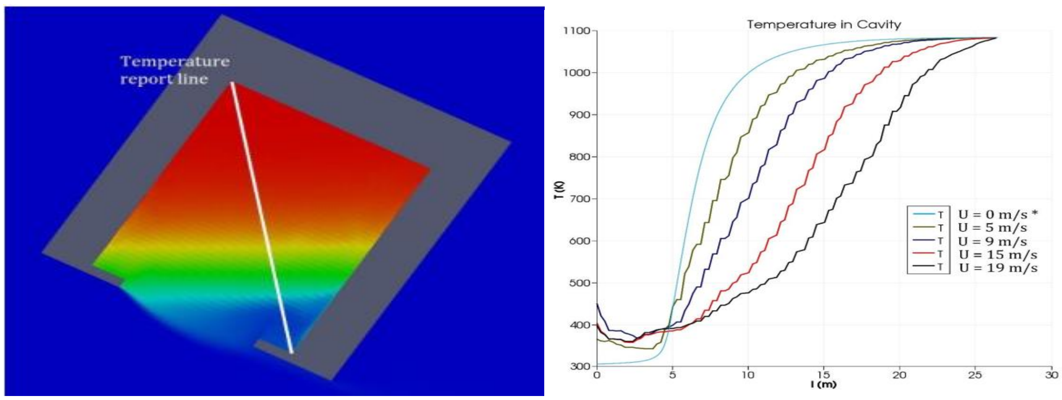

Figure 2.5: Convective heat loss inside the receiver cavity (Seyed, 2017).

Shown in figure 2.3 almost linear relation between the convective heat losses and wind velocity**.** Shrinkage of the stagnation zone has been observed with all wind velocities and stagnation zone become smaller with higher wind speeds. As the convective heat losses in the stagnation zone are very small, the shrinkage of the stable stagnation zone and consequently a bigger convective zone with lower temperature and natural and forced convective flows in it, has been recognized as the main reason for the increase of the convective heat losses from the cavity.

Madessa *et al*. (2011) investigated the thermal performance of two similar flat solar absorbers made of different materials (stainless steel fiber wire mesh and Silicon carbide honeycomb) in a small-scale parabolic dish concentrator collector.

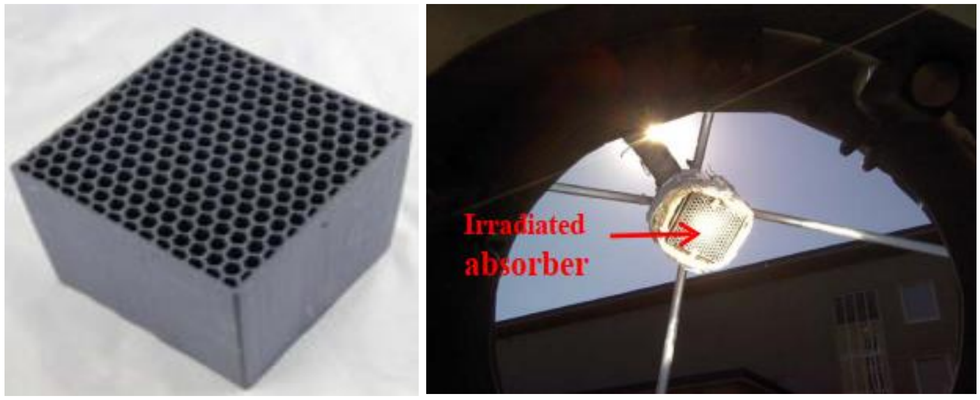

Figure 2.6: Honeycomb solar absorber (Madessa *et al*., 2011).

The finding points out that heat transfer fluid temperature and flow rates correlate negatively, while efficiency and flow rates correlate positively. In either case, the stainless-steel absorber had a good performance as compared to honeycomb absorber.

Shown in figure 2.4 indicates the honeycomb solar absorber, the solar radiation reflected and strikes on the absorber has positive response on the thermal efficiency of the collector.

Evangelos *et al*. (2019) investigated the Optical and thermal analysis of different cavity receiver designs for solar dish concentrators. The objective of the work was investigation of five different cavity receivers under different operating temperature levels and the selection of the most appropriate designs. More specifically, the examined cavities have the following shapes: cylindrical, rectangular, spherical, conical and cylindrical-conical. All the cavities were optimized in order to determine the best design which maximizes the thermal efficiency of the solar collector. The optimization variables are different for every design and they regard the cavity length, the cone angle and the distance from the concentrator base. According to the results, the best design was the novel one with cylindrical-conical shape, while the conical and the spherical are the next choices. The worst design was rectangular, while the cylindrical was the fourth design in the performance sequence. For operation at 300°C, the cylindrical conical design is found to have 67.95% thermal efficiency, 35.73% exergy efficiency while the optical efficiency is 85.42%.

Munir (2010) a flat surface absorption receiver was experimentally investigated with a parabolic dish solar concentrator in order to study the effect of receiver temperature distribution on heat gain and losses. The addition of specially designed metal fins in the inner surface of the receiver surface side the receiver transfers the incident heat flux to heat transfer fluid. The receiver surface temperature increased with increase in concentration ratio, intensity of beam radiation, ambient temperature, but decrease with wind speed. The maximum heat loss occurred from the outermost regions due to the more exposed surface area of the receiver even though there is more difference between receiver surface temperature and ambient temperature. The maximum and minimum of average surface temperatures were 350 °C and 210 °C without HTF during stagnation test whereas 200 °C and 145 °C with the circulation of water respectively. The average receiver surface temperature was around 280 °C during the test without heat transfer fluid and 140 °C with heat transfer fluid. The average receiver surface temperature was reduced by 100 ˚C due to the circulation of heat transfer fluid in the receiver when compared to the receiver at stagnation conditions.

2.6 Local Literatures on Areke Production System

To the best of the author’s knowledge there were no significant amount of studies that have been done so far in the area of improving and using solar energy as a source of energy for traditional Areke production in Ethiopia. However, some efforts have been made on the way of assessing the potential of biogas and solar energy for Areke production.

Shewangizaw (2016) conducted numerical and experimental analysis of biogas stove for local Areke distillation by using angle iron, flat iron and square pipe. The burner port diameter was 3mm and 62 holes manifold diameter 130 mm. In this study, the biogas flow rate was determined to meet the power input required for the process knowing the power required of the process being 1.547 kW, calorific value of biogas 22 MJ/m^3 and setting optimum biogas stove efficiency of 50%. the result showed at high flame intensity the overall efficiency was 54.8% and at low flame intensity the overall efficiency was 43.6%.

Figure 2.7: Biogas stove for local Areke production (Shewangizaw, 2016).

Yohannes (2011) conducted an experiment with First batch fed gasifier reactor having an internal diameter of 39cm was designed and fabricated, operating period of 25-35min, amount of biomass fuel consumed of 4.5kg, temperature at various points of 560 – 735C were monitored and analyzed. From this experiment fuel type, smoke and primary and secondary air inlet were evaluated using water boiling test and controlled cooking test methods by actually boil and cooking food. The experimental result shows thermal efficiency around 31.8% and the outer surface of stove was recorded as about 95°C. From the result by varying the available biomass fuels it was possible to increase thermal efficiency by decreasing heat loss to the surrounding.

Kebede (2018) studied the potential benefits of improved Areke distilling stoves with respect to the indoor air quality and specific fuel consumption as well as the time taken for distillation. The indoor concentration of two major pollutants, CO and PM were monitored using HOBO CO loggers and UCB PM Monitors, respectively. The test was conducted in real kitchens where the stoves perform the actual Areke distillation, whereas under controlled settings the possible efforts are made to minimize the source of variability to 30- minutes and 15- minutes intervals respectively to analyze the data. The improved stoves have shown statistically significant reduction in CO concentrations of 8.10% and 4.8ppm ($p<0.05$; $n= 9$) during complete distillation time whereas PM concentration was reduced to 19.05% and 69.70ppm. the result of the study indicated that the correlation between CO and PM were positive correlated and Pearson correlation of traditional stoves and improved stoves conditions were 0.32 ($p = 0.39$; $n = 9$) and 0.35; $n = 9$) respectively. Controlled Cooking test results showed that the improved stove significantly reduced the specific fuel consumption by 33.3% and 50.2% as well as reduction of time taken for distillation was observed.

Adane (2015) presented experimental analysis of parabolic dish solar collector system for Areke distillation. Took the data for parabolic dish frame of aperture diameter of 1.2 m, depth of 0.3 m and focal length of 0.3 m. Aluminum foil laminated galvanized sheet is used as reflective surface for dish concentrator. The parabolic dish tracks the sun ray manually based on the shadow of pin on the edge of dish aperture. Especially made clay pot with capacity of 4 liters, and having effective surface area of 0.071 m^2 was used as absorber. 2.5 liters of difedif was used to conduct the test in three different days. The test result showed it was possible to obtain from 2.5 liters of difedif 0.25 liters of Areke with alcohol content of 44% and on the average, it took 3 hours. And on average it took 1 hour and 15 minutes to reach temperature of 70.4℃ which is the boiling point temperature of alcohol in Addis Ababa at atmospheric pressure of 0.746 atm.

Figure 2.9: Direct solar thermal Areke distillation (Adane, 2015).

Gemedo (2016) studied design of a hydro/biogas based electric supply system as distributed generation applied for katikala distillation in significant parts of Ethiopia, case study at Arsi Negele. The work began by investigating hydro and biogas energy potentials of the site, capacity, demand and the total number of electric customers; and then compiling data from different sources and analyzing it using HOMER software. The Software simulation result showed, the most cost-effective system was the hydro-grid–biogas generator set-up. The designed power of hydro, biogas and grid was 2.835 MW, 7.5 MW, and 8 MW, respectively. The distillation using new still proceeded using 12 litter fermented wash. The cooling water temperature was around 40 ℃ and as the cooling water temperature rises the output distillate slows down. At a temperature of 89 ℃ the purity of alcohol collected was 46 ABV and at 92 ℃ it was 43 % ABV which was equal to the best *katikala* known as *„Arefa Areke‟* meaning which forms foam when shacked.

2.7 International Literatures on Areke Production System

Rajiv *et al.* (1991) reported the successful use of solar energy for distillation of alcohol. A flat plate solar collector (Aluminum fins with copper tube risers mechanically bonded and coated with selective Ni) system with a collector area of 38 m^2 was coupled to a pilot-scale distillation plant with a capacity of 1.8 l/h of 95 % v/v ethanol. The number of flat plate collector were 19. The average daily solar collection was 1.68 kWh/m^2 and the collection efficiency was 28 %. The average specific ethanol production rate was 0.63 liter per meter square per day. And yearly solar load was 65 %. The angle of inclination of the flat plate collector was 25° to horizontal and the collector run 70℃ hot water. The reboiler and condenser were shell and tube heat exchangers with heat transfer areas 0.236 m^2 and 1.29 m^2, respectively. Economic analysis of the system reveals that solar distillation of ethanol using flat plate collectors is not an economically viable proposition. The collector costs are 80% of the total plant cost. However, this study has also shown that it was feasible to run the plant at reboiler temperatures as low as 42 ^{0}C. Thus, low temperature solar collector systems like solar ponds could become a viable alternative.

Pierre *et al*. (2004) presented an experimental study about single and two compartments solar stills, a single-compartment and a two-compartment type. The single compartment still was optimized under local climate conditions. An experimental study of the cover slope showed that a cover angle of 16 ° ensures a very good transfer of solar radiation within the still while preventing the drops of the distillate to into the basin. In the two compartments, the glass of the compartment was transparent cover with apart of condensation happening on it, while the other compartment also made of glass is a non-transparent material which shade the sun; it was used only as a condenser. The result showed that the distillation of a 38 % alcohol initial solution yields a product containing 48 % of alcohol when using the single-cover model, while under the same climatic conditions the two compartments still gives a 71 % alcohol distillate.

Toure *et al*. (1999) studied on a small solar still of a domestic type with two distinct compartments has been led. The two compartments which communicated by slit. The frame was made of wood and measuring $1.095 \times 0.6 \times 0.4$ m^3. compartment one made of tank or absorber which was well insulated at the back and on the sides. The absorber made from stainless steel of 0.0015 m thick and 0.035 m high. There was a glass of 0.005 m thick and inclination of 16° this glass was used as a condenser. The second compartment was protected from solar radiation, because it was placed outside wooden cover which was 0.05 m from the glass in parallel position. The slit that permit communication between two compartments was 0.01 m wide and 0.6 m. And the result showed solar energy can perfectly be used to produce alcohol.

Ayuthaya *et al.* (2013) developed a mathematical model for predicting the productivity of an ethanol solar still of basin type a basin solar still was integrated with a set of fin-plate fitting in the still basin. The stainless-steel and basin solar still of $0.7\ m\ \times 0.7\ m$ area with a double glass cover of 14 inclination and the average height of 10.3 cm on a 100 cm stand was constructed. The cover inclination was selected in order to ensure that all condensate could flow to a collecting flask. A 1500 W heater with a controller heated the solution in the basin. The ethanol solution temperature was within the range of 40-90 ^{0}C. The condensing surface temperature range was 35-80 ^{0}C. The glass cover temperature was controlled by cool water passing through the glass cover channel. The ethanol solution input with known concentrations of 10, 30, 50, 70 and 90 %v/v was fed continuously to keep the solution concentration constant during the test period. Data obtained from this still set were used to develop mathematical models to predict the output of the still at the outdoors It was found that the productivity of the modified solar still was increased by 15.5 %, compared to that of a conventional still.

Vorayos *et al*. (2006) conducted mathematical model and simulation for performance analysis of solar ethanol distillation. The component from the simulation start up with 10 % alcohol concentration and yield 12,500 liter per year. The solar collector area is 3.6 m^2 for the heat pipe collector and 4 m^2 for the flat plate collector. heat pipe collector is higher than that of the system using flat plate collector. It results from the efficiency of the flat plate collector is greatly reduced when it is operated under high temperature condition. The result showed that the ethanol–water mixture was fed into the system with the rate of 0.08 l/min. The initial concentrations of the mixture are varied from 10% to 45% by volume. With the economic analysis, the results showed that the use of solar distillation systems appear to be economical compared to the conventional distillation system using fuel oil as heat source. The minimum production cost of the system was 0.39 US$ per liter.

Yuelei *et al*. (2012) investigated an ethanol distillation system has been developed to remove the water contents from the original wash that contains only around 15 % of the ethanol. The system has an ethanol production capacity of over 100,000 liters per day. One unique characteristic of this system is that it utilizes the waste heat rejected from a power plant to vaporize the ethanol, thus it saved a significant amount of energy and at the same time reduces the pollution to the environment.

Namprakai and Hirunlabh (1996) investigated alcohol distillation in a solar still with a horizontal evaporating surface and an inclined condensing surface was carried out, based on the model modified by Spalding (Arnold, 1963) and (Kiatsiriroat *et al*.,1986). The experiment was carried out under steady-state conditions with the evaporating and condensing surface temperature ranges 40-70°C and 35-50°C, respectively. The temperatures of the evaporating and condensing surfaces were monitored with a set of K-type thermocouples and concentration of the products was read by an alcoholometer. The production rate was read directly with a measuring cylinder. The mass fluxes of concentrated ethanol, pure alcohol and water distillate yielded from the unit could be estimated. The predicted results agreed well with those of the experiment that distill alcohol content of 50 % by volume.

Pablo *et al*. (2013) proposed thermal analysis of a solar distillation system for ethanol-water solutions. The dimensions, volumetric flow rates, and thermal capacities of an ethanol distillation system where solar energy used as primary energy were examined in the study. A rigorous thermodynamic equilibrium analysis was applied to obtain the critical design parameters for the solar distillation of an ethanol-water solution with different feed stream concentrations (5%, 7%, and 10% wt. ethanol) to obtain a distillate product of 95 % wt. ethanol. The volumetric flow of the feed stream is varied and a sensitivity analysis was performed to study its impact on the design of the solar distillation system. Important technical details, such as the configuration of the solar distillation system, the size of the distillation columns, reboiler heat duty, energy consumption per unit mass of distillate product, solar fraction, and collector area, among others, are evaluated and presented as a guideline for designers. The methodology developed herein was used to design the solar ethanol distillation system and can be extended to other geographical locations, weather conditions, and operational parameters.

2.8 Solar Thermal Energy for Heating Application

Joshua (2009) studied the design, construction and testing of a parabolic dish solar steam generator. Using concentrating collector, heat from the sun is concentrated on a black absorber located at the focus point of the reflector in which water is heated to a very high temperature to form steam. It also describes the sun tracking system unit by manual tilting of the lever at the base of the parabolic dish to capture solar energy. The whole arrangement is mounted on a hinged frame supported with a slotted lever for tilting the parabolic dish reflector to different angles so that the sun is always directed to the collector at different period of the day. On the average sunny and cloud free days, the test results gave high temperature above 200℃.

Yaseen *et al.* (2018) developed two solar dish concentrators (SDC) with diameter of (2 m) have been designed for water heating purpose. This study was applied on solar steam water heater. Both of the dishes coated with thick layer of steel (galvanized), while its interior surface covered with a reflector layer.

Figure 2.10: Parabolic dish concentrator for water heating purpose (Yaseen et al., 2018).

The first dish interior surface covered with a layer of reflectivity up to 80%, whereas the second one covered by a piece of mirrors with a reflectivity of 95%. The receivers have been fixed in the focal position of both dishes. The measurement of temperature and solar power for both types have been documented and recorded. The optical energy for the 1st dish is 1909 W, the final energy is 1551 W, and the efficiency is 61%, while the optical energy for the 2nd dish is 1607.68 W, the final energy is 1853 W, and the efficiency is 73%.

Lifang *et al*. (2011) developed a new concept of large parabolic dish concentrator for oil heating. The dish mirror was formed from several optimal-shaped thin flat metal petals with highly reflective surfaces. Attached to the rear surface of the mirror petals were several thin layers whose shapes optimized to reflective petals form into a parabola when their ends were pulled toward each other by cables or rods. The result showed that the concentrator reaches maximum temperature of 680 ℃

Ibrahim (2012) reported the design and development of a parabolic dish solar water heater for domestic hot water application. The result showed that the heater is providing 40 liters of hot water a day for a family of four members, assuming that each member of the family requires 10 liters of hot water per day. Initially the expected the thermal efficiencies of 50% by the design but the obtained thermal efficiencies of 52% - 56% and this range of efficiencies was higher than the expected designed value.

Fareed *et al.* (2012) studied portable solar dish concentrator and reported design and fabrication of solar dish concentration with diameters 1.6 meters for water heating application and solar steam was achieved. The dish was fabricated using metal of galvanized steel, and its interior surface was covered by a reflecting layer with reflectivity up to (76%), and equipped with a receiver (boiler) located in the focal position. The dish equipped with tracking system and measurement of the temperature and solar power. Water temperature increased up to 80 ℃, and the system efficiency increased by 30% at mid noon time.

Ibrahim (2013). designed and constructed Parabolic dish solar thermal cooker. The cooker was designed to cook food equivalent of 12 kg of dry rice per day, for a relatively medium size family. For effective performance, the design required that the solar cooker track the sun frequently, and a linear actuator (super jack) was adopted for this purpose. Preliminary test results show that the overall performance of the solar thermal cooker was satisfactory. The cooker was capable of cooking 3.0 kg of rice within 90 – 100 minutes, and this strongly agrees with the predicted time of 91minutes.

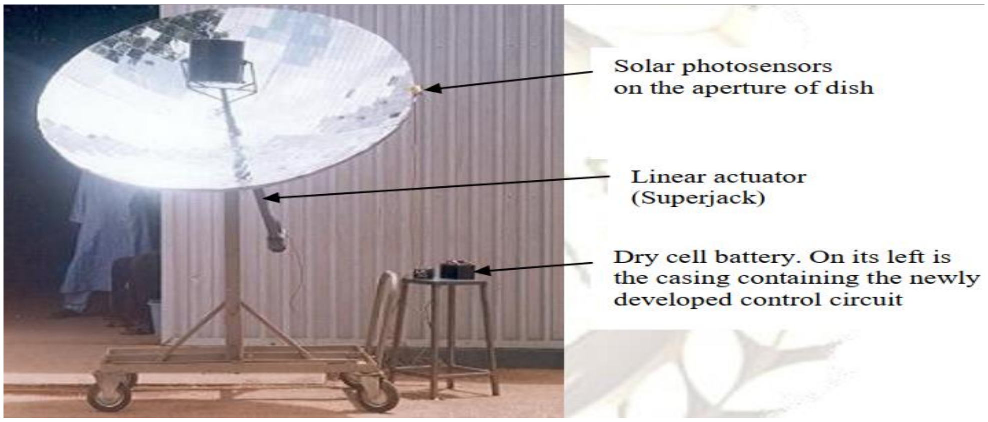

Figure 2.11: Parabolic dish concentrator for water heating system (Ibrahim, 2013).

2.9 Solar Thermal Energy for Cooking Application

Amos *et al*. (2017) investigate the thermal performance of a point focus solar concentrating collector comprising a 2000 mm diameter, and a 665 mm focal length symmetric parabolic dish concentrator covered with reflective aluminum tiles of 0.9 reflectivity and SiC honeycomb volumetric absorber, which use atmospheric air as heat transfer fluid was experimentally investigated. The absorber was tested for two different mass flow rates

Figure 2.12: Indirect solar cooker (Amos *et al*., 2017).

The test was intended to assess the potential of this collector as a component of solar cooker with heat storage, a prototype that has a potential to enable indirect and off-sun cooking. The prototype of a solar cooker under investigation was intended to be used in rural areas (in Mozambique) to meet multiple domestic needs in thermal energy as part of a global effort to mitigate the consequences of one of the severe problems the world faces today (desertification and deforestation), some of which are attributed to climate change

Asfafaw *et al*. (2014) the second experimental study was a solar thermal stove which generates steam by concentrating suns ray using a parabolic dish on the receiver. The steam flows through a pipe to the injera baking stove and condenses by transferring heat to the baking pan which is placed on the steel plate that is in contact with steam. The important conclusion drawn from this study was the possibility of baking injera using indirect steam in a temperature range from 135 to 160 °C. The indicated temperature was less than the literature or experimental values obtained earlier by other researchers or developers working on an injera baking stove.

Figure 2.13: Solar thermal injera baking stove (Asfafaw *et al*., 2014).

2.10 Heat Exchanger

Heat exchangers are devices designed to transfer heat between two or more fluids-i.e., liquids, vapors, or gases of different temperatures. Depending on the type of heat exchanger employed, the heat transferring process can be gas-to-gas, liquid-to-gas, or liquid-to-liquid and occur through a solid separator, which prevents mixing of the fluids, or direct fluid contact (Ashkan 2017).

Yang *et al*. (2008) studied condensation heat transfer of the ethanol–water mixtures on the vertical tube over a wide range of ethanol concentrations was investigated. The condensation curves of the heat flux and the heat transfer coefficients revealed nonlinear characteristics and had peak values, with respect to the change of the vapor-to-surface temperature difference. This characteristic applies to all ethanol concentrations under all experimental conditions. With the decrease of the ethanol concentrations, the condensation heat transfer coefficient increased notably, especially when the ethanol concentration was very low. The maximum heat transfer coefficient of the vapor mixtures increased to 9 times as compared with that of pure steam at ethanol vapor mass concentration of 1%. With the increase of the ethanol concentrations, the condensation heat transfer coefficient decreased accordingly. When the ethanol concentration reached 50%, the heat transfer coefficient was smaller than that of the pure steam.

Ashkan (2017) presented the effect of operational and geometrical parameters on the thermal effectiveness of shell and helically coiled tube heat exchangers was investigated. Analysis was performed for the steady state. The working fluid is water vapor and liquid water, that its viscosity and thermal conductivity was assumed to be dependent on temperature.

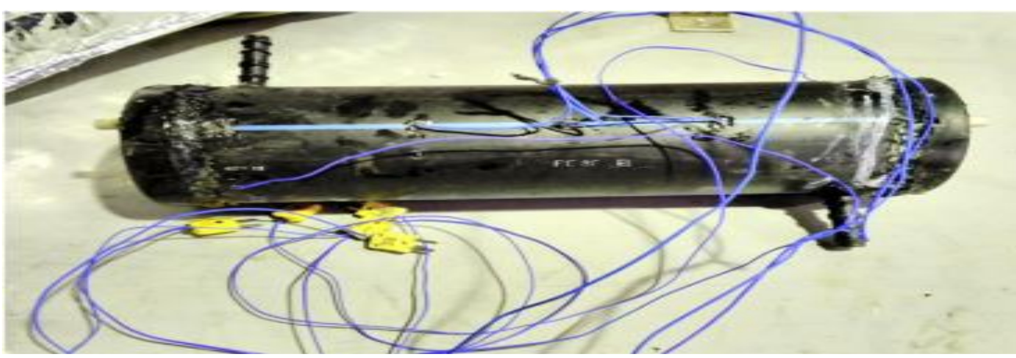

Figure 2.14: Shell and coil heat exchanger (Ashkan 2017).

Based on the results, two correlations have been developed to predict the thermal effectiveness, for wide ranges of mass flow rates ratio, dimensionless geometrical parameters and product of Reynolds numbers. Furthermore, it was found for same values of NTU and Cr, the effectiveness is averagely 12.6% less than the effectiveness of parallel flow heat exchangers and this difference is approximately constant. The cold water reaches to a prescribed temperature (65-85℃).

Adams (2012) developed a Liebig condenser for ethanol condensation. It had a tube going straight through, and a surrounding tube with a water inlet and a water outlet. The outer tube works as a jacket of water. The flow of water through the jacket condenses the alcohol vapor in the inner-tube. It was used in both pot still and reflux still designs.

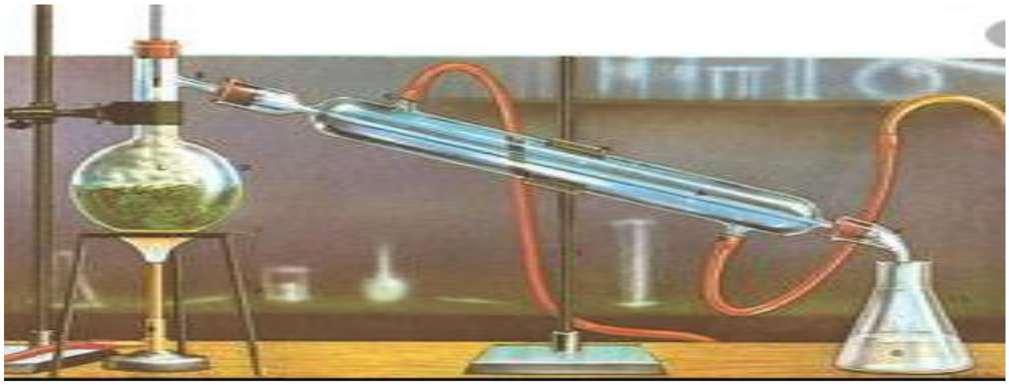

Figure 2.15: Liebig alcohol vapor condenser (Adams 2012).

Russel (2003) study shell and tube crossflow condenser, a concept used extensively in large-scale steam recovery systems for ethanol distilling, it is particularly suitable for coolant recirculating (recycling). Its advantages over other condensers are: very low coolant friction, therefore low-power pumping requirements; compact size compared to product volume output; Large heat transfer surface. Design-wise, it was the reverse of the so-called "shotgun" condenser in that the coolant flows through the tubes and the vapor passes over the tubes at right angle, allowing much larger volumes of vapor to be condensed for no increase in condenser size.

Figure 2.16: Shell and tube cross flow condenser for alcohol vapor condensation (Russel 2003).

2.11 Summary from Literature Review

For many years local Areke production activity takes place using energy from biomass wood. But in developing countries, like Ethiopia sunlight is unrivaled source of energy. Solar thermal energy is used for different applications such as cooking, distillating, heating and electric power generation. Alcohol/Areke production system takes place using different technologies from this, Biogas technology and solar technology were applied. Researchers conducted numerical and experimental analysis for alcohol/Areke production process by considering time taken, fuel consumption and environmental pollution. In this thesis providing improved design of solar thermal Areke distillator with locally available and low-cost materials and finding out the performance of solar thermal energy and how long it can maintain the required temperature inside a distillation column using solar radiation are mainly focused area. That aim to divert people living in rural area from fire-wood powered oven to solar powered distillation system. As explained in literature reviews above some researches have been taken with an intensive experimental and numerical investigation of solar thermal Areke production system. However, still there is a wide research gap to fulfill societies need and to design socially acceptable solar thermal Areke production system.

2.12 Research Gap

From the literatures which were conducted on the local Areke production system there was a gap on heating system of the Difdif, Putting the distillation pot directly on the focal point is not advisable because, for large volume of the distillation pot it creates shading on the reflector due to this effect shading loss increases, performance of the collector decrease and difficult to track the dish concentrator. The energy consumption using biomass/wood for Areke distillation was very high and time taken to complete one round of distillation process was maximum. By considering such gaps this study conducted on the performance of solar thermal energy for local Areke production system using modified solar absorber and by indirect heating system.

CHAPTER THREE

MATERIALS AND METHODS

3.1. Materials

The materials and instruments used for the experimental setup and test are listed in Table 3.1.

Table 3.1: List of materials and instruments used for experimental work.

No	Equipment	Measuring instruments
1	Distillation column made from clay	Thermocouple (K-type)
2	Copper/Aluminum sheet metal	Mercury Thermometer
	Copper coil	Alcoholmeter
4	Satellite dish	
5	Reflective glass	
6	Polystyrene foam (insulator)	
7	Difdif (mixture of Gesho, Kita, Bikl and Water)	
8	Water (working fluid)	
9	Fluid transport pipe	

3.2. Methodology

To perform this research work different methodologies have been employed; that are, overview of the prior related works, experimental tests and traditional Areke production system. Testing has been performed by two ways stagnation testing and load testing. For developing prototype, low cost and locally available materials were used. The software's used for this study are SOLIDWORK, Microsoft office word, ANSYS Fluent 16.2.

To achieve the general and specific objectives the following steps are adopted.

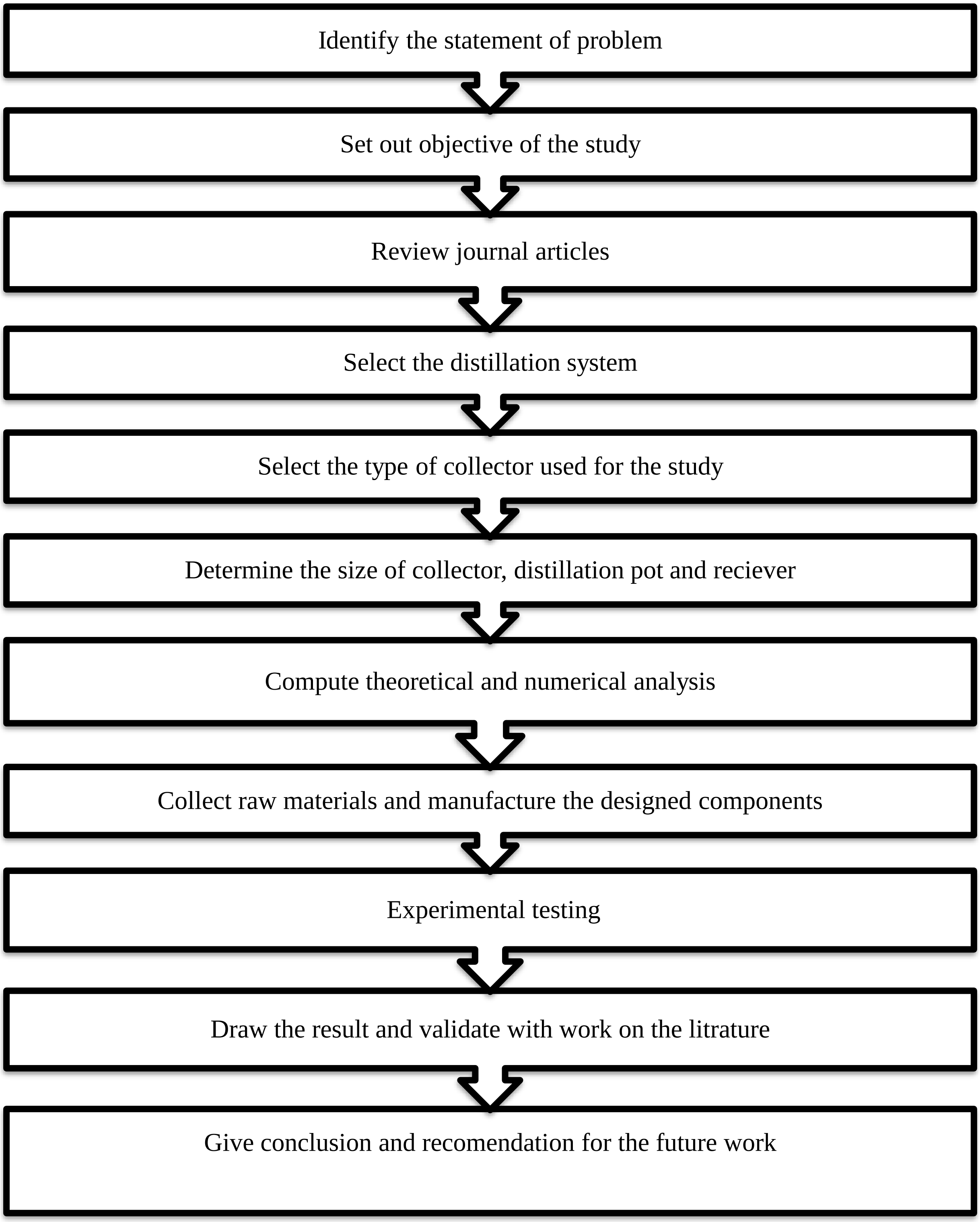

Figure 3.1: Work flow diagram of solar thermal Areke production system.

3.2.1. Areke Difdif Preparation Process

Generally, in traditional Areke distillation Difdif preparation process is divided into three phases.

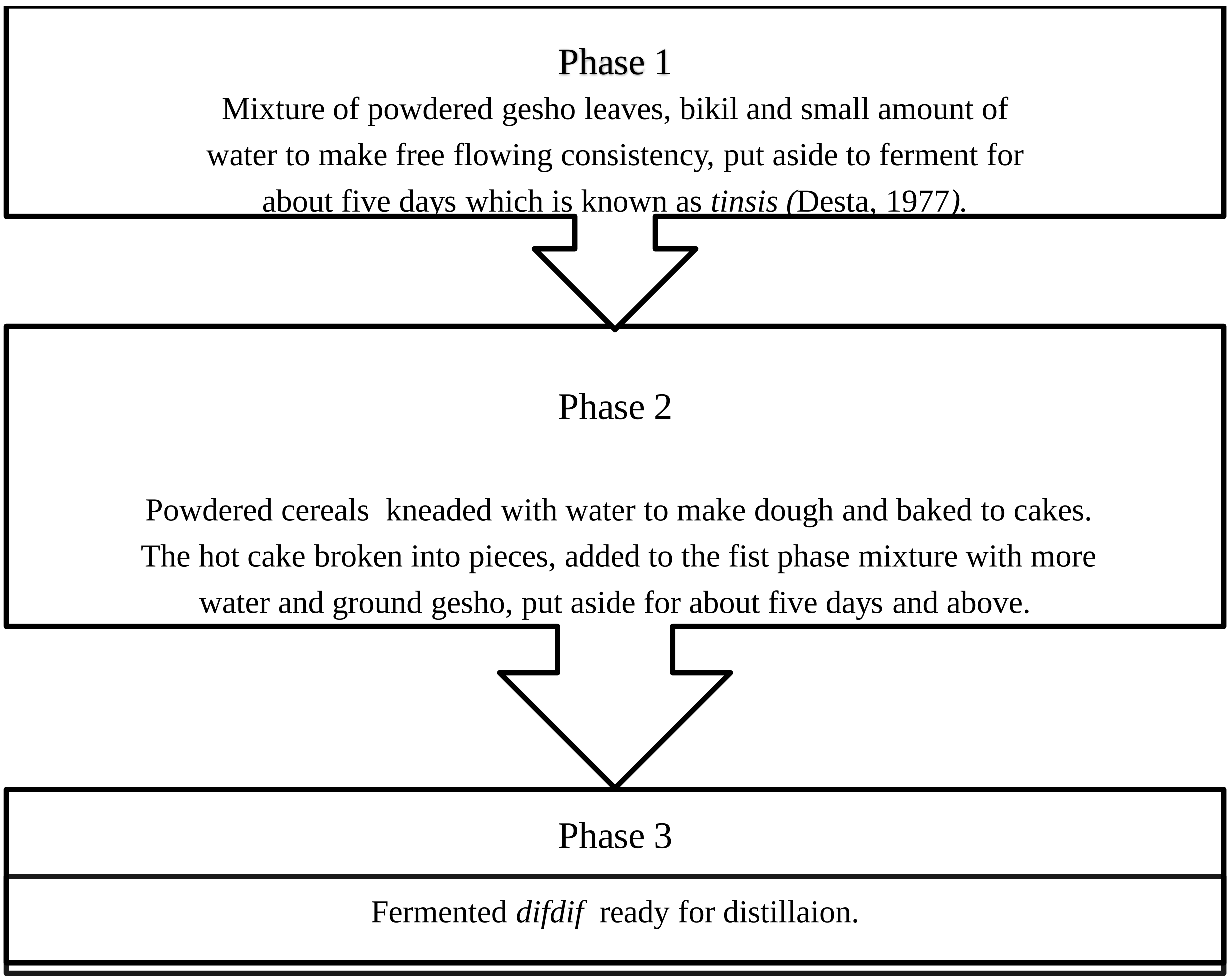

Figure 3.2: Difdif preparation procedures.

3.3. Traditional Areke Distillation Apparatus

Traditional Areke distillation system generally comprises the following components: distillation pot made of clay with thickness of approximately 8-12mm, pot lid made of clay, condensate tube made of bamboo, distillate collector flask and condenser tub-made of clay filled with cooling water.

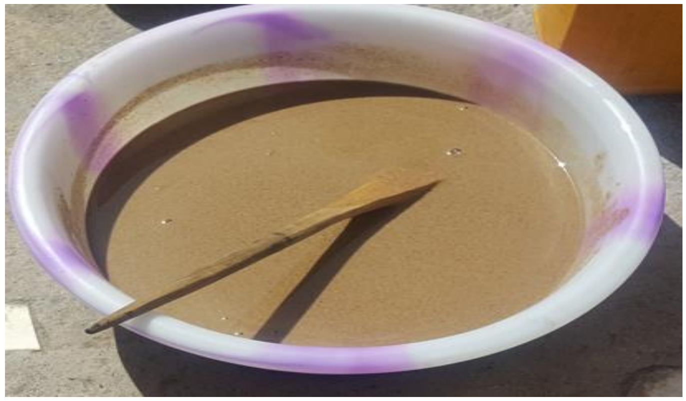

Figure 3.3: Photograph of difedif ready for distillation (Adane, 2015).

3.3.1. Distillation pot

The traditional Areke distillation pot has spherical shape and made from clay soil, which has separate fuel and air inlet and combustion chambers are made of refractory bricks which can withstand high temperature and gives strength to stove.

Figure 3.4: Traditional distillation stove (Girma, 2008).

3.3.2. Condensate Tube

In traditional Areke distillation process the condensate tube made of bamboo with approximate internal diameter of 60mm is used. The condensate tube has small opening at one end where bamboo tube having smaller diameter is inserted and connects the collector flash with the pot, while the larger opening at the other end is inserted in to the opening on the lid of distillation pot. cooling tub made of clay filled with cooling water, tie rope and the distillate collector flask. The distillate collector is immersed up to its neck into the water filled tub. One end of condensate tube made of bamboo is inserted into the opening of distillate collector flask, while the other end is inserted into the outlet of the distillate pot.

After condensate tube is inserted into the flask and the flask is inserted in the cooling water, it will be tied down to the tub by tie rope to prevent the movement. The evaporate coming from the Difdif in distillate pot flows through the condensate tube and enters into the collecting flask. The hot steam that enters into the flask cools by releasing the heat to the cooling water in the cooling tub. When the cooling water in the tub gets hot, it will be drained and replaced by cool water if the flask is not already full of distillate-areke.

3.4. Solar Data Collection

Solar energy data was collected from different websites and from National Meteorology Agency of Ethiopia (NMA).

Website based solar radiation data were collected from:

- ✓ HelioClim-1 Database, http://www.soda-is.com, data provider is MINES ParisTech -Armines (France).
- ✓ MERRA-2 meteorological data, http://gmao.gsfc.nasa.gov/reanalysis/MERRA-2,data provider is National Aeronautics and Space Administration (NASA)/ Goddard Space Flight Center.
- ✓ HOMER energy, http://www.homerpro.com, as a resource of National Solar Radiation Database.

The data collected from the above websites are used to analysis solar potential of Debre Birhan city and compare the result with National Meteorology Agency (NMA) of Ethiopia. The data's collected from NMA are sunshine hour, wind speed, maximum and minimum ambient temperature.

3.5. Design of Solar Thermal Areke Production System

Schematic diagram of solar thermal Areke production system in figure 3.3 drawn by using SOLIDWORK 2018.

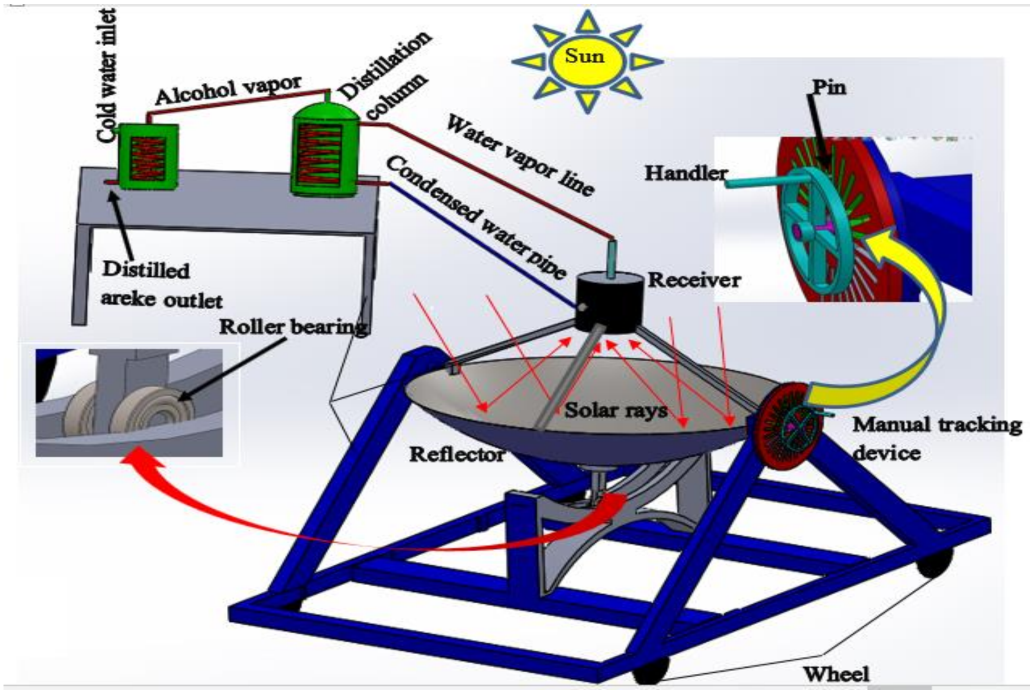

Figure 3.5: Schematic diagram of solar thermal Areke distillator.

The schematic diagram of the proposed system is shown in Figure. 3.3 The cold water which is stored in the main receiver that kept at the focal point of the parabolic dish collector, gets heated up because of concentration of solar radiation at the focus of the concentrating collector. The hot water is then allowed to flow through the copper tube and move to the top of the distillation column from where it can be taken out for distillation purposes.

CHAPTER FOUR

SOLAR ENERGY POTENTIAL OF DEBRE BIRHAN TOWN

4.1. Introduction

Detail data about solar radiation is the main input in designing of solar collector thermal systems, even in building designing and agroindustry processes solar radiation data is very important (Dlamini *et al.*, 2017).

Figure 4.1: Geographical location of Debre Birhan Town.

Developing countries like Ethiopia has no enough technological instruments to conduct detail meteorology related measurements including solar radiation. So to overcome this problem, different analytical models have been assessed and developed to estimate solar radiation in different parts of the world by using geographical data and simple meteorological data by using air temperature such as in Swaziland (Dlamini *et al*., 2017), by using sunshine hour such as in USA (Allen, 1997), Nigeria (Umoh, 2013). In fully organized meteorological agencies, all meteorological parameters such as temperature, atmospheric pressure, relative humidity, the number of sunshine hours, wind speed, cloud cover, and rainfall are available. Ethiopia has an annual mean average solar radiation of about 5.2 kWh/m^2, and the range of 4 – 6 kWh/m^2 with average sun light length of more than 10 hours per day throughout the year and has high potential of solar irradiation (UNCC, 2002).

4.2. Estimation of Global Solar Radiation Using Sunshine Duration

Sunshine duration is the length of time that the ground surface is irradiated by direct solar radiation and used to characterize the climate of sites. Debre Birhan is a town and woreda in central Ethiopia. Located in the Semen Shewa Zone of the Amhara Region, about 130 kilometers north east of Addis Ababa on the paved highway to Dessie, the town has a latitude and longitude of 9.633°N 39.5°E and an elevation of 2,750 m. The data obtained from national meteorology agency of Ethiopia is sunshine hour and calculated using software (Microsoft excel), since the solar radiation data was not active for Debre Birhan, it was difficult to take global solar radiation the only option was calculating the solar data by using sunshine hour.

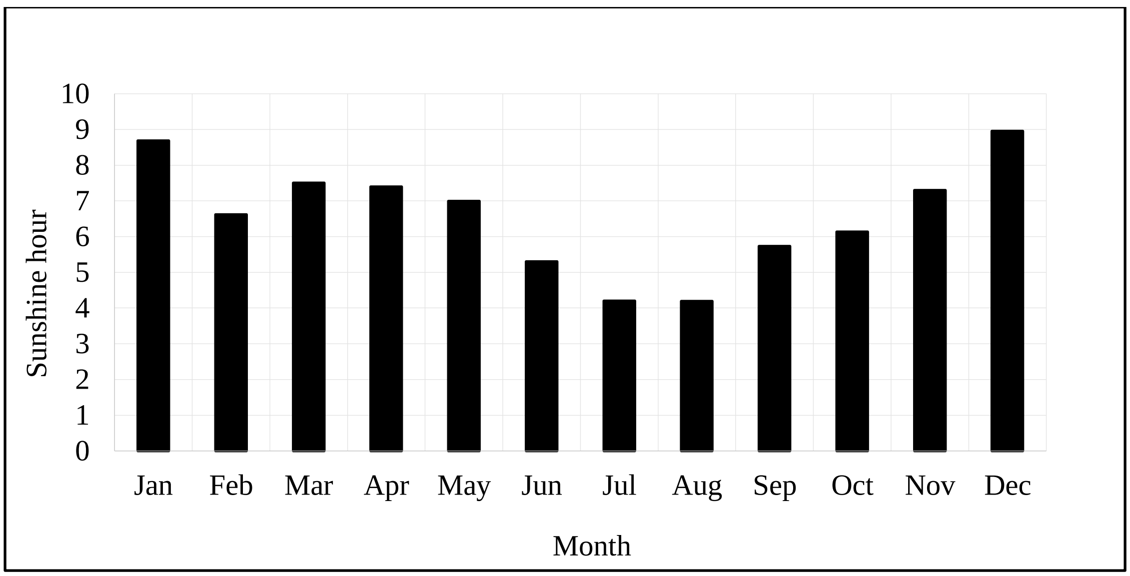

Figure 4.2: Sunshine hour for the representative day of each month in Debre Birhan for an average climatic condition of five years.

Figure 4.2 indicates that the sunshine hour attains maximum and minimum value on the month December and August respectively, this is due to behavior of the season, sunshine hour is maximum during Winter of Ethiopia because, most of a time it is clear sky. During the summer season there is a cloud so the sunshine hour leads to minimum value.

4.3. Fundamental Angles of Sun with Earth

Fundamental angles of sun are hour angle, latitude, and declination. Other angles like solar incidence, azimuth etc. must be related to these fundamental angular quantities (Duffie and Beckman, 2013).

Solar Time: Time based on the apparent angular motion of the sun across the sky with solar noon the time the sun crosses the meridian of the observer. Solar time is the time used in all of the sun-angle relationships. So, it is necessary to convert standard time to solar time by applying the equation of time which takes into account the perturbations in the earth's rate of rotation which affect the time, the sun crosses the observer's meridian (Duffie & Beckman, 2013).

$$\text{solar time} - \text{standard time} = 4(\mathrm{L_{st}} - \mathrm{L_{loc}}) + \mathrm{E} \tag{4.1}$$

where:

L_{st} -is the standard meridian for the local time zone

L_{loc} -is the longitude of observers the location, and longitudes are in (◦) West, that is, 0°< L < 360°.

The parameter *E* is the equation of time (min) and sited (Kalogirou, 2014).

$$\mathrm{E} = 229.2(0.000075 + 0.001868 \cos 2\mathrm{B} - 0.032077 \sin \mathrm{B} - 0.014015 \cos 2\mathrm{B} - 0.04089 \sin 2\mathrm{B}) \tag{4.2}$$

where:

$B = \frac{360}{365}(n-1), [°]$

n −is day of the year

Solar Hour angle (ω): is the angular displacement of the sun east or west of the local meridian due to rotation of the earth on its axis at 15° per hour (morning negative and afternoon positive) (Duffie & Beckman, 2013).

$$\omega = (\text{solar time} - 12)(\text{in hours}) \times 15 \text{ degrees} \tag{4.3}$$

Zenith angle (θ_z): the angle between the vertical and the line to the sun or the angle of incidence of beam radiation on a horizontal surface (Tiwari *et al*., 2016).

$$\cos\theta_z = \cos\varphi\cos\delta\cos\omega + \sin\varphi\sin\delta \tag{4.4}$$

where, $\varphi -$ angular location north or south of the equator; $-90 \leq \varphi \leq +90$

$\delta -$ solar declination; $-23.45℃ \leq \delta \leq +23.45°$

Angle of incidence ($\boldsymbol{\theta}$): the angle between the beam radiation on a surface and the normal to that surface (Tiwari *et al.*, 2016).

$$\cos\theta = \cos\delta\cos\omega(\cos\varphi\cos\beta + \sin\varphi\sin\beta) + \sin\delta(\sin\varphi\cos\beta - \cos\varphi\cos\beta) \tag{4.5}$$

Sunrise and sunset times and day length

The sun is said to rise and set when the solar altitude angle (α) is zero. So, the hour angle at sunset, ω_{ss}, can be found by (Kalogirou, 2014).

$$\omega_{ss} = \cos^{-1}(-\tan\delta \times \tan\varphi) \tag{4.6}$$

where, ω_{ss} $-$is taken as positive for sunset

$\varphi -$ latitude angle

$\delta -$ declination angle

The length of sun shine hour (N_s) is computed from (Kalogirou, 2014).

$$N_s = \frac{2}{15}\omega_{ss} \tag{4.7}$$

Latitude Angle (φ) is the angular geographical location that made in between the line joining location with center of the earth and its projection equatorial plane. Northern hemisphere is positive -90◦ ≤ φ ≤ 90◦ (Tiwari *et al.*, 2016).

Declination Angle ($\boldsymbol{\delta}$): The declination is the angular position of the sun at solar noon, with respect to the plane of the equator. Its value in degrees is given by Cooper's equation (fekede, 2019).

$$\delta = 23.45\sin\left(360°\frac{284 + n}{365}\right) \tag{4.8}$$

where: n is the day of the year, ($1 \leq n \leq 365$)

4.4. Solar Radiation Analysis

4.4.1. Extraterrestrial Radiation

The extraterrestrial radiation on a surface normal to sun's rays kept at a distance of sun-earth (not the mean distance, but the actual distance on that day, that time), the I_{sc} will essentially be the solar constant, modified to take into account the varying distance between the sun and the earth extraterritorial radiation (I_0) is given by (Tiwari *et al.*, 2016):

$$I_0 = \frac{24 * 3600}{\pi} I_{SC} \left[1 + 0.033 \cos\left(\frac{360n}{365}\right)\right] \tag{4.9}$$

where:

$I_{sc} -$ solar constant = $1367 W/m^2$

$n -$ day of the year, 1 for January 1st

4.4.2. Daily Extraterrestrial Radiation on a Horizontal Surface

Corresponding to I_{sc} the solar radiation intensity under extraterrestrial conditions, the intensity on a horizontal plane I_0 in W/m^2 is given by (Tiwari *et al.*, 2016):

$$I_0 = \frac{24 * 3600}{\pi} I_{SC} \left[1 + 0.033 \cos\left(\frac{360n}{365}\right)\right] \cos \theta_z \tag{4.10}$$

where, θ_z is zenith angle

By integrating Equation above from sunrise to sunset we can obtain the daily extraterrestrial solar radiation on a horizontal surface as:

$$H_0 = \frac{24x3600 I_{sc}}{1} \left[1 + 0.033 \cos\left(\frac{360n}{365}\right)\right] \left(\cos \varphi \cos \delta \cos \omega_{ss} + \frac{\pi \omega_{ss}}{180} \sin \varphi \sin \delta\right) \tag{4.11}$$

where, ω_{ss} is the sunset hour angle

4.5. Prediction of Monthly Average Daily Global, Beam and Diffuse Radiation on a Horizontal Surface

4.5.1. Global Monthly Average Daily Radiation

In Ethiopia sunshine data based solar energy estimation has been used frequently in different researches for solar radiation energy estimation and for designing purpose of solar system. (Addisu *et al.*, 2013) estimated solar radiation by using sunshine data of the different sites based on well-known Angström model. Surface solar radiation on a ground level was suggested by Angstrom, who relate it with the amount of sunshine hour in the day, using some empirical constant obtained by regression analysis (Tiwari *et al.*, 2016):

$$\mathrm{H_G} = \mathrm{H_0}(\mathrm{a} + \mathrm{b}\left(\frac{\bar{\mathrm{n}}_\mathrm{s}}{\mathrm{N_s}}\right)) \tag{4.12}$$

where, a and b are regression constant given by:

$$\mathrm{a} = -0.11 + 0.23\,cos\,\varphi + 0.323\,\frac{\bar{\mathrm{n}}_\mathrm{s}}{\mathrm{N_s}} \tag{4.12a}$$

$$\mathrm{b} = 1.449 - 0.533\,cos\,\varphi - 0.694\,\frac{\bar{\mathrm{n}}_\mathrm{s}}{\mathrm{N_s}} \tag{4.12b}$$

where, H_G is global daily solar radiation on a horizontal surface, $\bar{n}_s$ is the daily hours of bright sunshine hour and N_s is the maximum possible daily hours of bright sunshine.

4.5.2. Diffuse Monthly Average Daily Radiation

The monthly average daily diffuse solar radiation on a horizontal surface can be determined from the monthly average daily global radiation and the number of bright sunshine hours (Tiwari *et al.*, 2016):

$$\mathrm{H_D} = \mathrm{H_G}(0.931 + 0.814\,\frac{\bar{\mathrm{n}}_\mathrm{s}}{\mathrm{N_s}}) \tag{4.13}$$

4.5.3. Beam Monthly Average Daily Radiation

Beam solar radiation is direct solar radiation which reaching the earth surface without scattering in the atmosphere. Monthly average daily beam radiation on a horizontal surface (H_B) is the difference between global and diffuse monthly daily average radiation.

$$H_B = H_G - H_D \tag{4.14}$$

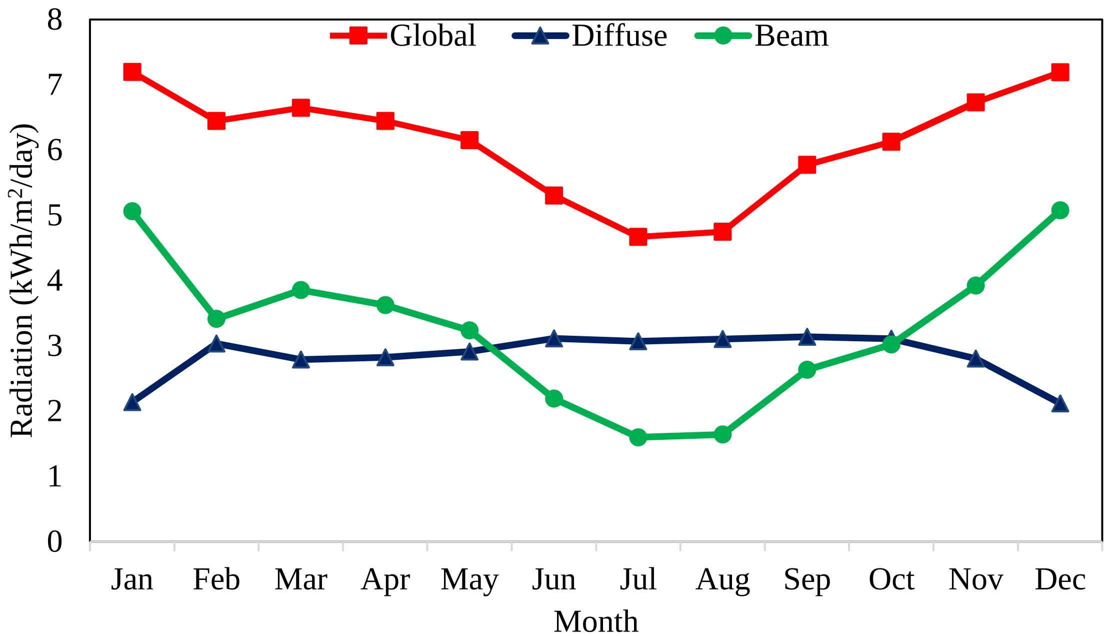

Figure 4.3: Monthly average daily global, diffuse and beam radiation on a horizontal surface in Debre Birhan.

4.6. Prediction of Monthly Average Hourly Global, Beam and Diffuse Radiation on a Horizontal Surface

The monthly average hourly global and diffuse radiation on a horizontal surface can be calculated from the knowledge of the monthly average daily global and diffuse radiation on a ground level.

4.6.1 Global Hourly Solar Radiation Estimation

Prediction of monthly average hourly global radiation on a horizontal surface (I_G) (Tiwari *et al.*, 2016).

$$I_G = \frac{H_G\pi}{24}(a_1 + b_1\cos\omega)\frac{\cos\omega - \cos\omega_{ss}}{\sin\omega_{ss} - \frac{\pi\omega_{ss}\cos\omega_{ss}}{180}} \tag{4.15}$$

where, a_1 and b_1 regression constant given by:

$$a_1 = 0.409 + 0.5016\sin(\omega_{ss} - 60) \tag{4.16a}$$

$$b_1 = 0.6609 - 0.4767\sin(\omega_{ss} - 60) \tag{4.16b}$$

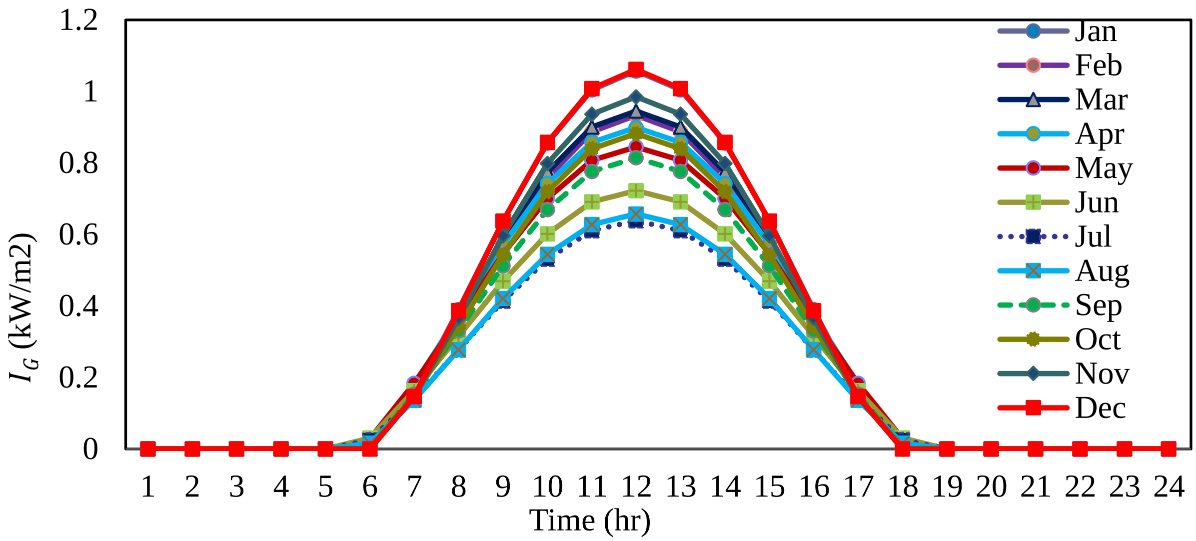

Figure 4.4: Monthly average hourly global radiation on horizontal surface.

4.6.2. Diffuse Hourly Solar Radiation Estimation

Prediction of monthly average hourly diffuse radiation on a horizontal surface (I_D) (Tiwari *et al*, 2016).

$$I_D = \frac{H_D\pi}{24}\frac{\cos\omega - \cos\omega_{ss}}{\sin\omega_{ss} - \frac{\pi\omega_{ss}\cos\omega_{ss}}{180}} \tag{4.17}$$

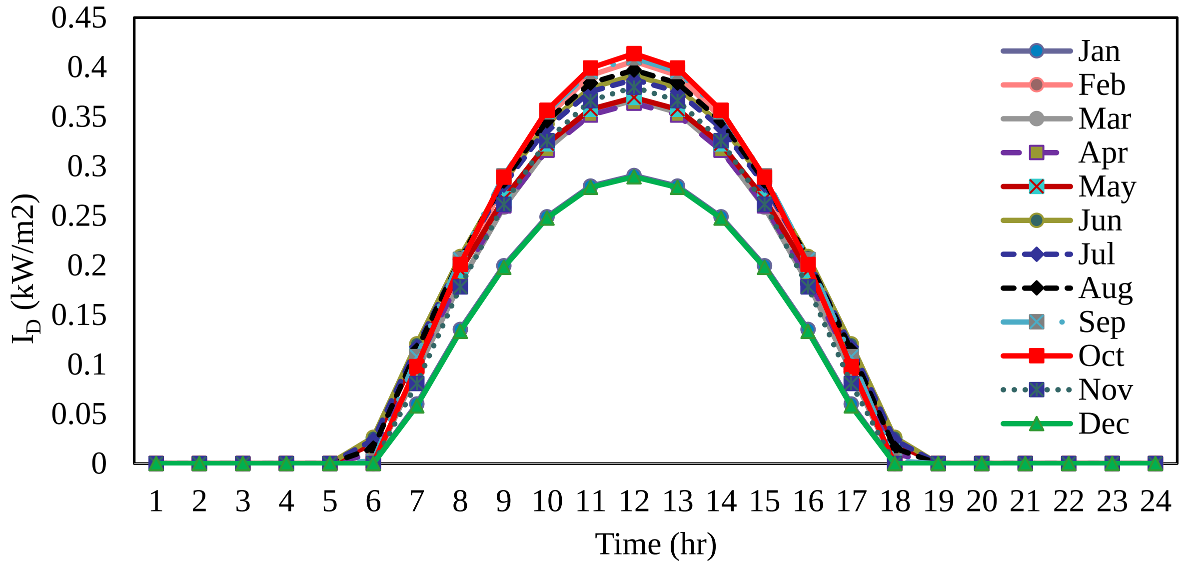

Figure 4.5: Monthly average hourly diffuse radiation on horizontal surface.

4.6.3. Beam Hourly Solar Radiation Estimation

Estimation of monthly average hourly beam radiation on a horizontal surface (I_B)

$$I_B = I_G - I_D \tag{4.18}$$

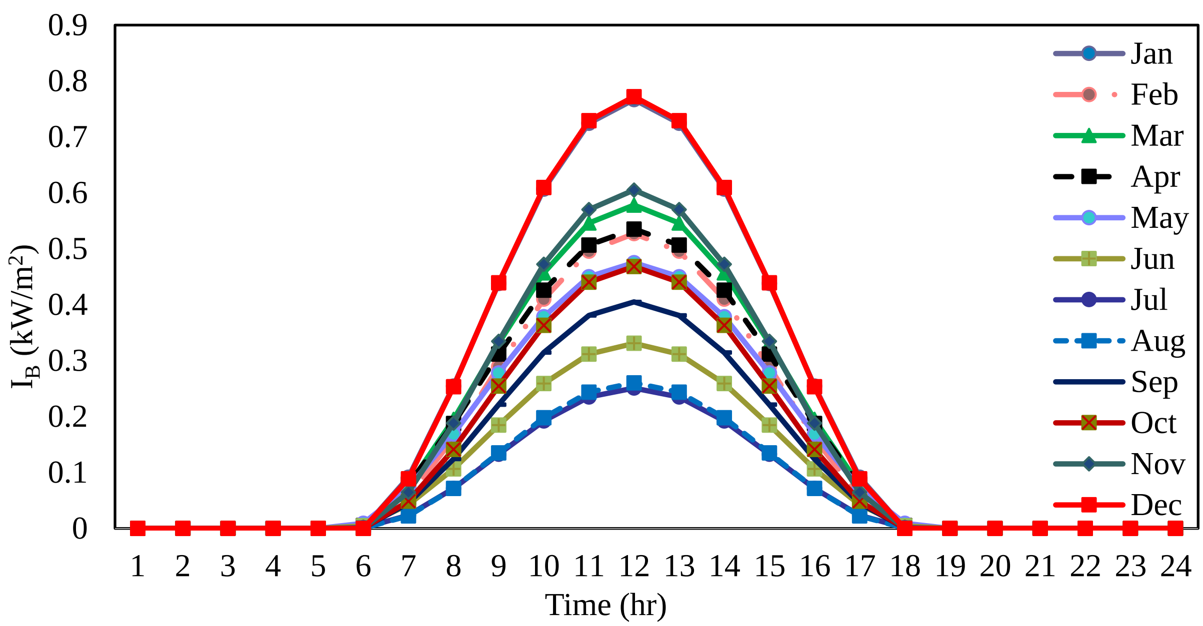

Figure 4.6: Monthly average hourly beam radiation on horizontal surface.

4.7. Meteorological Data of Average Ambient Temperature and Wind Speed for Debre Birhan Town

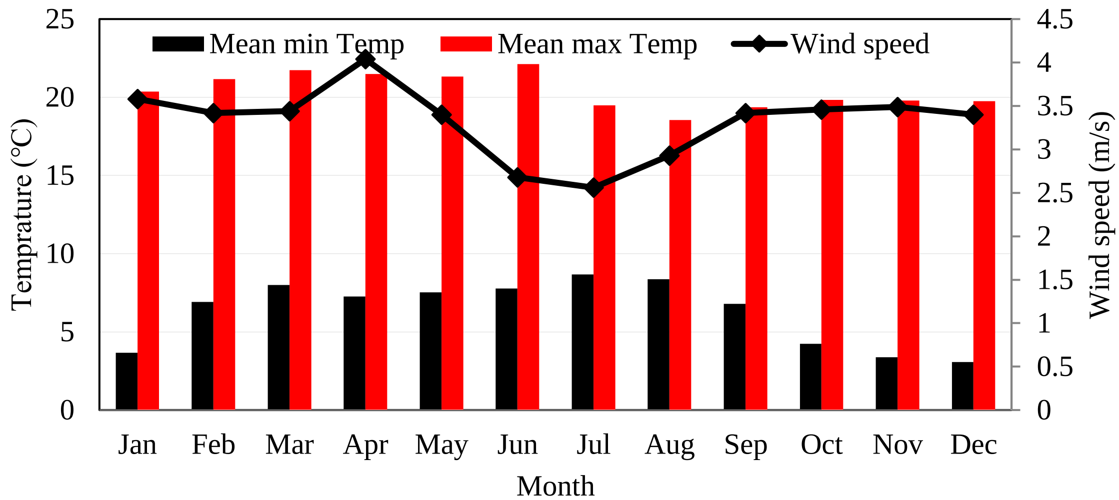

Figure 4.7: Metrological data for temperature and wind speed of Debre Birhan, for an average climatic condition of five years.

4.8. Prediction of Hourly Variation of Ambient Temperature

A sinusoidal variation of the dry bulb temperature through the day and maximum temperature occurs at 15:00 hour sun time is assumed. T(t) represent the temperature variation at any time t, as given by (Jones., 1994).

$$T(t) = \frac{T_{max} + T_{min}}{2} + \frac{T_{max} - T_{min}}{2}\left[sin\left(\frac{\pi(t-9)}{12}\right)\right] \quad (4.19)$$

where, T_{max} = mean daily maximum temperature at 15:00 h sun time

T_{min}= mean daily minimum temperature

t = Time of the day

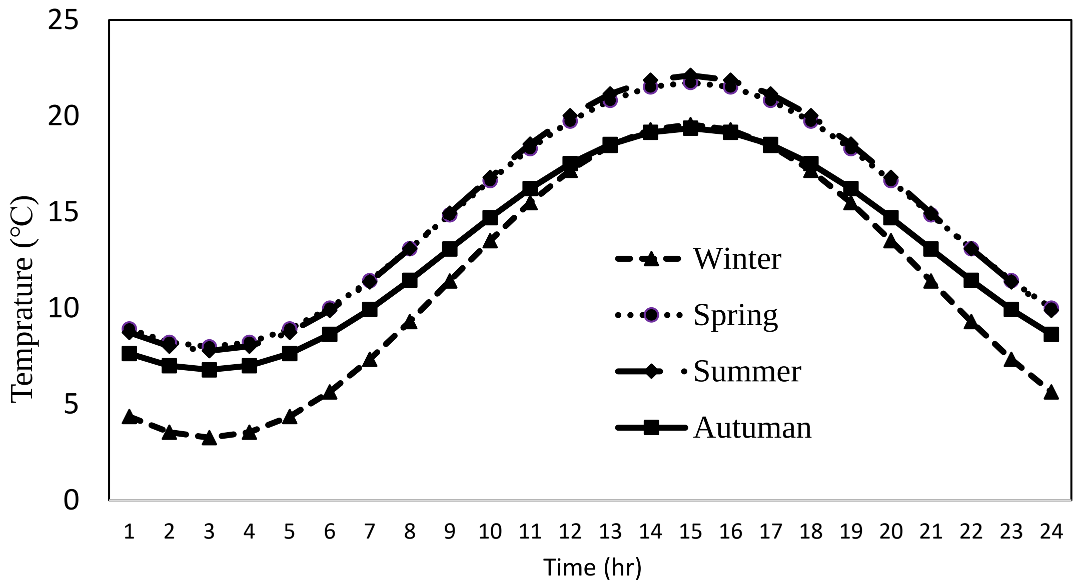

Figure 4.8: Atmospheric temperature variation of Debre Birhan.

4.9. Summary from Solar Energy Potential

Table 4.1: Summary of monthly average daily and hourly solar radiation.

	Global solar radiation (kWh/m^2/day)	Diffuse solar radiation (kWh/m^2/day)	Beam solar radiation (kWh/m^2/day)	Beam total average (kWh/m^2/day)
Monthly average daily solar radiation (kWh/m^2/day)	Maximum average solar radiation			3.4
	7.2	3.1	5.1	
	Minimum average solar radiation			
	4.6	2.1	1.6	
Monthly average hourly solar radiation (kW/m^2)	Maximum average solar radiation			0.5
	1.06	0.41	0.77	
	Minimum average solar radiation			
	0.64	0.28	0.25	

Shown from Table 4.1 monthly average daily solar radiation maximum average daily solar radiation of global, beam and diffuse is obtained on January (7.2 kWh/m^2/day), December (5.1 kWh/m^2/day) and September (3.1 kWh/m^2/day), respectively. And minimum average daily solar radiation of global, beam and diffuse is obtained on July (4.6 kWh/m^2/day), July (1.6 kWh/m^2/day) and December (2.1 kWh/m^2/day), respectively. Total monthly average daily global, beam and diffuse radiation is 6.12, 3.4 and 2.84 kWh/m^2/day, respectively. From monthly average hourly solar radiation analysis of maximum global, beam and diffuse radiation is obtained on December (1.06 kW/m^2), December (0.77 kW/m^2) and October (0.41 kW/m^2), respectively. And monthly average hourly solar radiation analysis of minimum global, beam and diffuse radiation is obtained on July (0.64 kw/m^2), July (0.25 kW/m^2) and December (0.28kW/m^2), respectively. Total monthly average hourly global, beam and diffuse radiation is 0.87, 0.5 and 0.372 kW/m^2, respectively. The average wind speed for Debre Birhan is predicted as 3.5 m/s.

CHAPTER FIVE

DESIGN AND ANALYSIS OF SOLAR THERMAL AREKE PRODUCTION SYSTEM COMPONENTS

5.1. Introduction

The main components of solar thermal local Areke production system are:

- Distillation column
- Solar receiver
- Dish concentrated solar collector
- Condenser

5.2. Sizing of Distillation column

Distillation pot is a type of distillation apparatus or still used to distill alcoholic spirits. During distillation, the alcohol vapor travels up the swan neck at the top of the pot still and down the lyne arm, after which it travels through the condenser, where is cooled to yield a distillate with a higher concentration (40-60%) of alcohol than the original liquid (Connor, 2015). The Difdif is heated by the hot spiral coil that contain steam coming from the receiver. The temperature of Difdif rise for some extent and vaporization of ethanol occur. And the water vapor coming from the receiver change its state into liquid. As reviewed on the literature the volume of Difdif required for local Areke distillation is 8-12 liter (Adane, 2015). For this study the amount of Difdif taken for analysis is the average (10 liters).

To determine the size of distillation pot heat loss must be considered. This suggests height to diameter ration optimization should be done to decrease losses from the distillation pot to improve overall distillation time of the system. Proper set of the distillation pot on the surface and obtimum heat loss obtained for (H/D=1.45) (Rajput, 2012).

Volume of cylindrical distillation pot is determined by:

$$V = \frac{\pi D^2}{4} \cdot H \tag{5.1}$$

where: D- is diameter of the cylindrical pot

H- is the height of cylindrical pot

Diameter of the distillation pot is determined by rearranging the volume formula

$$\frac{\pi D^2}{4} \cdot H = 0.01$$

$$D = \sqrt[3]{\frac{0.01 * 4}{\pi * 1.45}}$$

$$= 0.21m$$

The height of distillation pot is determined as:

$$H = 1.45D = 0.31m$$

The coil length inside the distillation pot is determined by:

$$L_c = N\sqrt{(2\pi R_c)^2 + p} \tag{5.2}$$

where: N −number of turns of helical coil

R_c −radius of helical coil

p − pitch length of the coil

$$L_c = 6\sqrt{(2\pi * 0.08)^2 + 0.05} = 3.31m \tag{5.3}$$

The exchange surface area is determined (Giacomo and Roberto, 2015):

$$A = \pi D_c L_c \tag{5.4}$$

$$= \pi * 0.16 * 3.31 = 1.66\ m^2$$

Shell length is given by (Giacomo and Roberto 2015):

$$L_s = p.N \tag{5.5}$$

$$= 0.05 * 6 = 0.3m$$

Amount of sensible heat required to boil the Difdif is given by (Adane, 2015):

$$Q_d = mC_p\Delta T \tag{5.6}$$

where:

Q_d −heat required to boil the Difdif

m −mass of Difdif

C_p −Specific heat capacity of Difdif

ΔT −temprature difference of the Difdif

From local alcohol preparation, for 20 kg of corn meal, 12 kg of bikil, 2 kg of ground gesho leave and 5-liter water for tinsis. Additional 80 liter of water was added to make a mixture called didfdif from this mixture 17 liter of Areke was produced (Adane, 2015).

Depend on the above data it is possible to determine the amount of Difdif as follow:

The total mass of Difdif (m_d)is:

$$m_d = m_g + m_c + m_b + m_w = 119\text{kg} \tag{5.7}$$

where:

m_g −mass of ground gesho

m_c −mass of corn meal

m_b −mass of bikil

m_w −mass of water

Total volume of the Difdif calculated by the formula (Alem, 2011):

$$V_d = \frac{m_g}{\rho_g} + \frac{m_c}{\rho_c} + \frac{m_b}{\rho_b} + \frac{m_w}{\rho_w} \tag{5.8}$$

$$= \frac{2}{769} + \frac{20}{481} + \frac{12}{673} + \frac{85}{997}$$

$$= 0.148m^3 = 148L$$

In 148 liters of Difdif 57.4% is water and 42.6% is (mixture of corn meal, gesho and bikil) (Adane, 2015).

The volume each ingredient in 148L is given by dividing the mass of ingredients by its density:

$$V_g = 3L$$

$$V_c = 42L$$

$$V_b = 18L$$

$$V_w = 85L$$

The volume each ingredient in one liter of Difdif is given as:

$$V_g = 0.02L$$

$$V_c = 0.284L$$

$$V_b = 0.122L$$

$$V_w = 0.574L$$

Volume of each ingredient in 10L of Difdif is given as:

$$V_g = 0.2L$$

$$V_c = 2.84L$$

$$V_b = 1.22L$$

$$V_w = 5.74L$$

Mass of each ingredient in 10L of Difdif is (Alem, 2011):

$$m_i = \rho_i \times V_i \tag{5.9}$$

where, m_i mass of ingredient, ρ_i density of ingredient and V_i volume of ingredient.

Therefore;

$$m_g = 0.2L \times \frac{0.769kg}{L} = 0.1538\ kg$$

$$m_c = 2.84L \times \frac{0.481kg}{L} = 1.366\ kg$$

$$m_b = 1.22L \times \frac{0.673kg}{L} = 0.821\ kg$$

$$m_w = 5.74L \times \frac{0.997kg}{L} = 5.723\ kg$$

Thus, total mass of Difdif for this study is 8.1 kg.

Specific heat capacity of Difdif is calculated as follow (Shewangizaw, 2016). The specific heat capacity of each ingredient listed in (APPENDIX C):

$$\mathrm{C_{p,d}} = \frac{\mathrm{m_g C_{p,g} + m_c C_{p,c} + m_b C_{p,b} + m_w C_{p,w}}}{\mathrm{m_d}} \tag{5.10}$$

where:

$C_{p,g}$ −specific heat capacity of gesho (kJ/kgK).

$C_{p,c}$ −specific heat capacity of corn meal (kJ/kgK).

$C_{p,b}$ −specific heat capacity of bikil (kJ/kgK).

$C_{p,w}$ −specific heat capacity of water (kJ/kgK).

$$C_{p,d} = \frac{2 \times 1.8 + 20 \times 1.54 + 12 \times 1.674 + 85 \times 4.184}{119} = 3.45kJ/kgK$$

Amount of latent heat required to change liquid state of alcohol into vapor state (Adane, 2015):

$$\mathrm{Q_{Latent} = m_v L_v} \tag{5.11}$$

where, m_v is mass of alcohol vapor (ethanol) and L_v is latent heat of evaporation of ethanol (846kJ/kg).

Amount of sensible heat required to boil water is given by (Adane, 2015):

$$\mathrm{Q_w = mC_P \Delta T} \tag{5.12}$$

Amount of latent heat required to change liquid state of water in to vapor state is given by (Adane, 2015):

$$Q_{latent} = m_{v,w}L_{v,w} \tag{5.13}$$

where, $m_{v,w}$ is mass of water vapor and $L_{v,w}$ is latent heat evaporation of water (2260kJ/kg).

5.3. Heat Loss over the Distillation column

Heat loss from distillation pot is generally described in terms of a material constant, the thickness of the material and its cross-section area. Heat loss from the distillation column is through conduction, convection and radiation given by (Tanaka, 2016).

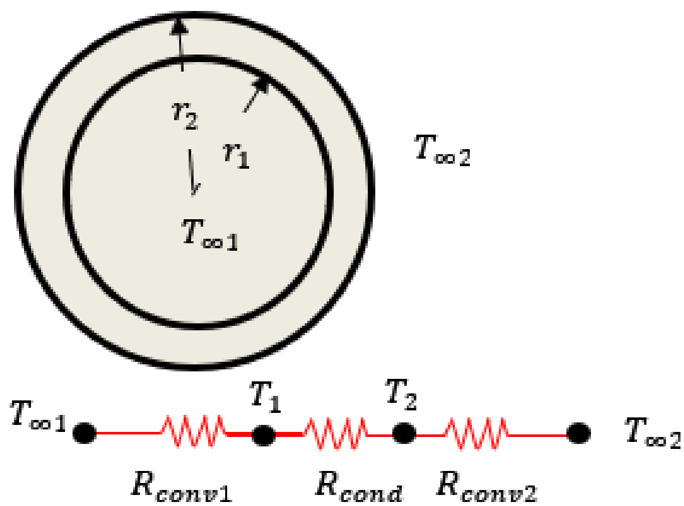

Figure 5.1: Thermal resistance network for distillation column.

5.3.1 Heat Loss at The Side Wall of The Distillation Column

Heat loss over the vertical wall side of the distillation column is given by

$$Q_{loss} = \frac{2\pi L(T - T_{amb})}{\frac{ln\left(\frac{r_2}{r_1}\right)}{k} + \frac{1}{h_i r_1} + \frac{1}{h_o r_2}} + 2\pi r_2 L\varepsilon\sigma({T_{sur}}^4 - {T^4}_{amb}) \tag{5.14}$$

where:

$k -$ Thermal conductivity of clay (W/Mk).

$A_r -$ Surface area of the distillator (m^2).

$T -$ Inside temperature of distillator (K).

$T_{sur} -$ Outer surface temperature of the distillator (K).

$r_1 -$ inner radius of distillator (m).

$r_2 -$ outer radius of distillator (m).

$T_{amb} -$ ambient temperature (K).

5.3.2 Heat Loss on The Upper Side of Distillation Column

The upper side of the distillation column has half spherical shape, and the equation given as (Tanaka, 2016):

$$\mathrm{Q_{loss}} = \frac{2\pi(\mathrm{T} - \mathrm{T_{amb}})}{\frac{1}{\mathrm{h_i r_1^2}} + \frac{\mathrm{r_2} - \mathrm{r_1}}{\mathrm{k_1 r_1 r_2}} + \frac{1}{\mathrm{h_o r_2^2}}} + 2\pi \mathrm{r_2^2} \varepsilon \sigma ({\mathrm{T_{sur}}}^4 - \mathrm{T^4}_{\mathrm{amb}}) \tag{5.15}$$

where:

$k -$ Thermal conductivity of clay (W/mK).

$r_1 -$ inner radius of the sphere (m).

$A_r -$ Surface area of the sphere (m^2).

$r_2 -$ outer radius of the sphere (m).

$T -$ Inside temperature of sphere (K).

$T_{amb} -$ ambient temperature (K).

$T_{sur} -$ Outer surface temperature of the sphere (K).

5.4 Solar Receiver Design

The solar receiver with outside diameter (D_0), internal diameter (D_i), and height (h) is made from copper for good thermal conductivity. The performance of the concentrator decreases due to shading of the receiver, to overcome this effect the diameter of the receiver must be less than or equal to the height (Vashi *et al*., 2015). If the receiver area is large, the losses will increase. On the other hand, if the receiver area is small, the value of heat loss will decrease (Rosnani *et al.,* 2015). To minimize vertical loss the length of the receiver has to be ranged from 1.1*D* up to 2.5*D* (Evangelos *et al*., 2019). For this study the receiver height (H) is made to be equal to the average of the given diameter range.

Table 5.1: Dimensional specification for the cylindrical shape of receiver (Evangelos *et al*., 2019).

Receiver parameters	Values (m)
Outer diameter	0.15
Thickness	0.012
Height	0.27

Table 5.2: Dimensional specification of conical shape receiver (Evangelos *et al*., 2019).

Receiver parameters	Values (m)
Outer diameter (bottom)	0.15
Outer diameter (top)	0.075
Thickness	0.004

Heat transfer over the solar receiver is enhanced by increasing the heat transfer area of the absorber that exposed to the solar radiation coming from the reflector or solar dish concentrator (Yen *et al.*, 2012).

$$\dot{Q} = UA\Delta T \tag{5.16}$$

where:

$\dot{Q}$ − Heat transfer rate

U − Over all heat transfer coefficient

A − Heat transfer area

ΔT −Temprature difference

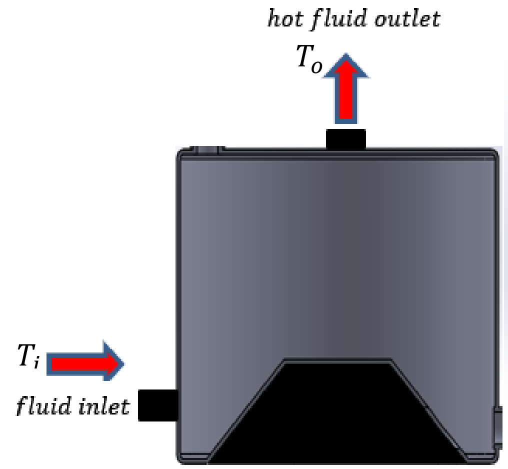

Figure 5.2: Truncated cone shape at the bottom of the receiver.

Figure (5.2) indicates the combined shape the cylindrical and the truncated cone at the bottom surface, since solar radiation reflected from the reflector strikes on the flat surface of the truncated cone surface uniform distribution of the heat over surface is obtained, to simplify the design analysis, it must be done separately as follow:

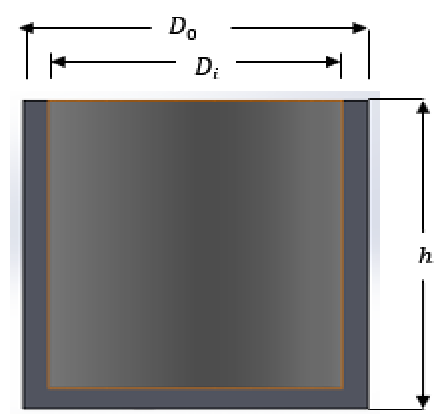

Figure 5.3: Cylindrical part of the receiver.

From the cylindrical part the volume of the cylinder is (Ibrahim, 2013):

$$V_{cylinder} = \frac{\pi D_i^2}{4} \times h \tag{5.17}$$

$$= \frac{\pi \times 0.138^2}{4} \times 0.27$$

$$= 0.003m^3$$

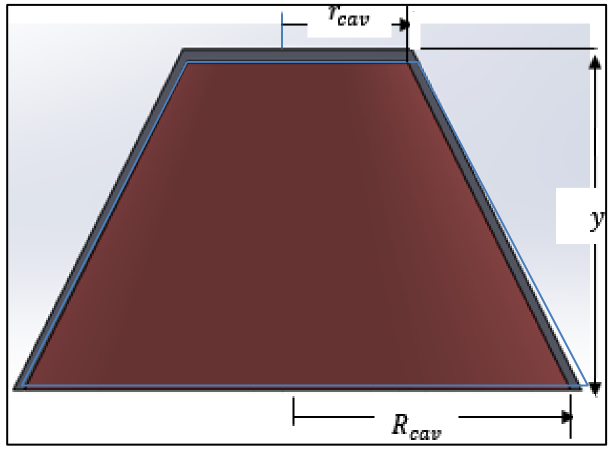

Figure 5.4: Geometry of the truncated cone.

Area of the cavity that have conical shape in which solar radiation concentrated is given by (Li *et al.*, 2015):

$$A_{cav} = \pi(r_{cav}^2 + R_{cav}^2) + \pi(r_{cav} + R_{cav})\sqrt{y^2 + [R_{cav} - r_{cav}]^2} \tag{5.18}$$

To get the height of the cone it is necessary to know the inclined angle

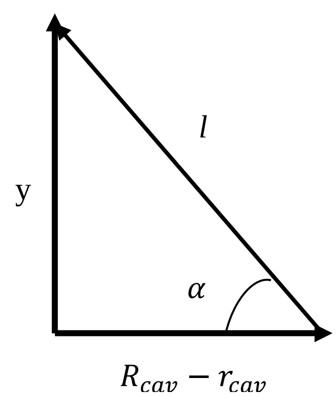

From the right-angle triangle given above it is possible to determine the angle of the cone using Pythagoras theorem:

$$y = l \, sin \, \alpha \tag{5.19}$$

$$= \frac{R_{cav} - r_{cav}}{\cos \alpha} \times \sin \alpha$$

$$= (R_{cav} - r_{cav}) \tan \alpha$$

$$\alpha = tan^{-1}\left(\frac{\mathrm{y}}{\mathrm{R_{cav}} - \mathrm{r_{cav}}}\right) \tag{5.20}$$

$$= \tan^{-1}\left(\frac{0.075}{0.035}\right)$$

$$= 63.4°$$

Therefore, the area of the cavity gives as:

$$A_{cav} = \pi(0.035^2 + 0.075^2) + \pi(0.035 + 0.075)\sqrt{0.075^2 + [0.075 - 0.035]^2}$$

$$= 0.05m^2$$

The volume of cavity is determined as (Li *et al.*, 2015):

$$\mathrm{V_{cav}} = \frac{\pi \times \mathrm{y}}{3}(\mathrm{r_{cav}^2} + \mathrm{r_{cav}R_{cav}} + \mathrm{R_{cav}^2}) \tag{5.21}$$

where:

r_{cav} − is the smallest radius of the cavity

R_{cav} −is the largest radius of the cavity

y −is the height of the cavity

$$V_{cav} = \frac{\pi \times 0.075}{3}(0.035^2 + 0.035 \times 0.075 + 0.075^2)$$

$$= 0.0008m^3$$

This is the volume of the cavity so; it must be subtracted from the original volume and the remaining is the receiver volume.

$$\mathrm{V_{reciver}} = \mathrm{V_{cylinder}} - \mathrm{V_{cav}} \tag{5.22}$$

$$= 0.003 - 0.0008 = 0.002m^3$$

Thus, the solar receiver contains 2 liters of working fluid.

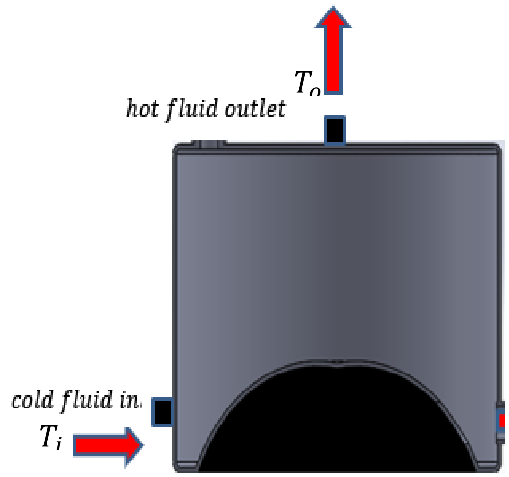

Figure 5.5: Dome shaped bottom surface of the receiver.

Figure (5.5) indicates the cylindrical and bottom spherical shaper of the receiver. For the cylindrical, the analysis is done on equation (5.17). Let as calculate area for the spherical shape then compare the area of the truncated cone with the spherical and take the maximum as heat transfer area for the solar receiver.

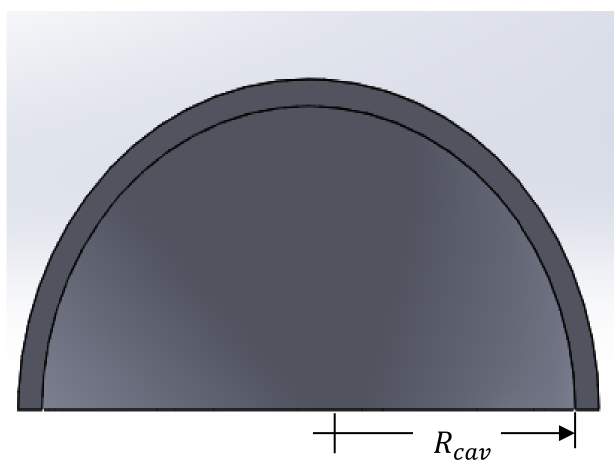

Figure 5.6: Geometry of sphere.

From Figure (5.6) let as determine the area of the sphere as follow (Amos *et al*., 2015):

$$\mathrm{A_{sphere}} = 2\pi \mathrm{R_{cav}^2} \tag{5.23}$$

$$= 2 \times \pi \times 0.075^2$$

$$= 0.035m^2$$

Total area of the receiver is given as (Amos *et al*., 2015):

$$A_{r,surface} = \pi D_0 h + A_{cav} \quad (5.24)$$

$$= \pi \times 0.15 \times 0.27 + 0.05$$

$$= 0.18\, m^2$$

5.5 Comparison of Heat Transfer Area

Table 5.3: Optimized area for different shape of absorber.

Shape of bottom surface of the receiver (absorber)	Aperture diameter of the absorber (m)	Area (m^2)
Flat	0.15	0.01767
Sphere	0.15	0.0353
Truncated cone	0.15	0.05

From the heat transfer area analysis done for the three geometrical shapes, the surface area of truncated cone is greater than the surface area of sphere(dome) and flat surface Table 5.3. Therefore, the heat transfer rate is maximum for truncated conical shape at the bottom of the receiver.

5.6 Energy Analysis of receiver

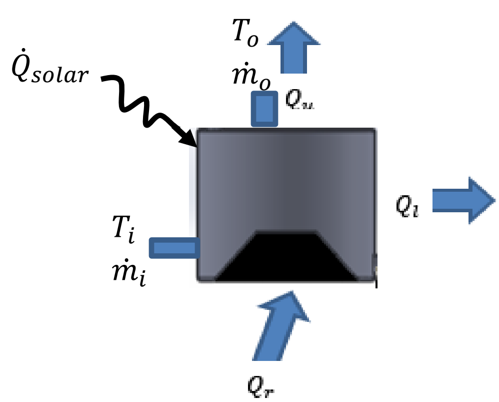

Figure 5.7: Energy analysis of solar receiver.

The energy balance equation for the receiver is given by (Pavlovic *et al*., 2016):

$$\dot{Q}_u = \dot{m}C_p(T_{out} - T_{in}) \tag{5.25}$$

where:

$\dot{m}$ − is mass flow rate of the fluid inside the receiver (kg/s).

C_p − specific heat capacity of working fluid (kJ/kgK).

$T_{out} - T_{in}$ = temperature difference of the working fluid (K).

And the total receiver efficiency is given by (Alexander *et al*., 2016):

$$\eta_r = \frac{\dot{Q}_u}{\dot{Q}_r} \tag{5.26}$$

The working fluid taken for this study is water because it has high specific heat capacity and easily available without any cost. Let as determine the heat required to boil and vaporize this working fluid in the receiver.

Sensible heat energy required to reach the water to its boiling point (Ibrahim, 2013):

$$\dot{Q} = \dot{m}C_p\Delta T \tag{5.27}$$

where:

$\dot{m}$ −mass flow rate of water (kg/s).

C_p −specific heat capacity of water (kJ/kgK).

ΔT −temprature difference between inlet and outlet of the receiver (K).

Latent heat energy required to change liquid state of water into vapor state (Ibrahim, 2013):

$$Q = m_v L_v \tag{5.28}$$

where, m_v is mass of vaporization of water and L_v latent heat of vaporization of water (2260 kJ/kg).

5.7 Heat Loss Analysis over the Receiver

The material used for solar receiver is aluminum sheet and the isolating material is polystyrene foam.

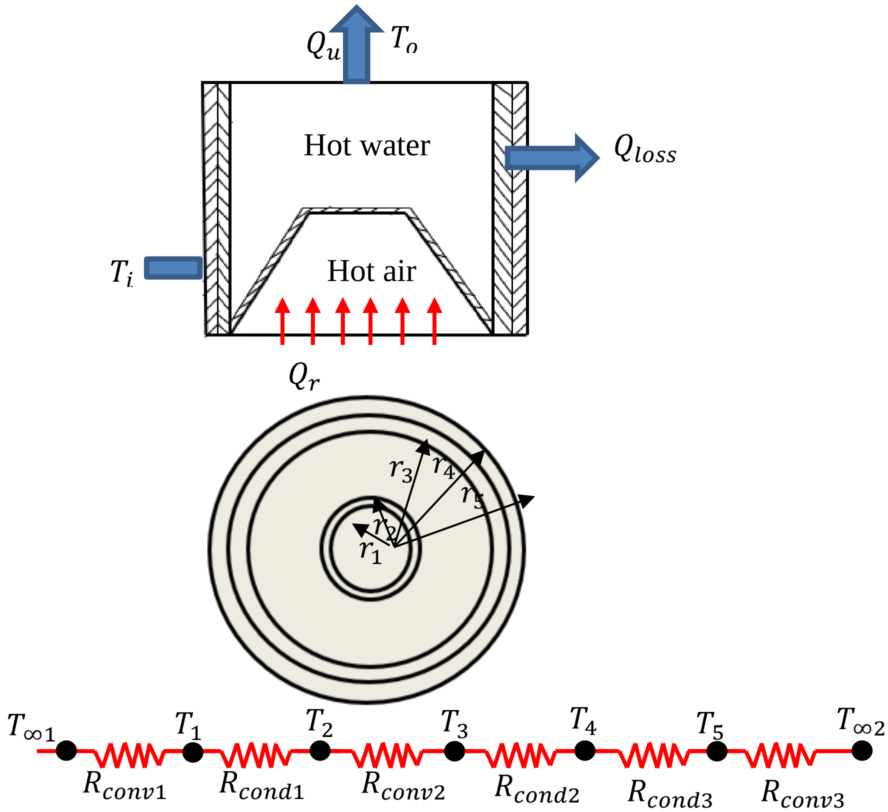

Figure 5.8: Thermal resistance network for solar receiver.

5.7.1 Convection Heat Loss

Convection is a highly nonlinear and complex problem, especially when external effects like wind are considered. As it is crucial to have an estimate for the convective losses, several studies dealt with an analysis of the convective losses of receivers. Head on wind flowing into the receiver cavity will be responsible for natural convection loss inside the cavity (Seyed, 2017).

$$Q_{conv} = h_{conv} A_r (T - T_{amb}) \tag{5.29}$$

where: h_{conv} − Convection heat transfer coefficient (W/m²K).

A_r − Surface area of receiver (m²).

T − Temperature on the outer surface of the insulator (K).

T_{amb} − Ambient temperature (K).

5.7.2 Conduction Heat Loss

Conductive heat loss from receiver is generally described in terms of a material constant, the thickness of the material and its cross-section area. The conduction heat loss in the cavity is transferred through the walls of the cavity (Vanita, 2015).

$$Q_{cond} = \frac{A_r(T - T_{out})}{\frac{ln\left(\frac{r_2}{r_1}\right)}{k_A} + \frac{ln\left(\frac{r_4}{r_3}\right)}{k_B} + \frac{ln\left(\frac{r_5}{r_4}\right)}{k_C}} \quad (5.30)$$

where:

$k_{A,B}$ − Thermal conductivity of receiver metal (W/mK). r_1 − inner radius of receiver (m).

k_C − Thermal conductivity of insulator (W/mK). r_2 − outer radius of receiver (m).

A_r − Surface area of the receiver (m2). r_3 − outer radius of insulator (m).

T − Inside temperature of receiver (K).

T_{out} − Outer surface temperature of the insulator (K).

5.7.3 Radiation Heat Loss

Radiative heat loss through the receiver aperture is described by operating temperatures only slightly above ambient, and becomes dominant for collectors operating at higher temperatures. The rate of radiation heat loss is proportional to the emittance of the surface and the difference in temperature to the fourth power (Vanita 2015).

$$Q_{rad} = \varepsilon A_r \sigma (T^4 - T^4{}_{amb}) \quad (5.31)$$

where:

ε − Emissivity factor

σ − Stefan-Boltzmann Constant (W/m^{2}K^4)

T − Outer surface temperature of insulator (K).

T_{amb} − Ambient temperature (K).

5.8 Theoretical Analysis of Solar Dish Concentrator

Based on the energy balance size of the dish concentrator could be determined.

5.9 Sizing of Dish Concentrator

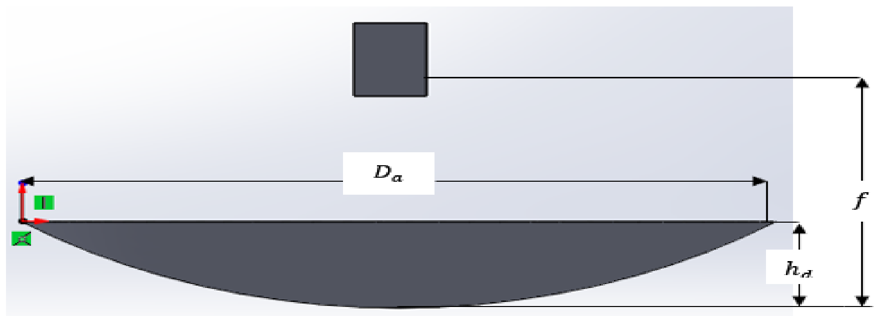

Figure 5.9: Geometry of dish concentrator.

Heat required to boil Difdif is less than heat required to boil water for equal volume of Difdif and water. Because, specific heat capacity of water is maximum. Using energy balance equation, it is possible to determine the size of the collector that rise water temperature to 100 ℃ and Difdif temperature to 78 ℃ from ambient temperature, respectively. From solar energy potential, the average beam solar radiation calculated for Debre Birhan is 500 W/m^2. For design simplicity losses from each component neglected and considering boiling point at sea level.

$$\mathrm{Q_{Difdif}} = \mathrm{Q_u} = \mathrm{Q_r} \tag{5.32}$$

$$\frac{\mathrm{m_d C_{p,d}(T_{df} - T_{di})}}{\mathrm{t_d}} = \frac{\mathrm{m_w C_{p,w}(T_{wf} - T_{wi})}}{\mathrm{t_w}} = \eta_o * \mathrm{I_b} * \mathrm{A_a} \tag{5.33}$$

where: m_d −mass of Difdif (kg). m_w −mass of water (kg).

$C_{p,d}$ − specific heat capacity of difdid (kJ/kgK). $C_{p,w}$ −specific heat of water (kJ/kgK).

T_{df} − final temperature of Difdif (K). T_{wf} −final temperature of water (K).

T_{di} − initial temperature of Difdif (K). T_{wi} − initial temperature of water (K).

t_d − time taken to rise temperature of Difdif (sec). $\mathrm{I_b}$ −beam solar radiation (W/m^2).

t_w −time taken to rise temperature of water (K). A_a −appparture area of dish (m^2).

Substituting the values in eq. (5.33).

$$\frac{8.1 * 3450(78-25)}{t_d} = \frac{2 * 4180(100-25)}{t_w} = 0.5 * 500 * A_a$$

$$\frac{1481085}{t_d} = \frac{815100}{t_w} = 250A_a \tag{5.34}$$

From equation (5.34) the aperture area of the collector is inversely proportional to the time taken to heat Difdif and water. Since one of the objectives this study is reducing the distillation time and increasing the production. Taking the diameter of aperture of the collector as 2m the time taken to rise the temperature of Difdif and water is 32 and 13.3 minutes respectively. But this result is without any loss. From the theoretical analysis aperture area of 3.14 m^2 dish concentrator collector heats up 2 L of water inside the solar receiver, which put on the focal point takes 13.3 minutes only.

The distance from the aperture to the vertex (h) can be calculated in terms of the focal length (f) and the aperture diameter (D_a), as the following expression:

$$h = \frac{D_a^2}{16f} \tag{5.35a}$$

$$\frac{f}{D_a} = \frac{1}{4\,tan(\psi_{rim}/2)} \tag{5.36}$$

In a same manner, the rim angle ψ_{rim} can be expressed as:

$$\psi_{rim} = tan^{-1}\left(\frac{1}{\frac{D_a}{8h} - \frac{2h}{D_a}}\right) \tag{5.37}$$

The concentrator is the component of the collector system which directs solar radiation onto the receiver surface. Receiver is the part of the collector system where incident radiation reflected from the concentrator is absorbed and useful energy is transferred to the working fluid. Radiation absorbed by the receiver is dependent on the concentration ratio of the collector. Increasing ratios mean increasing temperatures at which energy can be delivered and increasing requirements for precision in optical quality and positioning of the optical system.

Table 5.4: Design parameters of dish concentrator.

Parameters	Symbol	Value
Diameter of opening parabola	D_a	2m
Aperture area	A_a	$3.14m^2$
Area of receiver	A_r	$0.02m^2$
Depth of the parabola	h	0.25m
Focal distance	f	1m
Rim angle	ψ_{rim}	83.52°
Concentration ratio	C	177

5.9.1 Operating Parameters

Important measured parameters needed to be known to assess the performance of PDSC include solar insolation (DNI) incident on the collector, wind velocity, ambient temperature, inlet and outlet temperature of the fluid into and from the receiver, respectively, temperature inside the receiver cavity, angle of inclination of the receiver from the horizontal.

Direct Normal Irradiance (DNI): Is solar irradiance that comes in a direct line from the sun. On clear sky conditions, the DNI represents more than 80% of the solar energy reaching the earth's surface. Meanwhile, some of the solar radiation reaching the earth's surface is absorbed and scattered. The solar radiation is absorbed by ozone, oxygen and water vapor. Weather conditions such as storms and clouds become the primary factor that changed solar radiation to the surface. In which, on a cloudy day the direct beam radiation is almost zero (Rosnani *et al*., 2015).

Ambient temperature: The temperature of the surroundings (same as room temperature indoors).

Atmospheric pressure: The boiling point of any given liquid depends on atmospheric pressure of any given location. Since the atmospheric pressure of any location depends on the altitude of given place the pressure at sea level must be corrected to the required altitude. For altitudes between 0 and 10,973m the standard atmosphere is expressed by (NAG, 2006):

$$\mathrm{P} = \mathrm{P_0}(1 - 2.25 \times 10^{-5}\mathrm{Z})^{5.26} \tag{5.38}$$

where: $P_0 -$ standard atmospheric pressure at sea level

$Z -$ altitude, (Debre Birhan, 2750m)

$T_0 -$ standard temperature (288.15)

Using eq. (5.37) the atmospheric pressure at Debre Birhan is obtained as 72.2 kPa.

5.9.2 Derived / Calculated Parameters

Derived or calculated parameters include Concentration Ratio, Optical Efficiency and Thermal Efficiency, explained as follows:

Aperture area (A_a): The opening area of the concentrator at which solar incident from the sun is intercepted.

Absorber area (A_{abs}): The total area of surface of the absorber that receives the incoming reflected radiation from concentrator.

Concentration Ratio (C): The area of the collector aperture (A_a) divided by the surface area of the receiver (A_r) (Ibrahim, 2013).

$$\mathrm{C} = \frac{\mathrm{A_a}}{\mathrm{A_r}} \tag{5.39}$$

where:

$c -$ concentration ratio

A_a – aperture area of the concentrator (m^2).

$A_{abs} -$ area of receiver/absorber (m^2).

5.10 Energy Analysis for Dish Concentrator

Fig.5.10 represents schematic diagram of the heat flow though the dish concentrator collector. The plot is essential to describe step-by-step heat flow equation of dish concentrator collector. Under steady state conditions, the useful heat delivered by a solar collector system is equal to the energy absorbed by the heat transfer fluid, which is determined by the radiant solar energy falling on the receiver minus the direct or indirect heat losses from the receiver to the surroundings (Vanita *et al*., 2015).

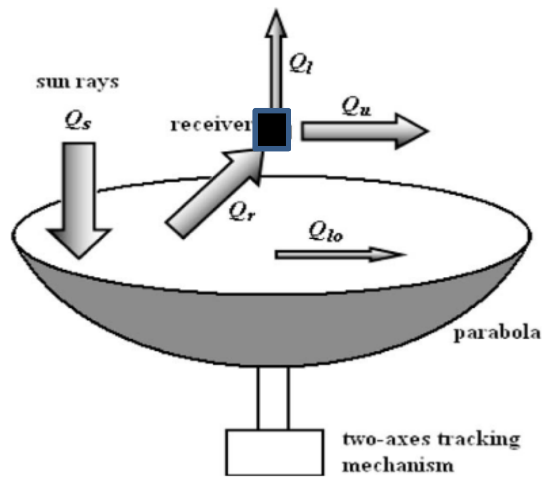

Figure 5.10: Dish concentrator 3D model.

$$Q_u = Q_r - Q_l \tag{5.40}$$

where:

$Q_r -$ energy reaches on the plane surface of the absorber (W).

$Q_l -$energy loss from the absorber (W).

The radiation falling on the receiver Q_r is a function of the optical efficiency η_o, which is defined as the ratio of the energy falling on the receiver to the energy incident on the concentrator's aperture. And the receiver efficiency η_r is defined as the ratio of the useful energy delivered to the energy falling on the receiver (Kalogirou, 2004). Considering that the dish concentrator has an aperture area (A_a) and that it receives solar radiation at the rate (Q_s) from the sun and the net solar heat transferred (Q_s) is proportional to aperture area A_a and the direct normal insolation

(DNI) per unit of collector area I_b, which varies with geographical position on the earth, the orientation of the dish concentrator, meteorological conditions and the time of day (Vanita, 2015).

$$Q_s = I_b A_a \tag{5.41}$$

where:

Q_s −energy captured by the reflector (W).

I_b − beam Solar radiation (W/m^2).

A_a − Aperture area of collector (m^2).

The generalized thermal analysis of a concentrating collector is similar to that of a flat plate collector. Although not necessary, it is convenient to derive appropriate expressions for the collector efficiency factor *F'*, the loss coefficient U_L, and the collector heat removal factor F_R. with F_R and F_R known, the collector useful gain can be calculated from an expression that is similar to that for a flat-plate collector. One significant difference between a concentrating collector and a flat-plate collector is the high temperatures encountered in the concentrating collector. High temperatures mean that thermal radiation is important, leading to the loss coefficient being temperature dependent. The loss and loss coefficient considering convection and radiation from the surface is given by (Duffie & Beckman, 2013).

$$Q_{loss} = A_r U_L (T_r - T_a) \tag{5.42}$$

where, A_r − receiver area (m^2)

U_L − loss coefficient of collector (W/m^{2}K)

T_r − receiver temperature (K)

T_a − ambient temperature (K)

the Reynolds number for an air temperature that is the average of the cover and ambient temperature given by (Duffie & Beckman, 2013).

$$R_e = \frac{\rho V D}{\mu} = \frac{1.2 * 3.5 * 0.075}{1.8 * 10^{-5}} = 17500 \qquad (5.43)$$

where V is the approximate wind velocity in Debre Birhan and v is the kinematic viscosity of air. The wind heat transfer coefficient is then found from Equation (Duffie & Beckman, 2013).

$$N_u = \frac{h_w D}{k} = 0.3(R_e)^{0.6} = 105 \qquad (5.44)$$

where, $N_u -$ Nusselt number

$\rho -$ density of air (kg/m^3)

$\mu -$ dynamic viscosity of air (N.s/m^2)

From the aforementioned, we have that $N_u = 105$, which is why the convection coefficient would be equal to (Jorge *et al*., 2013).

$$h_w = \frac{N_u k}{D} = 28.1\ W/m^2K \qquad (5.45)$$

The radiation coefficient is given by (Jorge *et al*., 2013).

$$h_r = 4\sigma\varepsilon T^3 = 2.84\ W/m^2K \qquad (5.46)$$

Loss coefficient of collector is given by (Jorge *et al*., 2013).

$$U_L = \left(\frac{1}{h_w + h_r}\right)^{-1} = 30.9\ W/m^2K \qquad (5.47)$$

Collector efficiency factor is given by (Duffie & Beckman, 2013).

$$F' = \frac{1/U_L}{\frac{1}{U_L} + \frac{D_0}{D_i h_i} + \left[\frac{D_0}{2k}\ln\left(\frac{D_0}{D_i}\right)\right]} \qquad (5.48)$$

where D_i and D_0 are the inside and outside tube diameters, $h_i$is the heat transfer coefficient inside the receiver, and k is the thermal conductivity of the receiver. The useful energy gain of collector is expressed in terms of the local receiver temperature and the absorbed solar radiation per unit of aperture area is (Duffie & Beckman, 2013).

$$Q_u = \frac{\dot{m} C_p A_a}{A_r U_l}\left[1 - exp\left(-\frac{A_r U_L F'}{\dot{m} C_p}\right)\right]\left[S - \frac{A_r}{A_a} U_L (T_i - T_a)\right] \tag{5.49}$$

where, $\dot{m}$ − mass flow rate of working fluid (kg/s)

C_p − specific heat capacity of working fluid (kJ/kgK)

A_a − aperture area of collector (m^2)

A_r − receiver area

U_L − loss coefficient of collector

S − absorbed solar radiation

Concentration ratio for the experimental testing is calculated by minimizing the actual size by 2.2, since the size is reduced by the dish concentrator size.

Therefore, the concentration is calculated by the equation (Duffie & Beckman, 2013).

$$C = \frac{A_a}{A_r} = \frac{R^2}{r^2} = \frac{0.9^2}{0.075^2} = 144 \tag{5.50}$$

5.11 Effect of Wind flow over Dish-Receiver System at Different Orientation on Convective Heat Loss

From the literature review, it was shown that the performance of CSP systems utilizing parabolic dishes were sensitive to heat losses from the receiver, particularly at high temperature. In particular, the heat loss from the receiver is affected by the surrounding air movement, and consequently exposure to this results in increased heat loss, and decreased thermal performance (Lupfert *et al*., 2001). For this work, CFD analysis was performed to examine the behavior of wind flow around a parabolic dish and receiver. Design correlations for estimating natural convective heat loss from cavity receivers were usually derived experimentally the equation given as (Robert, 1993).

$$N_u = \frac{hD}{k} \tag{5.51}$$

$$Q_{conv} = hA(T_{cav} - T_a) \tag{5.52}$$

$$R_e = \frac{VD}{v} \tag{5.53}$$

where,

A- exposed surface area of receiver (m^2)

T_{cav}- average temperature (K)

Ta- ambient temperature (K)

v -kinematic viscosity of air (kg/m.s)

N_u − Nusselt's number

V − wind velocity at different dish orientation (m/s)

k − thermal conductivity of air (W/mK)

h −Cconvective heat transfer coefficient of air (W/m^2K)

Convective heat transfer of air calculated as 28.1 W/m^2K. The convective effect also shown on (APPENDIX: G).

5.12 Laws of Thermodynamics

5.12.1 First Law of Thermodynamics

Energy efficiency of the solar dish concentrator collector can be defined as the ratio of the output Energy (gained by solar collector) to the input solar radiation Energy. Energy efficiency is given as (Kalogirou, 2004):

$$\eta_{collector} = \frac{\text{Energy output}}{\text{Energy input}} = \frac{Q_u}{Q_s} \tag{5.54}$$

where:

Q_u − Useful energy transferred (KJ).

$Q_s -$ Solar heat transferred (W).

$Q_l -$ total heat loss rate of the receiver (W).

$T_{wf} -$ final temperature of water (K).

$T_{wi} -$ initial temperature of water (K).

$A_c -$ collector area (m^2).

$$\eta_{distillator} = \frac{\text{Energy output}}{\text{Energy input}} = \frac{\mathrm{Q_{u,d}}}{\mathrm{Q}_i} \tag{5.55}$$

where, $\mathrm{Q_{u,d}} -$ useful energy of Difdif (J)

$\mathrm{Q}_i -$ input energy (J)

Overall efficiency of the system is given by the formula (Kalogirou, 2004):

$$\eta_{overall} = \eta_r \times \eta_d \times \eta_{pipe} \tag{5.56}$$

Optical Efficiency: The optical efficiency η_o depends on the optical properties of the materials involved (e.g. the reflectance of dish and the optical properties of the receiver glazing etc.), the geometry of the collector, and the various imperfections arising from the construction of the collector. It can be analyzed by identification of the different loss mechanisms (Kribus *et al.*, 2006).

The following equation form can be used to perform an approximated optical efficiency analysis;

$$\eta_o = \sigma\tau\alpha\gamma\, cos\, \theta \tag{5.57}$$

where:

$\sigma -$ Reflectivity

$\tau -$ Transmittance

$\alpha -$ Absorptivity

$\gamma -$ Intercept factor

As the solar parabolic dish concentrator maintains its optical axis always pointing directly towards the sun to reflect the beam, which means the incidence angle of solar beam into the dish is zero degree (Palavras, 2006).

$$\eta_o = \sigma\tau\alpha\gamma \tag{5.58}$$

Based on the analysis above, the optical efficiency considering losses can be assumed to be a value between 0.83-0.85 (Shuang *et al.*, 2010).

Production efficiency of the system is given by (Kebede 2018):

$$\eta_p = \frac{Distilled\ Areke\ product}{Input\ Difdif} \tag{5.58a}$$

5.13 Design Analysis of Condenser

The heat exchanger for this study is a condenser that cools vapor or steam by converting it to its liquid form. During distillation of alcohol, alcohol vaporizes at a lower temperature than water, this vapor travels to the condenser and then the condenser helps change the vapor to liquid alcohol. From the literature review the heat exchanger selected for the condensation process of alcohol vapor is water cooled shell and coil heat exchanger (condenser) according to the study of (Saunders, 1998) and (Salimpour, 2009).

Table 5.6: Dimensional specification of water-cooled condenser (Ashkan, 2017).

Parameters	Values (m)
Coil diameter	0.06, 0.08, 0.1
Shell diameter	0.1, 0.12, 0.14, 0.16, 0.22
Height of shell	0.24, 0.28, 0.32, 0.36, 0.4
Height of coil	0.12, 0.14, 0.16, 0.18, 0.2
Fluid inlet diameter of shell	0.01, 0.015, 0.02, 0.025, 0.03
Fluid inlet diameter of coil	0.007, 0.008, 0.01, 0.011, 0.013, 0.016
Pitch	0.0154, 0.02, 0.022, 0.025, 0.033, 0.04
Distance between inlet and outlet shell	0.12, 0.144, 0.20, 0.22, 0.251

Table 5.4 indicates the different dimensional specification of water-cooled condenser in the temperature range of 40℃ to 90℃ (Ashkan, 2017).

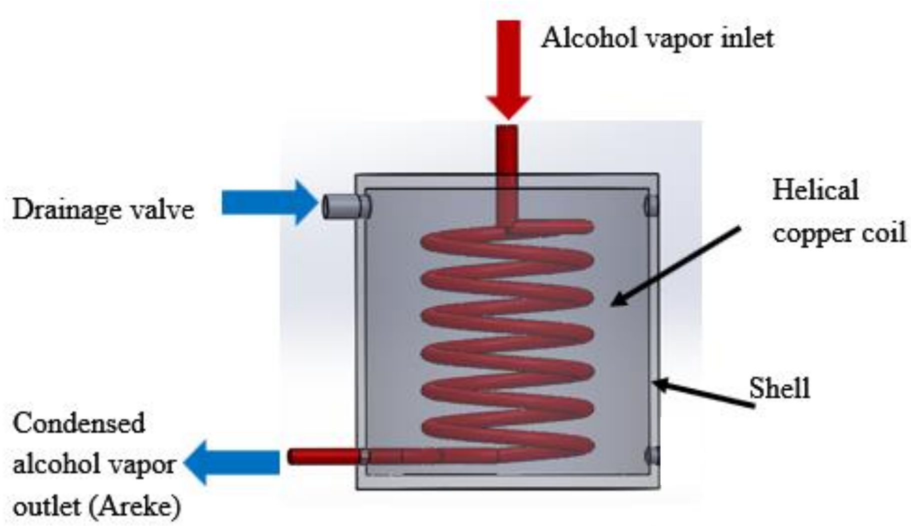

Figure 5.17: Geometry of condenser.

Figure 5.17 shows the alcohol condensing technique for this study is work by draining the water inside the condenser shell after temperature of the water is raised. The only moving fluid is ethanol vapor.

5.14 Material Selection for Condenser Coil

Copper is the preferred material in the construction of a still to impart flavor into the distilled spirits. According to Broad slab Distillery, both stainless steel and copper were excellent conductors of heat dispersing the heat evenly across the entire surface of the metal and creating a more even distillation. But where both stainless steel and copper will not put harmful chemicals into the final product, copper has the advantage over stainless in that whisky out of a copper still simply tastes better. When distilling in copper, the copper reacts on a molecular level with the sulfurs put out by the fermenting yeast. It “cancels-out” the sulfur taste which would otherwise be bitter and not as smooth. In the process of distilling, the sulfur coming from the yeast binds itself to the copper, making hydrogen-sulfide which in turn, forms copper sulfate. The copper sulfate sticks to the inside of the still after distillation is completed. After a thorough cleaning of the copper still, the copper sulfate must be washed down the drain (Gemedo, 2016).

5.15 Thermal Analysis of Condenser

The rate of condensation of alcohol vapor is given as (Rajput 2012);

$$heat\ lost\ by\ alcohol\ vapor = heat\ gained\ by\ water$$

$$\dot{m}_v \times h_{fg} = \dot{m}_c C_{pc}(T_{c2} - T_{c1}) \tag{5.59}$$

where:

h_{fg} − latent heat of alcohol vapor (kJ/kg)

$\dot{m}_c$ −mass flow rate of water (kg/s).

$\dot{m}_v$ −mass flow rate of alcohol vapor (kg/s).

C_{pc} −specific heat capacity of water (kJ/kgK).

T_{c2} −outlet temperature of water (K).

T_{c1} −inlet temperature of water (K).

Total heat transfer rate calculated in (APPENDIX: C).

$$Q = UA\theta_m = 208.7W \tag{5.60}$$

where:

U −overall heat transfer coefficient based on inner surface of the coil (W/m^2K).

A −surface area of the coil (m^2).

θ_m −logarithmic mean temperature difference

The logarithmic mean temperature difference is given by (Rajput, 2012):

$$LMTD(\theta_m) = \frac{\theta_1 - \theta_2}{ln\left(\frac{\theta_1}{\theta_2}\right)} = 26.78\ ℃ \tag{5.61}$$

where, θ_1 and θ_2 are the maximum and minimum temperature difference between the hot and cold fluid.

The coil length is determined by (Bonafoni and Capata, 2015):

$$L_c = N\sqrt{(2\pi R_c)^2 + p} = 3.68m$$

where: N −number of turns of helical coil

R_c −radius of helical coil

p − pitch length of the coil

The number of transfer unit (NTU) is given by (Rajput, 2012):

$$\mathrm{NTU} = \frac{\mathrm{UA}}{\mathrm{C_{min}}} = 1.4 \tag{5.62}$$

where, C_{min} − the minimum fluid capacity rate

In a condenser, C_{max} refers to the hot fluid which remains at constant temperature, therefore C_{min} refers to water (Rajput, 2012):

$$\mathrm{C_{min}} = \dot{\mathrm{m}}_{\mathrm{c}}\mathrm{C_{pc}} = 5.58\ \mathrm{kW/°C} \tag{5.63}$$

The effectiveness of the condenser (ε): is the ratio of actual heat transfer to the maximum possible heat transfer (Rajput, 2012). Thus, (APPENDIX: C).

$$\varepsilon = \frac{\mathrm{Q}}{\mathrm{Q_{max}}} = 1 - exp(-\mathrm{NTU}) = 0.75 \tag{5.64}$$

5.16 Pipe Line Design and Selection

A naturally circulating fluid flow is usually accompanied by pressure drop that is compensated by a hydraulic head between receiver and distillation column. The total pressure drop is summation of drop due to working fluid flow through receiver, vapor line and condensate line. The flow rate of the working fluid depends significantly on the value of the hydraulic head h; a design survey on solar water heater recommends the hydraulic head value can range from 0.2 to 2 m (Asfafaw *et al*., 2014), where lower head has higher flow rate and smaller heat loss at elevated temperature.

$$\Delta\mathrm{P_t} = (\rho_\mathrm{l} - \rho_\mathrm{v})\mathrm{gh} \tag{5.65}$$

The pressure drop of the system is computed by (Asfafaw *et al*., 2014).

$$\Delta\mathrm{P} = \mathrm{f}\frac{\mathrm{L}}{\mathrm{d}}\frac{\rho\mathrm{v}^2}{2} \tag{5.66}$$

The coefficient of friction given by:

$$f = \frac{64}{R_e} \tag{5.67}$$

The coefficient of friction of smooth copper coil surface is 0.03 (Asfafaw *et al.*, 2014). The Reynolds number helps to estimate the flow velocity of the working fluid.

$$R_e = \frac{\rho v D}{\mu} = 2133 \tag{5.68}$$

This indicates the fluid flow inside the pipe is laminar because $2133 \leq 2300$. The pressure drop is calculated as 0.002 N/m^2.

5.17 Pipe Loss Analysis

The heat loss from the pipe line through conduction, convection and radiation is computed using eq. (5.65). where, thermal conductivity and thickness of polystyrene foam insulation are 0.023 W/mK and 0.05m respectively.

$$Q_{\text{loss}} = \frac{2\pi k L}{ln\left(\frac{D_o + 2t}{D_i}\right)}\left[T_p - T_a\right] + A_p \sigma \varepsilon\left[T_p^4 - T_a^4\right] + h_c A_p\left[T_p - T_a\right] \tag{5.69}$$

where: $k -$ thermal conductivity of polystyrene foam (W/mK).

$T_p -$ temperature of pipe (K).

$A_p -$ area of pipe (m^2).

$h_c -$ convective heat transfer coefficient of air (W/m^{2}K)

$T_a -$ ambient temperature (K).

$\varepsilon -$ emissivity of the insulator

D_o *and* $D_i -$ outer and inner diameter of the pipe (m).

CHAPTER SIX

EXPERIMENTAL SETUP AND PROCEDURES

6.1. Introduction

This chapter presents the description of experimental setup consisting dish concentrator collector, solar receiver, flexible pipe, dish stand, distillation column and condenser. The experiment has been performed to study the performance of solar thermal energy for local Areke production system. Varies measuring devices used for the investigation of the result.

6.2. Experimental Setup

This experimental setup done by minimizing the original size of the designed components by the ratio of 2.22:1. The materials used for the prototype were purchased from local market. satellite dish is selected with aperture diameter of 90cm by using manual hand tracking system.

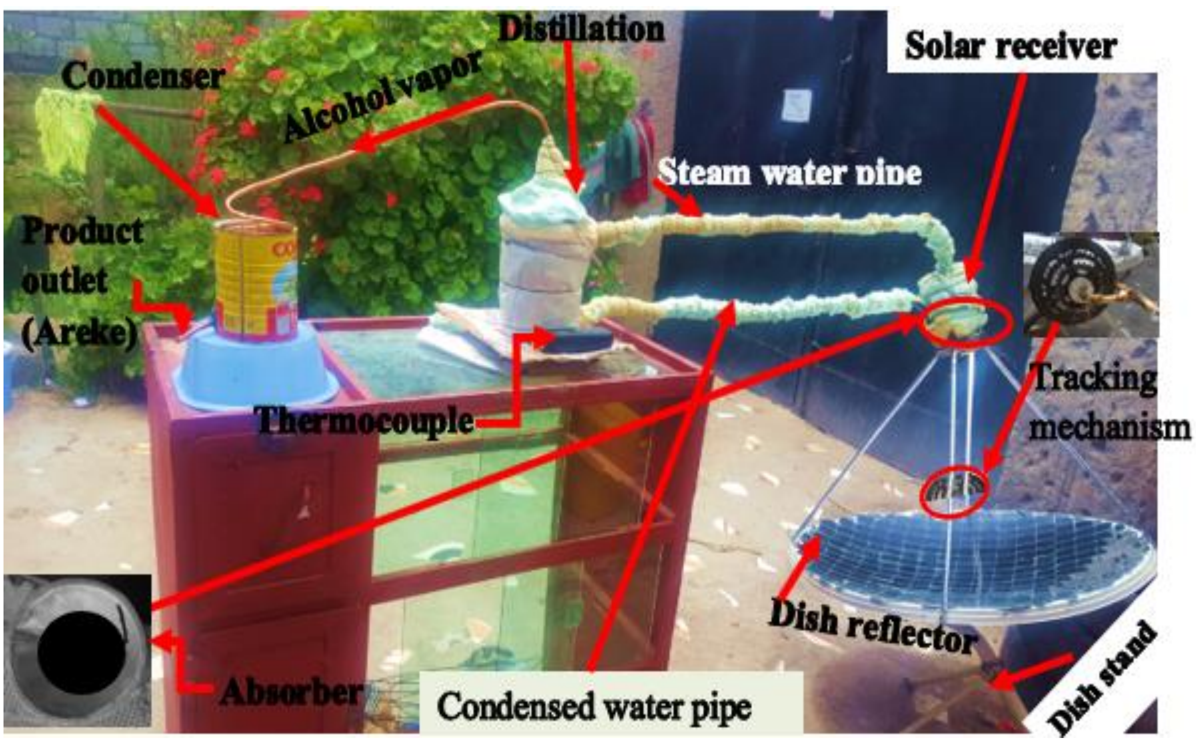

Figure 6.1: Experimental setup of solar thermal Areke production system.

.

6.3. Experimental Procedures

The following procedure were provided for the experimental work:

6.3.1 Installation Procedures

- ✓ Collect locally available materials for manufacturing of solar receiver and supporting structures.
- ✓ Select appropriate satellite dish for reflector.
- ✓ Insulate the receiver and distillation column to decrease energy loss.
- ✓ Connect the copper coil with solar receiver and distillation column.
- ✓ Connect the copper coil with the condenser.

6.3.2 Test Procedures

Figure 6.2: Thermocouple installation on each component.

Test procedures show on Figure 6.3 indicates the temperature reading of each component.

- ✓ Insert the water into the solar receiver.
- ✓ Insert the Difdif into the distillation column.
- ✓ Connect the temperature measurement thermocouple on the inlet and outlet of the receiver.

- ✓ Connect the port of the thermocouple on the bottom surface of the solar receiver/absorber to measure the surface temperature of the absorber.
- ✓ Put one end port the thermocouple inside the distillation column to record the temperature of Difdif.
- ✓ Put the other port of thermocouple on the condenser shell inlet to measure the temperature of the water.
- ✓ Test the quality of the product by percentage.

6.3.3 Alcohol Content Testing

The alcohol content of the distilled liquid Areke has been tested using alcoholometer at Debre Birhan university in chemical engineering laboratory, the test done by immersing the alcoholometer into the cylinder that contain liquid Areke, and the reading bar indicated 45% by volume shown in Figure 6.3.

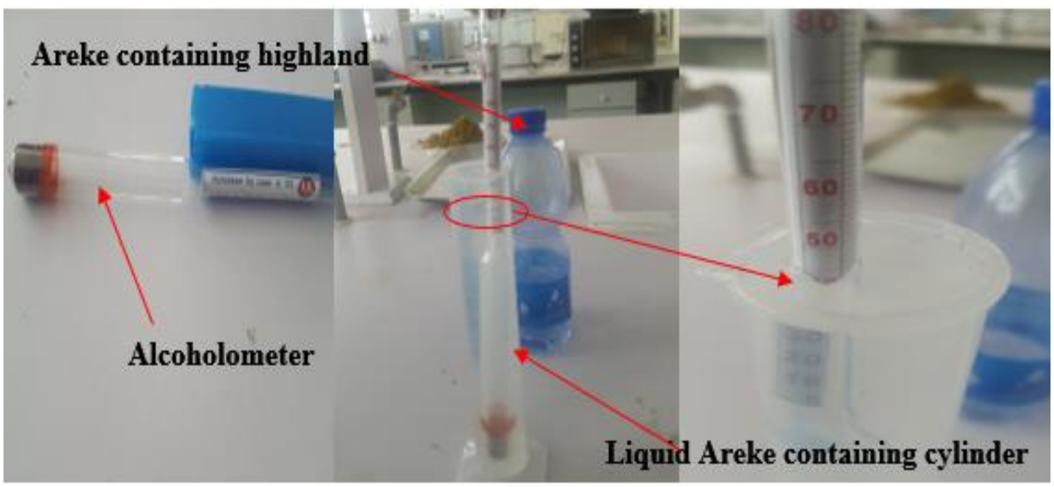

Figure 6.3: Alcohol content testing procedures.

6.4 Parameters for the Experimental Study

The parameters studied for this study are;

- ➢ Solar radiation
- ➢ Temperature
- ➢ Wind speed and
- ➢ Efficiency

CHAPTER SEVEN

RESULTS AND DISCUSSIONS

7.1. Average Solar Radiation

Solar radiation data for Debre Birhan has been collected from different sources. Data collected from NMA of Ethiopia is used to determine the solar energy potential of Debre Birhan city its average has been calculated from sunshine hour data because, the solar radiation was not active for Debre Birhan.

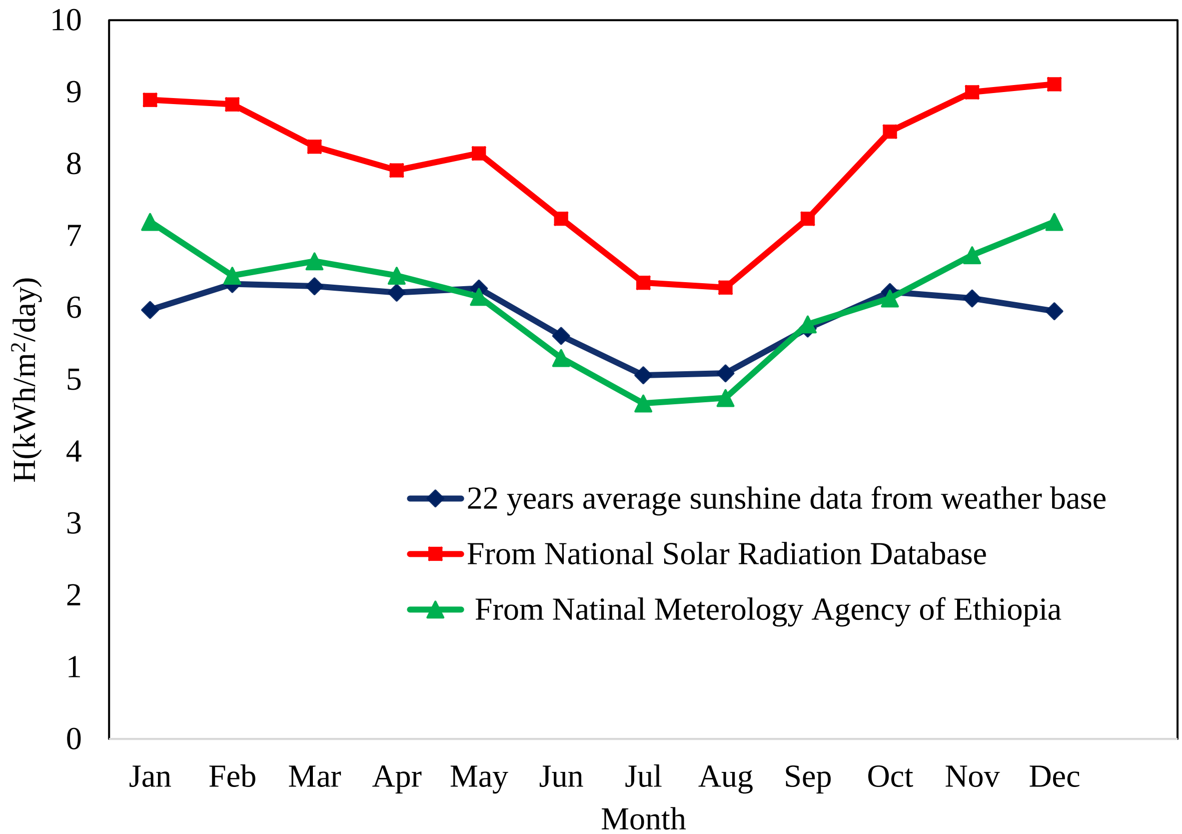

Figure 7.1: Comparison of calculated solar radiation with other data sources.

Radiation data from Weather base is calculated from twenty-two years averaged sunshine data that obtained from weather averages website (www.weatherbase.com). NASA surface meteorology and solar energy database is one of radiation data sources which provided also twenty-two years averaged data (July 1983- June 2005). Its cell midpoint that is near to Debre

Birhan city is Latitude 9.6 and Longitude 39.5 with cells dimension of 1° × 1°. The nearby data of National Meteorological Agency (NMA) of Ethiopia for Debre Birhan city collected from Addis Ababa. The result of calculated solar radiation from NMA has nearby result with NASA as shown in Figure 7.1. an average solar radiation is calculated as maximum in January (7.2 $kWh/m^2/day$) and minimum in July (4.6 $kWh/m^2/day$) and Annual average daily solar radiation is 6.1 $kWh/m^2/day$.

7.2. The Result of Direct Solar Radiation for Four Seasons.

Figure 7.2-7.5 shows that, an average hourly beam solar radiation is calculated as maximum in December (0.77 kW/m^2) and minimum in July (0.25 kW/m^2).

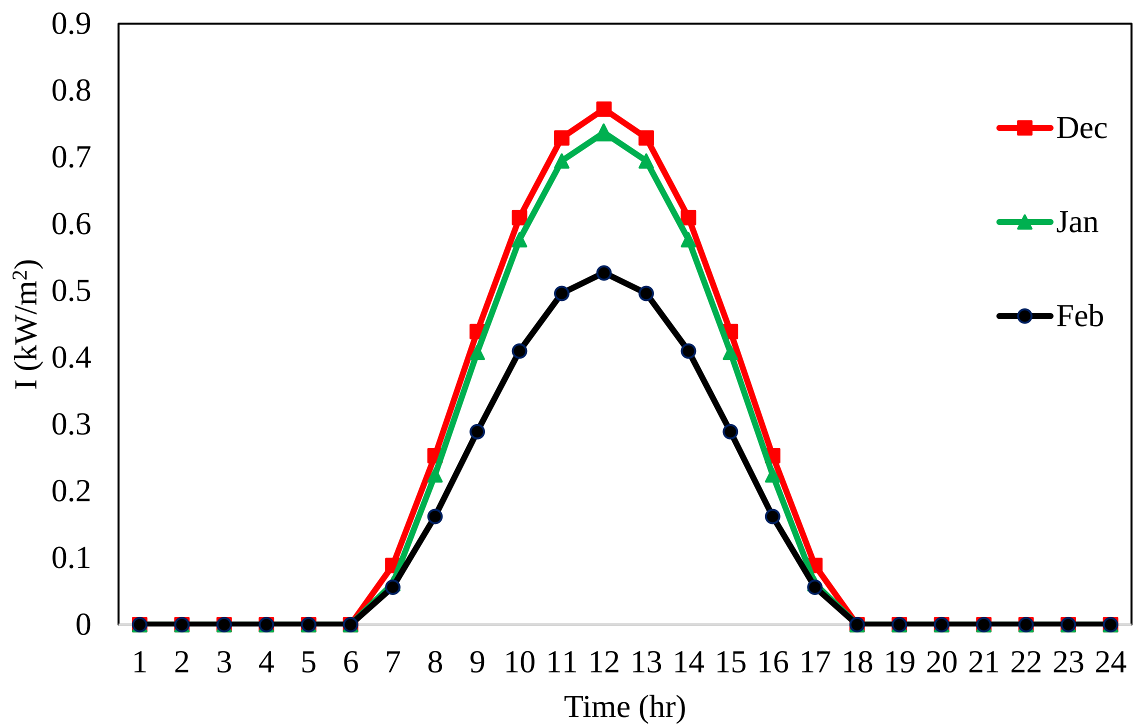

Figure 7.2: Monthly average hourly beam solar radiation of Winter season.

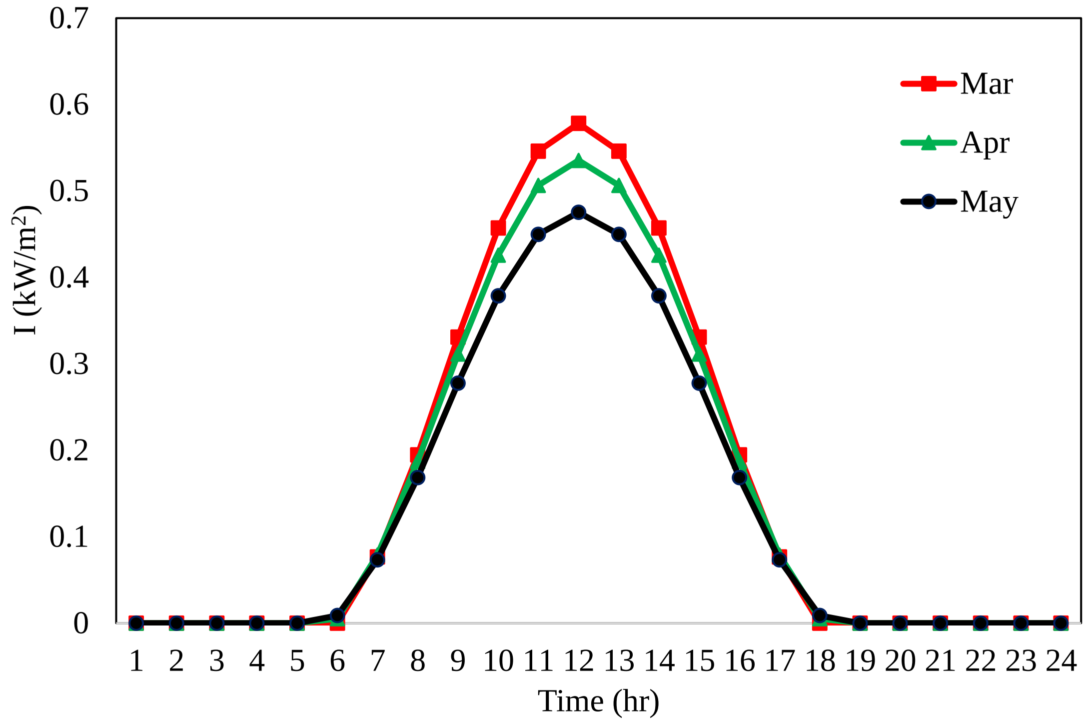

Figure 7.3: Monthly average hourly beam solar radiation of Spring season.

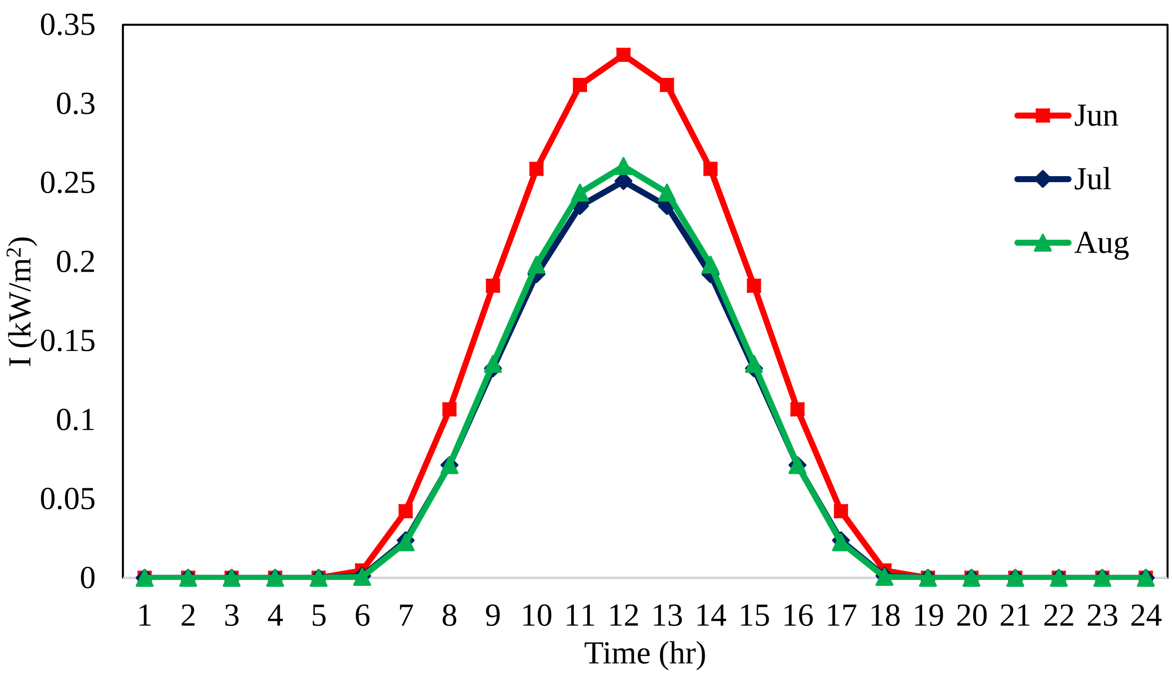

Figure 7.4: Monthly average hourly beam solar radiation of Summer season.

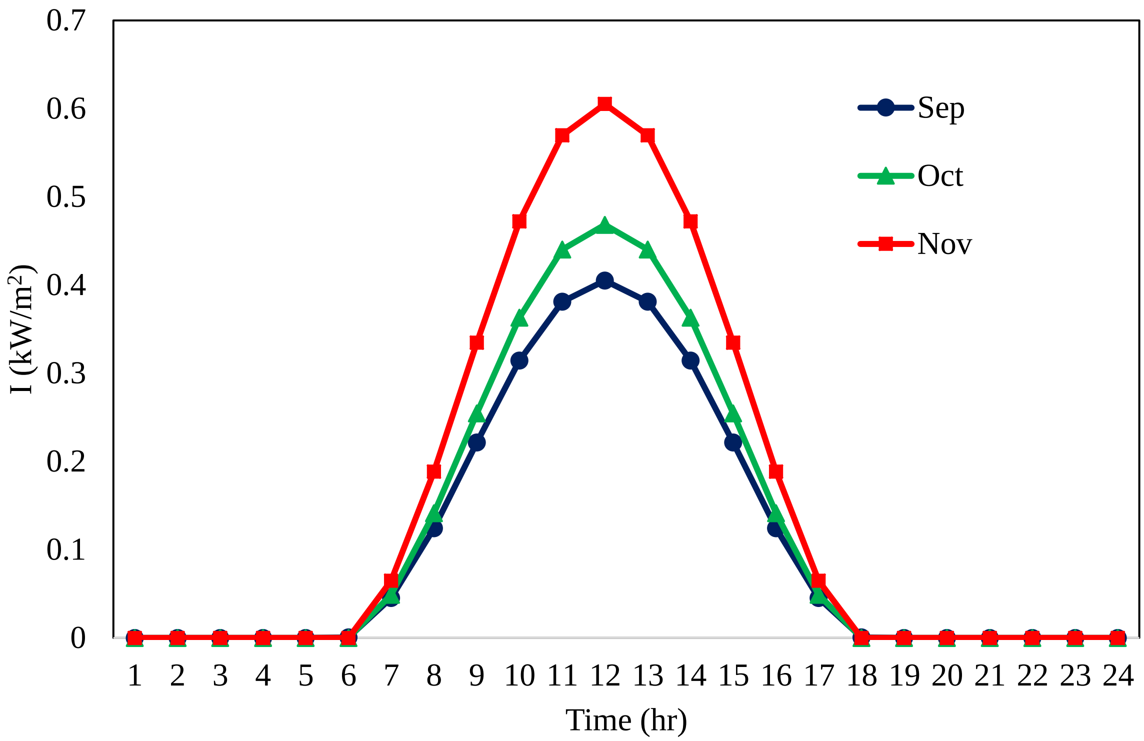

Figure 7.5: Monthly average hourly beam solar radiation of Autumn season.

7.3. Temperature Distribution

Figure 7.6 shows that absorber wall temperature, ambient temperature beam solar intensity throughout the day for each single hour are calculated by using Microsoft excel software. The solar beam insolation showed a parabolic path with the peak value attaining the mid-day which subsequently decreasing. Since the experimental testing has been conducted during the minimum solar intensity month, July. From Figure 7.4 the solar intensity indicated as 330 W/m^2. The temperature distribution over the wall of solar absorber had a fluctuated value due to the weather condition (cloud, wind). The maximum average wall temperature of modified absorber reaches 300.3 ℃ at the mid-day, 12:45AM, this maximum temperature is achieved by the effective geometrical shape of the absorber. Similar work from the literature review has been validated, the result of the study was the maximum temperature of the absorber with 400 W/m^2 was 270 ℃ has obtained (Munir, 2010). During the experimental testing that was conducted on clear sky day, the maximum absorber surface temperature reaches 313 ℃.

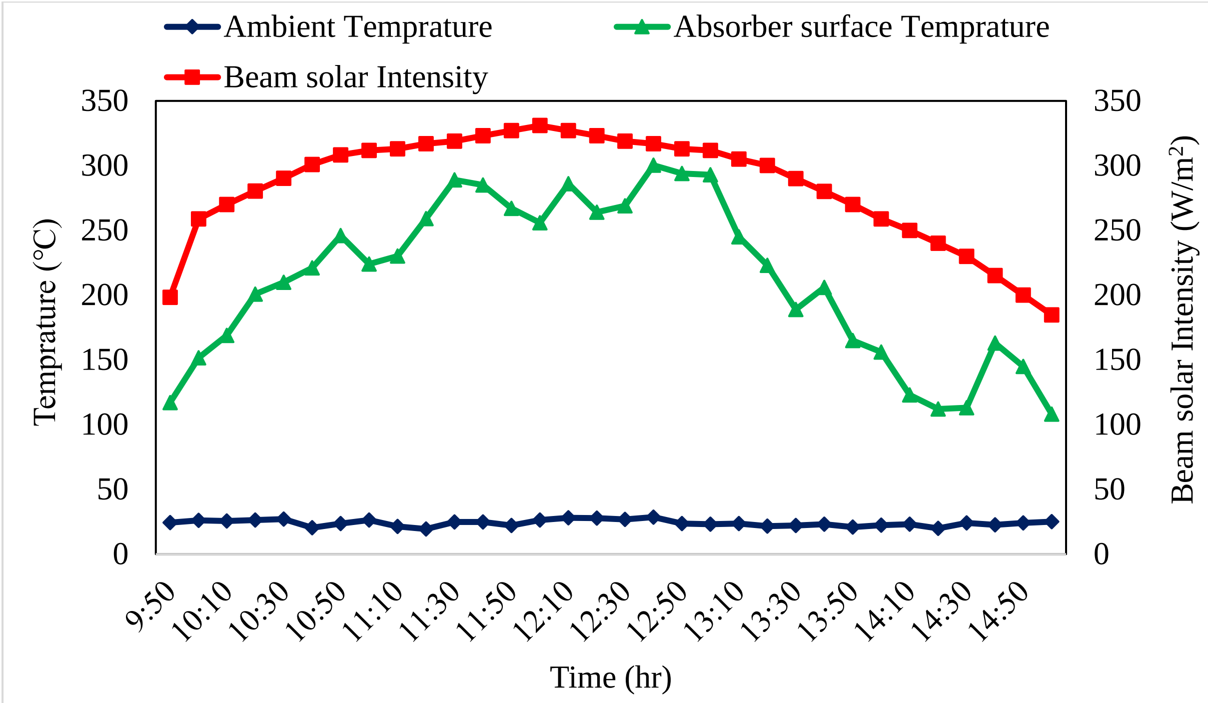

Figure 7.6: Result of temperature distribution over the solar absorber.

Figure 7.7 shows that the temperature variation inside the solar receiver with in a given ambient temperature, the temperature of water increases sharply at the beginning until the phase change of water occurred. The experiment has conducted at 9:45AM using 0.6 kg of water, the water boiled at 90.2 ℃ and the time taken to boil 0.6 kg of water is 25 minutes (APPENDIX B:). So, the boiling point of water at Debre Birhan is 90.2 ℃ with atmospheric pressure of 72.2 kPa. During water temperature testing, the temperature of water raised sharply up to 96 ℃ and again decrease to 94 ℃ then finally constant at 94.6 ℃.

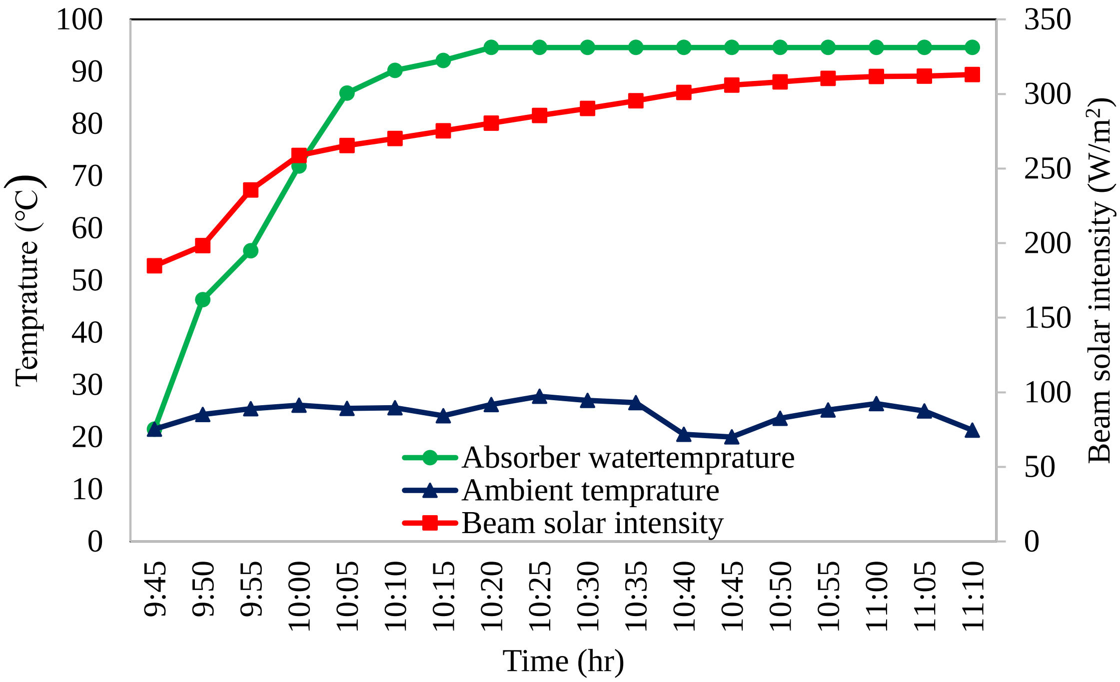

Figure 7.7: Absorber water temperature distribution.

Figure 7.8 indicates that the temperature variation of Difdif inside the distillation column, the Difdif starts to heat up after the water vapor inside the receiver flows through the pipe and rises the Difdif temperature to 71.4 ℃, at this temperature value ethanol starts to vaporize, this indicates the boiling point of ethanol at Debre Birhan weather condition is 71.4℃. The amount of Difdif poured into the distillation column is 2 L and total time taken to complete one cycle of distillation process is 65 minutes.

From the experimental result, 2 liters of Difdif 0.2 liter of Areke produced. Due to lack of flowmeter it was difficult to record the mass flow rate for each min or second, so the rate of production of Areke is measure after the total distillation which is obtained as 0.2 L/h.

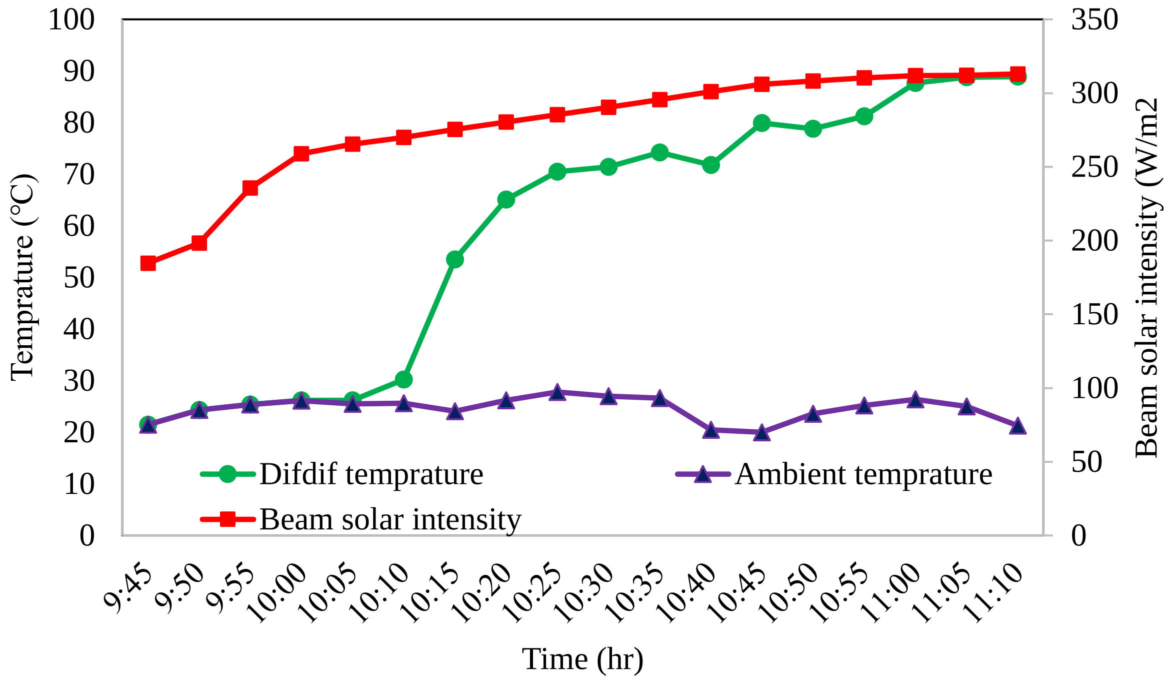

Figure 7.8: Difdif temperature distribution.

Figure 7.9 shows the temperature variation of water inside the condenser with in a given time taken, the condenser water starts to heat up after the Difdif is boiled and the vapor of ethanol flow through the copper tube that connect the distillation column and the condenser. The temperature of water inside the condenser raised to 59.1 °C.

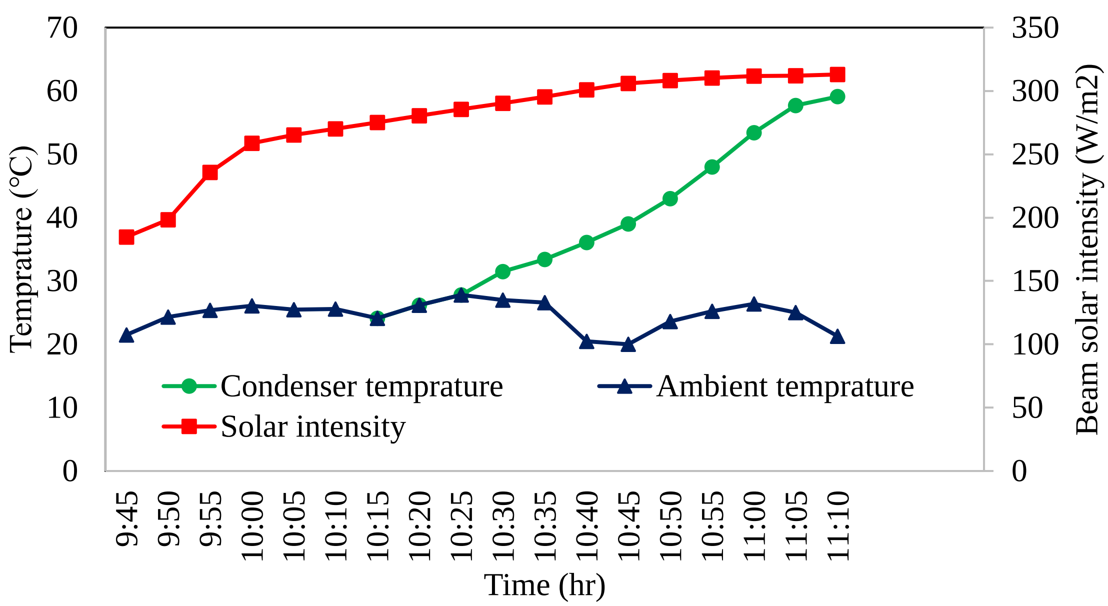

Figure 7.9: Condenser water temperature distribution.

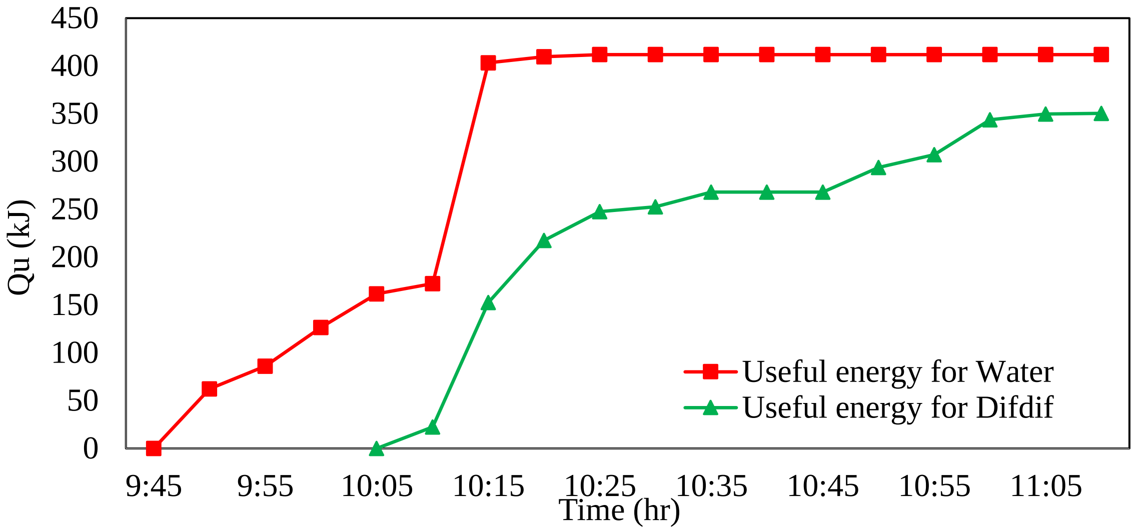

Figure 7.10: Useful energy gain of water and Difdif.

Figure 7.10 indicates the useful energy required to boil water and Difdif, sensible energy required to boil 0.6L of water is 172.5 kJ (eq. 5.25). And sensible energy required to boil 2L of Difdif obtained as 249.5 kJ. To reach the boiling point of water it takes around 25 minutes and time taken to complete a cycle distillation is 65 minutes. The latent heat required to vaporize the ethanol from the Difdif is 133.5 kJ (eq. 5.28) and latent heat required to vaporize water 226 kJ (eq. 5.28).

7.4. Results of heat loss analysis

7.4.1. Heat Loss from Solar Receiver

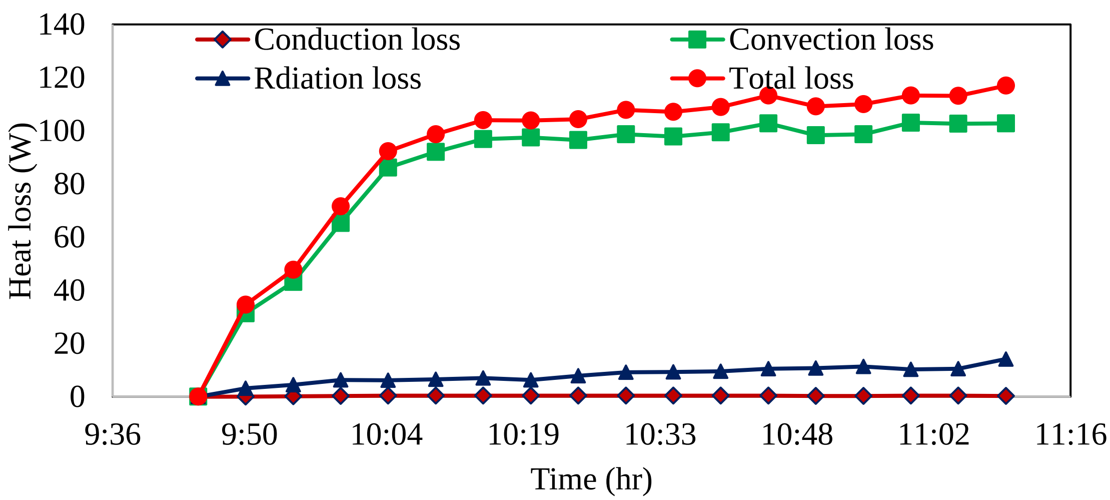

Figure 7.11: Heat loss from the solar receiver.

Figure 7.11 indicates that the heat loss from the receiver through conduction, convection and radiation mode, as seen from the graph maximum heat loss obtained by convection because, this is due to the wind flow around the receiver. minimum heat loss obtained by conduction mode because, the outer surface of the receiver is well insulated (eq. 5.29-5.31).

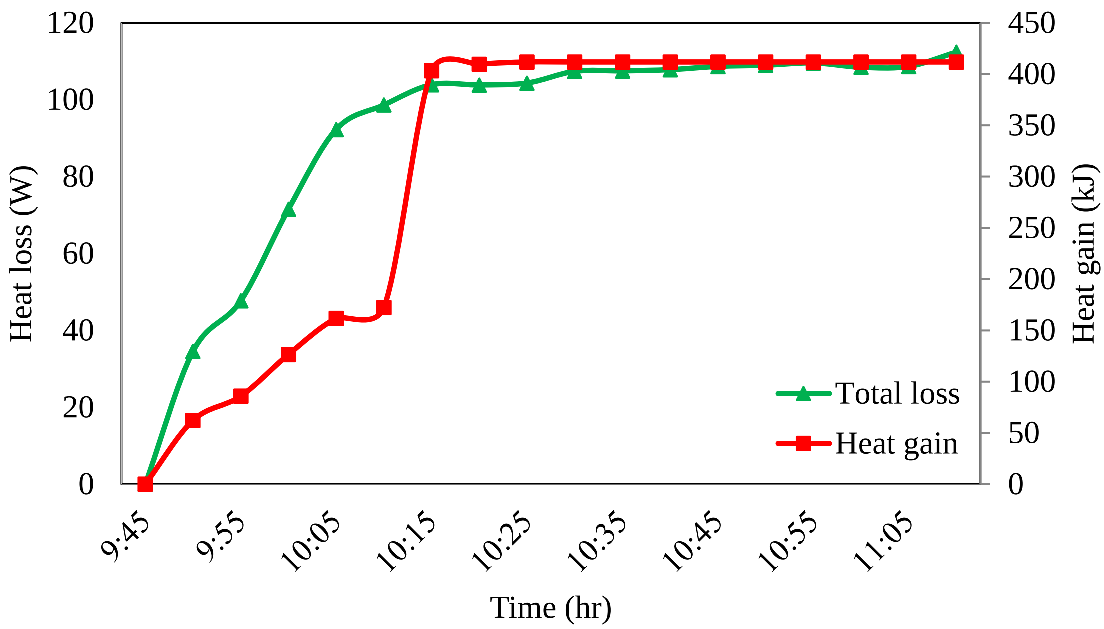

Figure 7.12: Heat loss versus heat gain inside the receiver by water.

Figure 7.12 shows the heat loss and heat gain by the water inside the receiver, the heat gain by the water is greater that the heat loss. at the beginning the heat graph is sharply increase then after becomes constant this is due to phase change of the water (liquid-vapor).

7.4.2. Heat Loss from Distillation Column

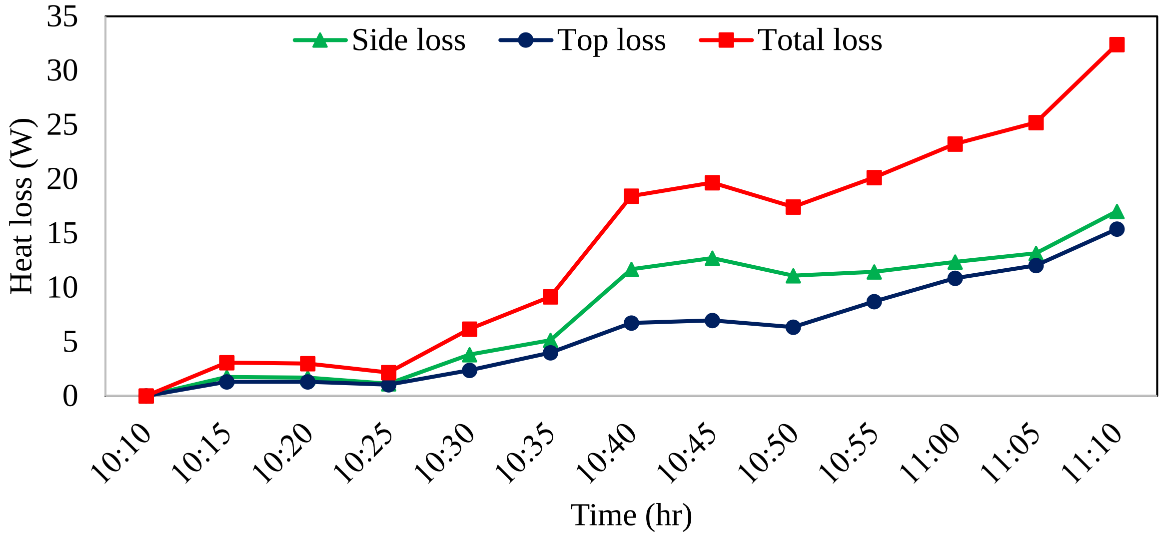

Figure 7.13: Heat loss over the distillation column.

Figure 7.13 indicates the heat loss over the distillation column, by considering conduction, convection and radiation heat loss the maximum heat loss has been obtained on the side part of the distillation column due to its maximum surface area compared to the top surface (eq. 5.14-5.15).

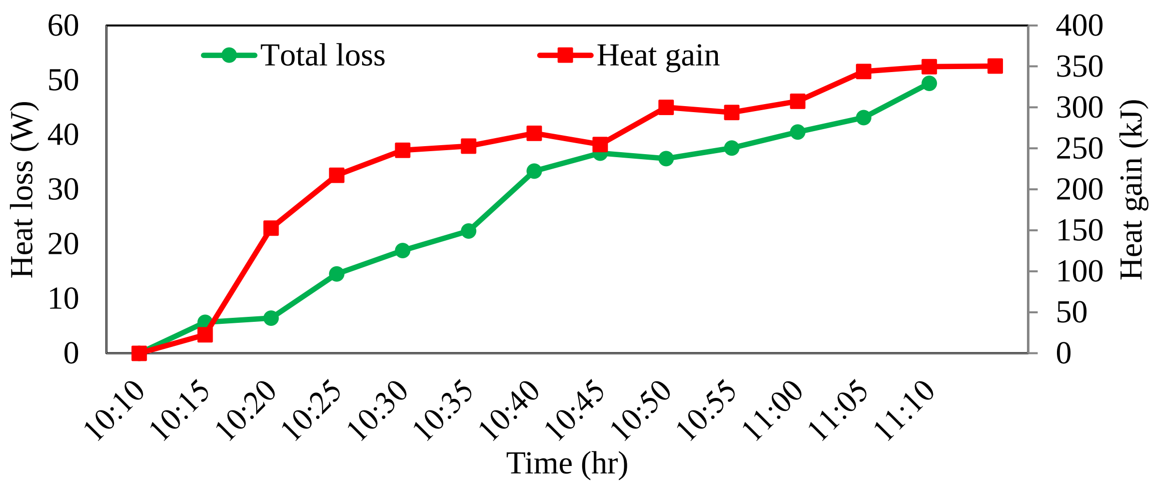

Figure 7.14: Total heat loss and heat gain by Difdif inside the distillation column.

Figure 7.14 shows the heat loss from the distillation column and heat gained by Difdif. As shown on the graph the heat loss is minimum rather than heat gain (eq. 5.14-5.15).

7.4.3. Heat Loss From Pipe Lines

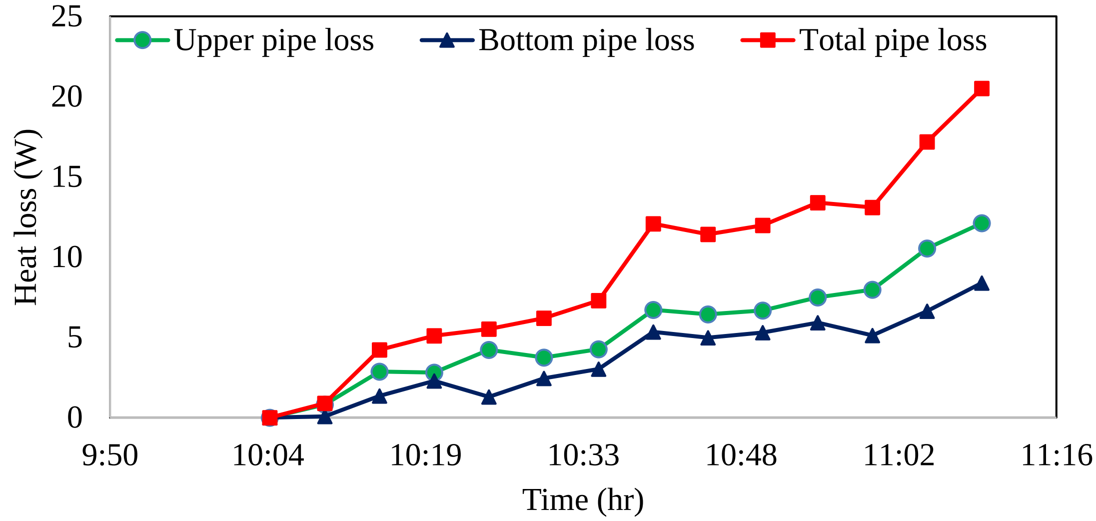

Figure 7.15: Heat loss from the fluid pipe lines.

Figure 7.15 indicates the heat loss over the fluid transport pipe, considering conduction, convection and radiation heat loss the maximum heat loss value is obtained on the hot fluid transport line. Since the fluid temperature inside the upper pipe line is maximum so the temperature difference with the ambient temperature goes maximum, due to this the heat loss also maximum (eq. 5.65).

Fig. 7.16 shows that the total heat loss analysis of distillation column, solar receiver and fluid transport pipes. As seen from the graph the maximum heat loss takes place on the solar receiver because it is exposed directly to the solar radiation reflected from the dish concentrator due to this maximum temperature obtained since, temperature has directly relationship with heat loss due to this heat loss is maximum on the receiver and minimum heat loss occurred on the fluid transport pipes. Total heat loss all over the system obtained as 150 W, and heat energy liberated to the surrounding until water is vaporized inside the receiver is 96.6W.

7.4.4. Total Heat Loss all over the System

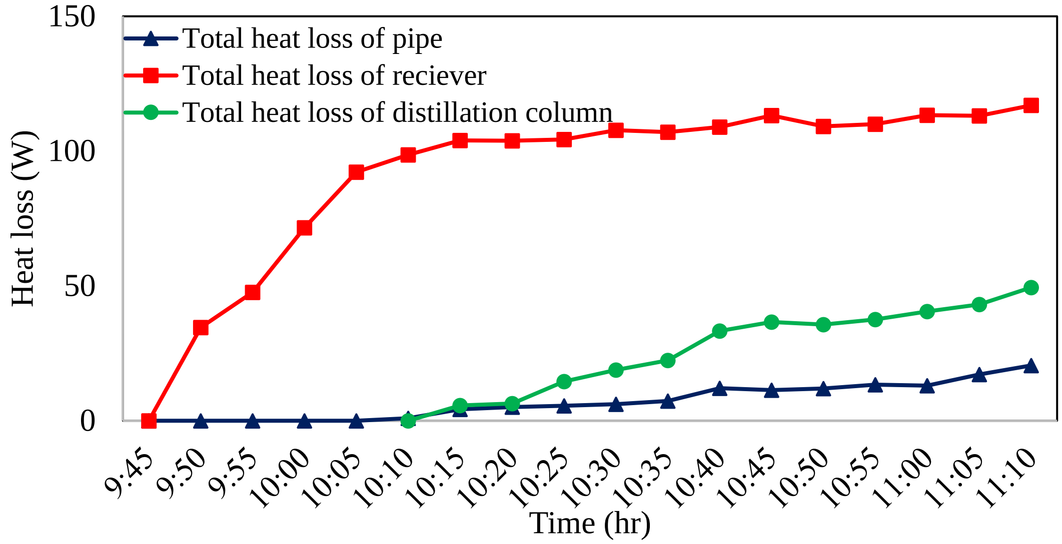

Figure 7.16: Heat loss analysis all over the system.

7.5. Results of Efficiency Analysis

To determine the efficiency of the collector, the heat loss must be subtracted from the input energy.

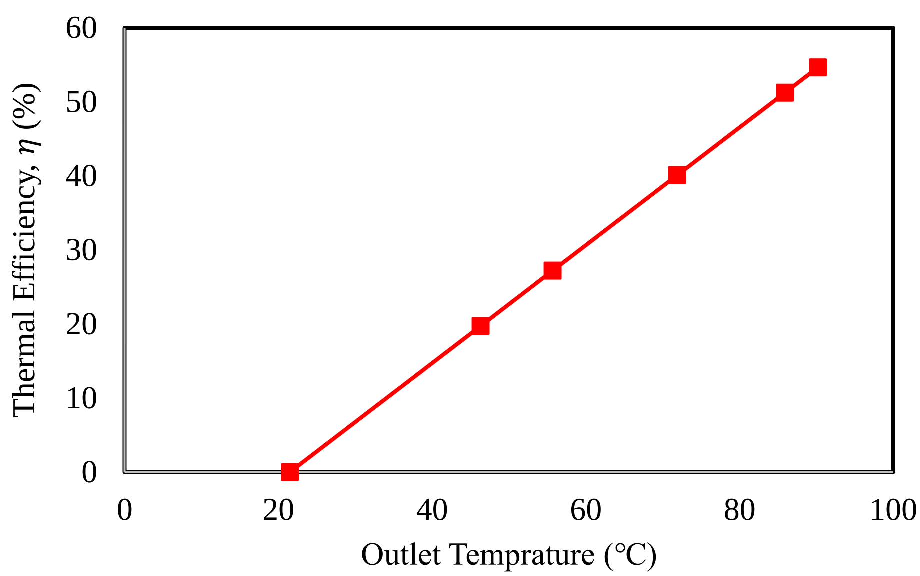

Figure 7. 17: Thermal efficiency of the collector.

The efficiency of dish concentrator collector is calculated from the thermal efficiency formula (eq. 5.54). Figure 7.17 shows the thermal efficiency versus outlet temperature of the working fluid inside the receiver, as the outlet temperature increase the thermal efficiency also increase, to know the effect of outlet temperature the inlet temperature must be constant. Theoretically if the inlet temperature of the working fluid enter into the receiver increases the thermal efficiency decrease. Production efficiency of the system is calculated from (eq. 5.58a) gives as 10%. From traditional distillation system 8.33 % of production efficiency was obtained.

7.6. Sankey Diagram

The Sankey diagram is done from the complete energy analysis of the system shown in Figure 7.18.

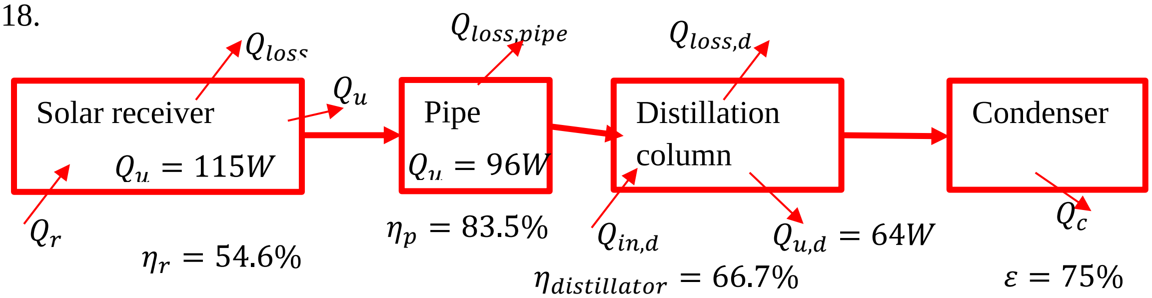

Figure 7.18: Block diagram of energy analysis of solar thermal areke production system.

The overall efficiency of the system is given by multiplying the thermal efficiency of the receiver, pipe and distillator. The overall efficiency is obtained as 30.4%.

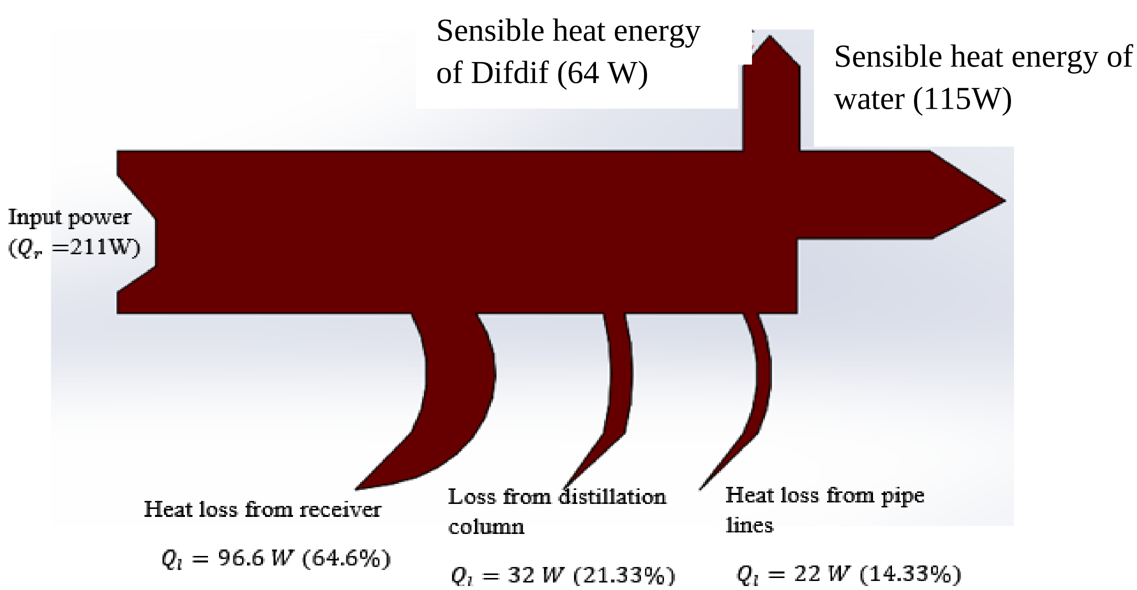

Figure 7.19: Sankey diagram of the system.

Figure 7.19 shows the power distribution all over the system with energy loss. The input power for the solar based local Areke production system is 211 W, the total heat loss from the system is 150 W. The useful energy for the water heating system in 115 W (shown in Table 7.1) and useful energy for Difdif heating is 64 W (shown in APPENDIX: C).

Table 7.1: Analytical result of the receiver system.

m (kg)	Cp (kg/kgK	Ti ℃	Tabs (K)	Tf (K)	Ta (K)	Temp. change (K)	mass flow rate (kg/s)	Qwater (kJ)	Qrate (W)
0.6	4186	21.5	82.9	25.6	21.5	4.1	0.0004	10.2975	6.86504
0.6	4186	21.5	117.1	44.2	24.3	22.7	0.0004	57.0133	38.0088
0.6	4186	21.5	144.8	56.2	25.4	34.7	0.0004	87.1525	58.1016
0.6	4186	21.5	151.6	69.4	26.1	47.9	0.0004	120.305	80.2037
0.6	4186	21.5	182.7	87.7	25.5	66.2	0.0004	166.267	110.845
0.6	4186	21.5	223	90.2	25.6	68.7	0.0004	172.546	115.031

7.7. Result of Distillation Test

In the first run of the fermented Difdif the temperature was stabilized at 89 ^oC and the purity of the collected alcohol was 45 % by volume. Then the temperature was rising gradually as the alcohol content in the wash decreases. There was corresponding change of purity of distillate/ ethanol as the head temperature change.

Table 7.2: Alcohol product testing.

No	Temperature (^oC)	Percentage of Alcohol	Remark	Rate of distillation (L/hr.)
1	89	45	High % ABV	
2	90	44	High % ABV	
3	91	43	High % ABV	

4	92	42	High % ABV	0.2
5	93	40	Low % ABV	
6	94	38	Low % ABV	

CHAPTER EIGHT

CONCLUSIONS AND RECOMMENDATIONS

8.1. Conclusions

In this study, solar thermal based local Areke production system is designed, constructed and tested for experimental investigation of the thermal performance at Debre Birhan, Ethiopia. For solar receiver system aluminum sheet metal with truncated shape on the bottom side has been selected to increase the heat transfer area and catch up effectively the solar radiation reflected from the reflector. For distillation column, clay has been selected because it retains heat energy. The insulator called polystyrene foam for the components is chosen from locally available materials. Wind flow over the dish-receiver system was analyzed to know the effect of wind on the convection loss.

From the study and the analysis of the collected data, the following conclusions have been drawn. The solar absorber was designed and fabricated for experimental testing with solar dish collector area 0.64 m^2 for Debre Birhan weather condition. The designed solar absorber can entrap maximum average temperature of 300.3 ℃ in between 9:45 AM up to 15:00 PM in minimum solar intensity month, July.

- ❖ From the experimental result, the water boiling point is 90.2 ℃ and boiling point of ethanol is 71.4 ℃ at atmospheric pressure of 72.2 kPa, this is due to the effect of the altitude.
- ❖ Time required to produce 0.2 L of liquid Areke from 2 L of Difdif is 65 min.
- ❖ Time required to vaporize 0.6 liter of water 25 min.
- ❖ Input power required for one cycle of distillation process is 0.211kW.
- ❖ The alcohol content of distilled Areke is 45%.
- ❖ The efficiency of dish concentrator is calculated as 54.6%.
- ❖ The production efficiency of the system obtained as 10%.

8.2. Recommendations for Future Work

- ✓ Areke production process takes place during night and day time, since solar energy performance is applicable during day time, to cover the night time integrating solar storage system is necessary to carry out the night work.
- ✓ Since Areke production system in Ethiopia takes place in wide range in Debre Birhan town, it is better to construct solar energy based small industry.
- ✓ On this study the solar absorber is designed with modified model that trap the solar radiation effectively, but the solar addition depends on the weather condition, fluctuation of temperature happen, so applying phase change material on the bottom side of the absorber will stabilize the fluctuation.
- ✓ Wind flow over the dish-receiver system analyzed for the hot air inside the cavity, it is better to analyze the effect external hot air escaping on the heat transfer fluid (Water inside the receiver).

REFERENCES

Abdulkadir AH, Demiss AA, Ole NJ. 2011. "Performance Investigation of Solar Powered Injera Baking oven for Indoor Cooking." *ISES Solar World Congress Proceedings, Kassel,* 186–96.

Abramzon, Boris, Jacob Danan, and Shlomo Ostersetzer. 1999. *Condenser Heat Exchanger.*

Adams, A. 2012. "The Distillation of Alcohol." *Journal of Industrial and Engineering Chemistry* 8-14.

Adane, Kassa. 2015. "Investigation of Parabolic Dish Solar Concentrator for Local Areke Distillation." *Msc. Thesis, Submitted to Addis Ababa University, Department of Thermal Engineering.*

Alem, K. 2011. " Design and Manufacturing of Parabolic Trough for Katikala Production." *Msc. Thesis, Submitted to Adama Science and Technology University, Department of Manufacturig Engineering.*

Alia H., M.S. Kamrana H.M. Alia S. Imran. 2019. "Condensation Heat Transfer Enhancement Using Steam-Ethanol Mixtures on Horizontal Fnned Tube." *International Journal of Thermal Sciences 41(3),* 87-95.

Alimoradi, Ashkan. 2017. "Study of Thermal Effectiveness and its Relation with NTU in Shell and Helically Coiled Tube Heat Exchangers." *Case Studies in Thermal Engineering 301(7),* 100-107.

Amós Veremachi, Azher Zia, Boaventura C. Cuamba, Jorgen Lovseth. 2017. "Parabolic Dish Concentrating Collector for Indirect Solar Cooking." *Global Journal of Science Frontier Research 76 (2),* 2249-4626.

Andrzejczyk, R. Muszynski, M. Gosz, T. 2018. "Experimental Investigations on Heat Transfer Enhancement in Shell Coil Heat Exchanger with Variable Baffles Geometry." *Chemical Engineering and Processing: Process Intensification* 114-126.

Anwar, M. M. 2014. "Solar Energy Resource Assessment of the Geba Catchment, Northern Ethiopia." *Energy Procedia 57,* 1266-1274.

Araya, A. 2013. "Horn of Africa Region Environment Centre and Network."

Asfafaw T., Mulu K., J.N. 2014. "Design and Development of Solar Thermal Injera Baking." *Energy Procedia, 57,* 46–55.

Ayuthaya, Rattanapol P., Pichai N., and Wirut A. 2013. "the Thermal Performance of an Ethanol Solar Still with Fin Plate to Increase Productivity." *Renewable Energy* 227-234.

Awash, B. 2014. "Indoor air pollution in developing countries and acute lower respiratory infection in children." , Thorax,55: 518-532.

Beggs, C. 2009. "Energy: Management Supply and Conservation." *Oxford, UK. Elsevier Publishers.*

Belay, Tefera. 2007. "Cleaner Production Assessment in the Ethiopian Alcohol Industries a Case Study in the Sebata Alcohol and Liquor Factor."

Bonafoni, Capata. 2015. "Proposed Design Procedure of a Helical Coil Heat Exchanger for an Energy Recovery System for Vehicular Application." *Mechanics, Materials Science and Engineering* ff10.13140/RG.2.1.2503.5282.

Bruce, N.L. 2006. "Indoor Air Pollution, in Disease Control Priorities in Developing Countries."

Daabo YB, He YL, Cui FQ, Lin CH. 2016. "Numerical study on coupling phase change heat transfer performance of solar dish collector.", Solar *Energy*. 90:84-93.

Dawit F. 1986. "The distribution of concentrated solar radiation in paraboloidal collectors." *Journal of Solar Energy Engineering*. 108(3):219-225.

Dizaji, S. Jafarmadar, M. Hashemian. 2015. "the Effect of Flow, Thermodynamic and Geometrical Characteristics on Exergy Loss in Shell and Coiled Tube Heat Exchangers." *Energy* 678–684.

Duffe J. A., Beckman W. A. 2006. "Principle of Solar Engineering." New Jersey.

El Ouederni1, A.R., M. Ben Salah, F. Askri, M. Ben Nasrallah and F. Alou. 2009. "Experimental Study of Aparabolic Solar Concentrator." *Revue Des Energies Renouvelables* 395-404.

Emin El, Gülsah Çakmak, Cengiz Yıldız. 2017. "Efficiency Analysis of Tank-Type Water Distillation System Integrated with Hot Water Collector." *Thermal Science and Engineering Progress 3,* 24-30.

Eswaramoorthy, S.Shanmugam, A R. Veerappan. 2013. "Experimental Study on Solar Parabolic Dish Thermoelectric Generator." *International Journal of Energy Engineering* 62-66.

Ethio Resource Group. 2009. "Diversity and Security for The Ethiopian Power System: Preliminary Assessment of Risks and Opportunities for the Power Sector, for Heinrich Boll."

Fareed. M. Mohamed, Auatf.S.Jassim, Yaseen. H. Mahmood, Mohamad A.K.Ahmed. 2012. "Design and Study of Portable Solar Dish Concentrator Fareed ." *International Journal of Recent Research and Review* 52-61.

Fekade, Yehualawork. 2019. "Study and Design of Solar and Micro-Hydro Hybrid System for Rural Area of Debre Berhan, Ethiopia." *Msc. Thesis Submitted to The School of Graduate Studies in Partial Fulfilment of the Requirement for the Degree of Master of Science in Electrical and Computer* 1-70.

Fletcher, Clive A. J. 2006. *Computational Techiniqques for Fluid Dynamics 1*. Sydney: Springer.

Funk, D. " Indoor smoke from the household use burden of diseases due to select factors," Thorax.

Gebreegziabher, Z. and G. C. Van Kooten. 2013. "Does Community and Household Tree Planting Imply Increased Use of Wood for Fuel Evidence From Ethiopia." *Forest Policy and Economics 34,* 30-40.

Gemedo, Dera. 2016. "Hydro/Biogas Based Distributed Generation for Katikala Distillation." *Msc. Thesis, Submitted to Addis Ababa University, Department of Electrical Power Engineering.* 1-86.

Gilbert, M. 2004. "Renewable and Efficient Electric Power Systems." New Jersey: John Wiley and Sons, In. Hoboken.

Girma, Gezahegn. 2008. "Evaluating the Efficiency of Improved Local Liquor (Areke) Distilling Stove by Measuring the Indoor Air Emission." *Msc. Thesis, Submitted to Addis Ababa University, Department of Environmental Science.*

GIZ. 2011. "The Energy Development Intervention in Ethiopia." *GIZ Energy Coordination Office Ethiopia* .

Hailu, D. 2010. "Ethiopian Energy Systems- Potentials, Opportunities and Sustainable Utilization." Msc Thesis, Uppsala University, Sweden.

Https:// Www.Alamy.Com.

Https://Www.En.Wikipedia.Org.

Https://Www.En.Wikipedia.Org/Wiki/World_Energy_Consumption.

Https://Www.Google.Com.

Https://Www.Worldwildlife.Org.

International Energy Agency. 2011. "Solar Energy Perspectives, Renewable Energy Technologies Division."

Jian Yan, Cheng. 2018. "Effect of Tracking Error of Double-Axis Tracking Device on the Optical Performance of Solar Dish Concentrator." *International Journal of Photoenergy* 1-13.

John A. Duffie, William A. Beckman. 2006. *"Solar Engineering of Thermal Processes Third Edition".* John Wiley & Sons, Inc.

Jorge Alexander Alarcón, Jairo Eduardo Hortúa, Andrea López. 2013. "Design and Construction of a Solar Collector Parabolic Dish for Rural Zones in Colombia." *DOI: Http:/Dx.Doi.Org/10.18180/Tecciencia, 14(2),.*

Kalbande S. R., Mathur A. N., Surendra Kothari and Pawar S. N. 2007. "Design, Development and Testing of Paraboloidal Solar Cooker." *Karnataka J. Agric. Sci.,20(3),* 571-574.

Kalogirou. 2014. "Solar Energy Engineering." *Processes and Systems (Second Edition Ed.).*

Kalogirou, S. 2004. "Solar Thermal Collectors and Applications." *Prog Energy Combust Sci* 231-295.

Kaushika, N. D., And K. S. Reddy. 2000. "Performance of a Low Cost Solar Paraboloidal Dish Steam Generating System." 713-726.

Kebede, Wakjira. 2018. "Evaluation of the Efficiency of Improved Local Liquor (Areke) Distillating Stove for Measure Indoor Air Pollution in the West Arsi Zone Oromia Region, Ethiopia." *Msc. Thesis, Submitted to Addis Ababa University, Department of Environmental Science.*

Klaisz H, Kohne R, Nitsch J, Sprengel U. 2003. "Solar Thermal Power Plants for Solar Countries—Technology, Economics and Market Potential." *Applied Energy* 165-183.

Kobari, Seyed Mohammad. 2017. "Numerical Modelling of Convective Heat Losses of a Real Scale Cavity Receiver Used in Solar Thermal Power Towers." *Master of Science in Energy Engineering.*

Ladisch, Michael R., and Karen Dyck. 1979. "Dehydration of Ethanol: New Approach Gives Positive Energy Balance." *Science* 898-900.

Lifang Li, Steven Dubowsky. 2011. "a New Design Approach for Solar Concentrating Parabolic Dish Based on Optimized Flexible Petals." *Mechanism and Machine Theory* 1536-1548.

Loni R., A.B. Kasaeian, E. Askari Asli-Ardeh, B. Ghobadian, W.G. Le Roux. 2016. "Performance Study of a Solar-Assisted Organic Rankine Cycle Using a Dish Mounted Rectangular-Cavity Tubular Solar Receiver,." *Applied Thermal Engineering* 1298-1309.

Mazengia, Dawit Hailu. 2010. "Ethiopian Energy Systems: Potentials, Opportunities and Sustainable Utilization."

Ministry of Water and Energy. June 22, 2013. "Ethiopia's Renewable Energy Power Potential and Development Opportunities." Slide Presented by Dereje Derbew in Abu Dhabi, UAE.

Mohammed, Ibrahim Ladan. 2013. "Design and Development of a Parabolic Dish Solar Thermal Cooker." *International Journal of Engineering Research and Applications* 179-1186.

Mohammed, Ibrahim Ladan. 2012. "Design and Development of a Parabolic Dish Solar Water Heater ." *International Journal of Engineering Research and Applications* 822-830.

Munir, A. 2010. "Design Principle and Calculations of a Scheffler Fixed Focus Concentrator for Medium Temperature Applications." *Solar Energy* 84, 1490–1502.

NAG, P K. 2006. *Basic and Applied Thermodynamics* . New Delhi: Tata Mcgraw-Hill Publishing Company Limited .

Pane, J. 2010. "Survey of the International Evidence on the Causal Relationship Between Energy Consumption and Growth." *Journal of Economic Studies, 37(1),* 53-95.

Pierre, Meukam, Donatien Njomo, Aboudramane Gbane, Siaka Toure. 2004. "Experimental Optimization of a Solar Still:." *Chemical Engineering and Processing.*

Rabl, A. 1985. "Active Solar Collector and Thier Applications." 503. Nework: Oxford University Press.

Rajiv M., Jorapur,. 1991. "Alcohol Distillation by Solar Energy." *in ISES Solar World Congress Proceedings, Vol. 1, No. Part II, Pp. 772-777 . Part II. Pergamon Press.*

Rajvanshi, Rajiv M. Jorapur and Anil K. 1991. "Alcohol Distillation by Solar Energy ." *Solar World Congress Proceeding.*

Ramakrishna, G. 2015. "Energy Consumption and Economic Growth: the Ethiopian Experience." *Journal of Economic and Financial Modelling 2(2),* 35-47.

Ramlow B., Nuszb. 2007. "Types of Solar Collectors."

Rattanapol, Panomwan Na Ayuthaya, Pichai Namprakai, Wirut Ampun. 2012. "The Thermal Performance of an Ethanol Solar Still with Fin Plate to Increase." *Renewable Energy.*

Reddy, K. S., Sendhil Kumar Natarajan, and G. Veershetty. 2015. "Experimental Performance Investigation of Modified Cavity Receiver with Fuzzy Focal Solar Dish Concentrator." *Renewable Energy* 148-157.

Rosnani Affandi, Mohd Ruddin Ab Ghani, Chin Kim Ghan, Liaw Geok Pheng. 2015. "the Impact of the Solar Irradiation, Collector and the Receiver to the Receiver Losses in Parabolic Dish System." *Procedia - Social and Behavioral Sciences* 2382 – 2390.

Russel, N. 2003. "Whisky Technology, Production and Marketing." *Chemical Engineering and Process* 27-35.

Salimpour, M.R. 2009. "Heat Transfer Coefficients of Shell and Coiled Tube Heat Exchangers." *Experimental Thermal and Fluid Science* 203-207.

Saša R. Pavlovic, Evangelos A. Bellos, Velimir P. Stefanov, Christos Tzivanidis and Zoran M. Stamenkov. 2016. "Design, Simulation, Annd Optimization of A Solar Dish Collector with Spiral-Coil Thermal Absorber." *Thermal Science 20(4),* 1387-1397.

Saunders, E. 1998. "Heat Exchangers: Selection, Design and Construction." New York.

Sergio. 2012. *Cereal Grains: Laboratory Reference and Procedures Manual*. Nework: Declan.

Shariah, Adnan, M-Ali Al-Akhras, And I. A. Al-Omari. ". 2002. "Optimizing the Tilt Angle of Solar Collectors." *Renewable Energy 26, No. 4:* 587-598.

Shawaqfeh, A. T., And Farid, M. M. 1995. "Distillation of Ethanol in a Solar Still: Studies on Heat and Mass Transfer." *Journal of Solar Energy Engineering* 236-241.

Shewandagnaw, W. Demissie, Venkata A. Ramayya, Derese T. Nega. 2016. "Design, Fabrication and Testing of Biogas Stove for 'Areke' Distillation: the Case of Arsi Negele, Ethiopia, Targeting Reduction of Fuel-Wood." *International Journal of Engineering Research and Technology (IJERT).*

Skog, K. E., & Nicholson, G. A. 1998. "Carbon Cycling Through Wood Products: the Role of Wood and Paper Products in Carbon Sequestration." *Forest Products Journal* 75-83.

Solomon, Haileyesus. 2011. "Potential of Solar Energy for Areke Production." *Msc Thesis Submitted to Addis Ababa University, School of Graduate Studies, and Environmental Science Program,.*

Tanaka, Hiroshi. 2016. "Thermal Distillation System Utilizing Biomass Energy Burned In Stove by Means of Heat Pipe." *Alexandria Engineering Journal 55,* 2203–2208.

Tiwari G.N. 2006. "Solar Energy Design Fundamentals, Modeling and Applications." *Alpha Science International Ltd* 525.

Tiwari, G.N., Arvind Tiwari, Shyam. 2016. "Handbook of Solar Energy Theory." *Springer.*

Toure, Siaka, Hassan, Salami And Pierremeukam. 1999. "Theoritical and Experimetal Studies of a Solar Still Type Suitable for Alcoholic Distillation." *Renewable Energy.*

Vorayosa, N.,T. Kiatsiriroatb, N. Vorayosb. 2006. "Performance Analysis of Solar Ethanol Distillation." *Renewable Energy*.

World Development Indicators. 2016. "World Bank." *Http://Data.Worldbank.Org.*

Yadav Avadhesh, Manoj Kumar, Balram. 2013. "Experimental Study and Analysis of Parabolic Trough Collector with Various Reflectors." *International Journal of Mathematical, Computational, Physical and Quantum Engineering* 1161-1165.

Yang Li, Junjie Yan, Lei Qiao & Shenhua Hu. 2008. "Experimental Study on the Condensation of Ethanol–Water Mixtures on Vertical Tube." *Heat and Mass Transfer* 607-618.

Yogi Goswami, D. 2014. *Principles of Solar Engineering* . 3rd Edition, CRC Press.

Yuelei, Yang, Kevin Boots And Dan Zhang. 2012. " a Sustainable Ethanol Distillation System." *Sustainability*.

Zanis, Jesko. 2008. "Clssification of Solar Collectors." *Engineering for Rural Development* 1-27.

Zied Guidaraa, Mahmoud Souissia, Alexander Morgenstern, Aref Maalej. 2017. "Thermal Performance of a Solar Box Cooker with Outer Reflectors: Numerical." *Solar Energy* 347-359.

APPENDIX

APPENDIX A: Thermocouple Calibration

The most popular thermocouple is the type K, which is high sensitive for measuring temperature, consisting of Chromel and Alumel (trademarked nickel alloys containing chromium, and aluminum, manganese, and silicon, respectively), with a measurement range of –200°C to +1250°C. Calibration of thermometers can be carried out using a reference thermometer in a temperature calibration test by comparing both measurement values of a reference thermometer and other thermometers. Calibration test for four channel digital k-type thermocouple was conducted at home with mercury thermometer as a reference by using 0.6kg water boiling and cooling test for 23 minutes.

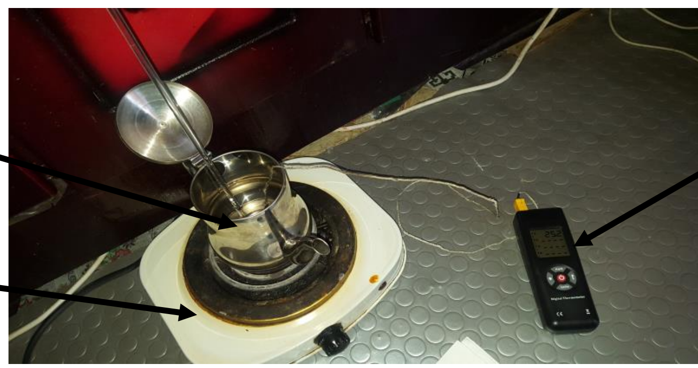

Figure A. 1: Calibration Setup.

Table A. 1: Water temperature measuring test by using k-type thermocouple.

Time (min)	T_{w1} (k type Thermocouple) (K)	T_{w2} (mercury Thermometer) (K)	Uncertainty (%) $[(T_{w1} - T_{w2})/T_{w2}] \times 100$
1	25.6	25.1	1.992031873
2	31.5	31.2	0.961538462
3	38.9	38.4	1.302083333
4	43	42.6	0.938967136
5	47	46.5	1.075268817
6	51.6	51.3	0.584795322
7	57.9	57.4	0.871080139
8	60.8	60.2	0.996677741
9	62.9	62.5	0.64
10	64.3	64.1	0.31201248
11	68.8	68.4	0.584795322

12	71	70.9	0.141043724
13	72.9	72.5	0.551724138
14	76.9	75.1	2.396804261
15	77.9	77.3	0.776196636
16	80.6	80.5	0.124223602
17	82.9	82.6	0.363196126
18	83.7	83.4	0.35971223
19	86.3	86.1	0.232288037
20	86.3	86	0.348837209
21	88	87.6	0.456621005
22	88.6	88.1	0.56753689
23	90.2	89.8	0.445434298
Average uncertainty (%)			0.74012473

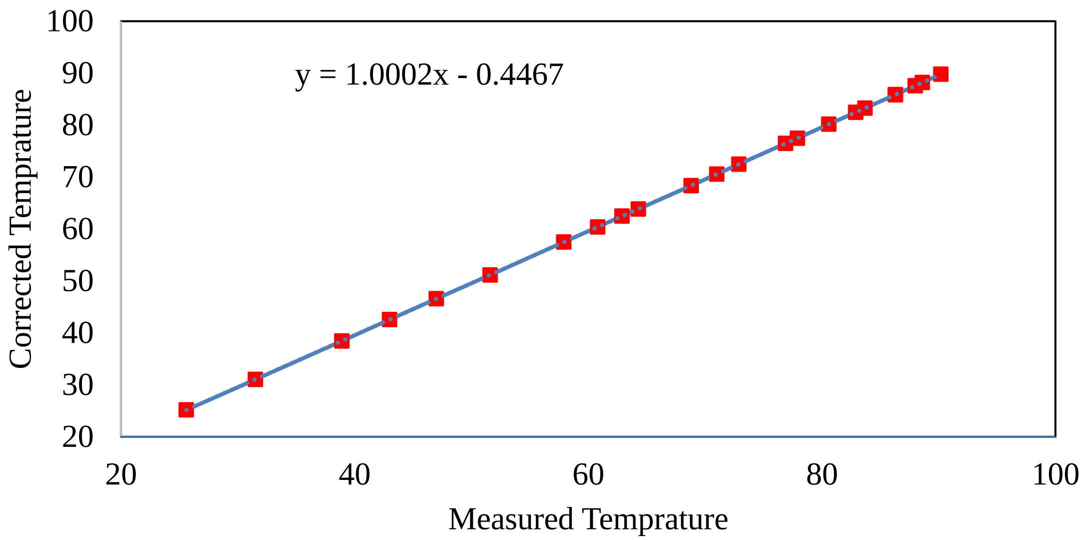

Figure A. 2: Measured temperature versus corrected temperature.

So, it can be concluded that the four-channel K- type thermocouple has uncertainty of 0.74%.

Four channel digital thermometer Specifications

- Serial Number: 2019002867
- Temperature range: -50 to 1350°C or -58 to 2462 °F
- Accuracy: [0.015%rdg+1°C (1.8°F)]
- Resolution: 0.1 °C for <1000°C; 1 °C for >1000°C
- Storage temp. and Humidity: -10 to 60°C and 10 to 75% RH
- Power supply: 9V

- Weight: approx. 230g

APPENDIX B: Results of Experimental Tests

Table B.1. Absorber Surface Temperature Test without Load.

19-20/06/2020 G.C Friday/Saturday

Local time	Ta (°C)	Tabs (°C)		12:30	26.8	289
9:45	21.6	84.1		12:45	24.5	317
10:00	26.8	171.5		13:00	26	313
10:15	24.6	188.3		13:15	24.5	255
10:30	21	230		13:30	22	209
10:45	20	259		13:45	22	226
11:00	26.4	243		14:00	22.3	176
11:15	25.8	250		14:15	22.5	135
11:30	24.8	309		14:30	24	165
11:45	22.3	305		14:45	25.8	176
12:00	26.3	300		15:00	24.9	126
12:15	26.7	284				

Table B.2. Absorber Surface Temperature Test with Load (Water).

20/06/2020 G.C Saturday

Local time	Ta (°C)	Tabs (°C)		13:20	21.6	223
9:50	24.3	117.1		13:30	22	189
10:00	25.5	182.7		13:40	23	206
10:10	26.2	169		13:50	21	165
10:20	26.6	200.7		14:00	22.3	156
10:30	23.6	210		14:10	23	123
10:40	25	221		14:20	20	112
10:50	19.4	246		14:30	24	115
11:00	19.6	223.9		14:40	22.6	163
11:10	22.1	230.2		14:50	24	145
11:20	25.7	259		15:00	25	108
11:30	24.8	289				
11:40	24.9	285				

11:50	22.1	267	
12:00	26.3	256	
12:10	28.1	286	
12:20	27.7	264	
12:30	26.8	269	
12:40	28.6	300.3	
12:50	23.6	294	
13:00	23	293	
13:10	23.6	245	

Table B.3. Water Temperature Test.

22-23/06/2020 G.C Monday/Tuesday

Local time	Ta (℃)	Tabs (℃)	Water temperature of absorber		10:20	26.2	200.7	94.6
9:45	21.5	82.9	21.5		10:25	27.8	172.3	95.5
9:50	24.3	117.1	46.3		10:30	19	187	95.8
9:55	25.4	144.8	55.7		10:35	26.6	190	95.2
10:00	26.1	151.6	71.9		10:40	20.5	163.1	96.3
10:05	25.5	182.7	85.9		10:45	20	172.6	96.7
10:10	25.6	223	91.9		10:50	23.6	166	95.6
10:15	24.1	189.4	92.1		10:55	25.2	169.9	95.8

Table B.4. Difdif Temperature Test.

24-25/06/2020 G.C Wednesday/Friday

Local time	Ta (℃)	TDifdif (℃)		10:45	20	81.2
10:05	25.5	26.2		10:50	23.6	78.6
10:10	25.6	30.2		10:55	25.2	79.8
10:15	24.1	53.5		11:00	26.4	83.1
10:20	26.2	59.6		11:05	25	85.4
10:25	27.8	70.5		11:10	21.3	86.6
10:30	19	71.4		11:15	24.8	88.6
10:35	26.6	79.9		11:20	19.4	87.1
10:40	20.5	80.3		11:25	22.9	85.3

APPENDIX C: Results of Theoretical Analysis

Table C.1. Analytical Result of Distillation Column.

Time (min)	m (kg)	Cp (kg/kgK)	Ti (℃)	Tf (K)	Tamb (K)	Temperature change(K)	Qd (J)	Qd rate (W)
0	1.62	3450	26.2	299.35	299.35	0	0	0
5	1.62	3450	26.2	303.35	300.95	4	22356	74.52
10	1.62	3450	26.2	326.65	292.15	27.3	152579.7	254.2995
15	1.62	3450	26.2	338.25	299.75	38.9	217412.1	241.569
20	1.62	3450	26.2	343.65	293.65	44.3	247592.7	206.3273
25	1.62	3450	26.2	344.55	293.15	45.2	252622.8	168.4152
30	1.62	3450	26.2	352.85	294.45	53.5	299011.5	166.1175
35	1.62	3450	26.2	354.35	292.55	55	307395	146.3786
40	1.62	3450	26.2	358.55	297.95	59.2	330868.8	137.862
45	1.62	3450	26.2	359.75	296.75	60.4	337575.6	125.028
50	1.62	3450	26.2	360.25	298.25	60.9	340370.1	113.4567
55	1.62	3450	26.2	360.85	294.25	61.5	343723.5	104.1586
60	1.62	3450	26.2	361.95	299.55	62.6	349871.4	97.1865
65	1.62	3450	26.2	362.05	298.75	62.7	350430.3	89.85392

r_1 (m)	r_2 (m)	r_3 (m)	hi W/m^{2}K	ho W/m^{2}K	L(m)	k_1 W/mK	k_2 W/mK	**ε**	**σ**
0.08	0.085	0.105	60	22.7	0.21	0.15	0.03	0.91	5.67E-08
0.08	0.085	0.105	60	22.7	0.21	0.15	0.03	0.91	5.67E-08
0.08	0.085	0.105	60	22.7	0.21	0.15	0.03	0.91	5.67E-08

0.08	0.085	0.105	60	22.7	0.21	0.15	0.03	0.91	5.67E-08
0.08	0.085	0.105	60	22.7	0.21	0.15	0.03	0.91	5.67E-08
0.08	0.085	0.105	60	22.7	0.21	0.15	0.03	0.91	5.67E-08
0.08	0.085	0.105	60	22.7	0.21	0.15	0.03	0.91	5.67E-08
0.08	0.085	0.105	60	22.7	0.21	0.15	0.03	0.91	5.67E-08
0.08	0.085	0.105	60	22.7	0.21	0.15	0.03	0.91	5.67E-08
0.08	0.085	0.105	60	22.7	0.21	0.15	0.03	0.91	5.67E-08
0.08	0.085	0.105	60	22.7	0.21	0.15	0.03	0.91	5.67E-08
0.08	0.085	0.105	60	22.7	0.21	0.15	0.03	0.91	5.67E-08
0.08	0.085	0.105	60	22.7	0.21	0.15	0.03	0.91	5.67E-08

Tsur side(K)	Tsur top(K)	Qloss side wall (W)	Qloss top wall (W)	Qloss total (W)
299.35	299.35	0	0	0
301	305.15	0.047146767	1.986197	2.033343387
301.15	306.15	8.189838038	6.411019	14.60085679
303.75	307.75	3.796028762	3.805743	7.601771692
315.25	318.45	20.97931781	12.04019	33.01950375
315.75	317.45	21.95275638	11.72372	33.67647193
316.35	320.75	21.43731859	12.93532	34.37263823
315.45	324.25	22.16299678	15.70542	37.86842151

318.95	326.05	21.07231565	14.33294	35.40525426
319.35	326.25	22.60759	14.98816	37.59575099
320.75	326.55	22.77426058	14.48266	37.25692172
321.75	327.2	27.51290317	16.64281	44.15571589
326.45	326.4	28.02368105	13.803	41.82667965
326.65	328	28.99855873	15.09044	44.08900069

Table C.2. Analytical Result of Solar Receiver.

m (kg)	Cp (kg/kgK	Ti ℃	Tabs (K)	Tf (K)	Ta (K)	Temp. change (K)	mass flow rate (kg/s)	Qwater (kJ)	Qrate (W)
0.6	4186	21.5	82.9	25.6	21.5	4.1	0.0004	10.2975	6.86504
0.6	4186	21.5	117.1	44.2	24.3	22.7	0.0004	57.0133	38.0088
0.6	4186	21.5	144.8	56.2	25.4	34.7	0.0004	87.1525	58.1016
0.6	4186	21.5	151.6	69.4	26.1	47.9	0.0004	120.305	80.2037
0.6	4186	21.5	182.7	87.7	25.5	66.2	0.0004	166.267	110.845
0.6	4186	21.5	223	90.2	25.6	68.7	0.0004	172.546	115.031

Table C.3. Analytical Result of Heat Loss.

Qloss side (W)	Qloss top (W)	Qloss total (W)		
Heat loss over the distillation column				
0.047146767	1.98619662	2.033343387		
1.422418568	4.540709018	5.96312759		
2.009215918	5.881516507	7.89073243		
7.27825705	3.21712557	10.49538262		
8.95275638	3.72371555	13.67647193		
9.43731859	7.93531964	16.37263823		
12.16299678	5.70542473	21.86842151		
14.07231565	9.33293861	23.40525426		
17.60759	4.98816099	25.59575099		
20.77426058	7.48266114	27.25692172		
22.51290317	8.64281272	30.15571589		
24.02368105	7.8029986	31.82667965		
26.99855873	6.09044196	32.08900069		
Qcond (W)	Qconv (W)	Qrad (W)	Qt loss (W)	Pipe loss (W)
Heat loss over the receiver				
0.067182485	31.36232	4.88903382	36.25135	2.249053
0.10155492	43.194468	6.50575968	49.70023	8.460106

0.142958079	65.290648	10.9508315	76.24148	6.511116
0.300758801	86.103824	8.43400747	94.53783	4.6896
0.306227143	92.091176	9.96240833	102.0536	16.90618
0.334350044	96.652968	9.64549964	106.2985	7.70403
0.32810051	93.944404	9.35877167	103.3032	17.00381
0.310133101	95.227408	10.9466376	106.174	17.45688
0.382783928	98.221084	7.66953134	105.8906	13.49845
0.385127503	98.648752	7.66953134	106.3183	11.64256
0.380440353	97.793416	7.66953134	105.4629	11.32754
0.389033462	99.361532	7.66953134	107.0311	13.94935
0.407782062	102.78288	7.66953134	110.4524	19.2547

Table C.4. Condenser Effectiveness Analysis.

Tc_1℃	Tc_2℃	$\boldsymbol{\theta_1}$℃	$\boldsymbol{\theta_2}$℃	Q(W)	A ($\mathbf{m^2}$)	U (W/m^2K)	mv (kg/s)	mc (kg/s)	Cmin (kJ/℃)	**ε**
21.7	59.1	49.7	12.3	208.7	0.0125	623	0.00025	0.0013	5.58	0.75

C.5. Conducted Experiments in Each Day

Day 1,2: First absorber temperature test without load (Exp. 1&2, 9:45-15:00)

Day 3,4: water boiling test using 0.6kg (Exp. 3&4, 10:20-10:45)

Day 5,6: Absorber temperature test with load (Exp. 5&6, 9:45-15:00)

Day 7,8: Difdif temperature test using 2L (Exp. 7&8, 9:45-15:00)

During collecting materials and manufacturing for experimental setup, the main difficulty was searching materials at different places due to fear of corona virus (Covid 19) pandemic.

APPENDIX D: Governing Equation for CFD Analysis of Dish-Receiver System

The objective of this CFD analysis is to know the wind effect at different orientation of the dish receiver system and obtain the convective heat transfer coefficient of wind. The governing equation used for the simulation of wind flow over the dish receiver system are carried out based on assumptions. These assumptions are: (i) steady and continuous fluid flow (ii) heat loss from the receiver is occurred by convection and mainly depend on the wind speed (iii) effects of gravity is negligible. Based on the assumptions,

The continuity equation was determined by the expression (Fletcher, 2006).

$$\frac{\partial \mathrm{u}}{\partial \mathrm{x}} + \frac{\partial \mathrm{v}}{\partial \mathrm{y}} = 0$$

The momentum equation was determined by the relationship

X-momentum

$$\mathrm{u}\frac{\partial \mathrm{u}}{\partial \mathrm{x}} = \frac{1}{R_e}\left(\frac{\partial^2 \mathrm{v}}{\partial \mathrm{y}^2}\right)$$

Energy equation is given by

$$\mathrm{v}\frac{\partial \mathrm{T}}{\partial \mathrm{y}} = \frac{1}{R_e P_r}\left(\frac{\partial^2 \mathrm{T}}{\partial \mathrm{x}^2}\right)$$

Boundary conditions

- ✓ Inlet velocity of, 3.5 m/s and ambient temperature of 288.15 K
- ✓ Absorber surface temperature of 573.15 K
- ✓ Turbulent intensity, 0%
- ✓ Turbulent viscosity ration, 10
- ✓ Pressure outlet, 0 pa
- ✓ Stationary wall and no slip condition

D.1. Meshing Geometry of Dish Receiver System

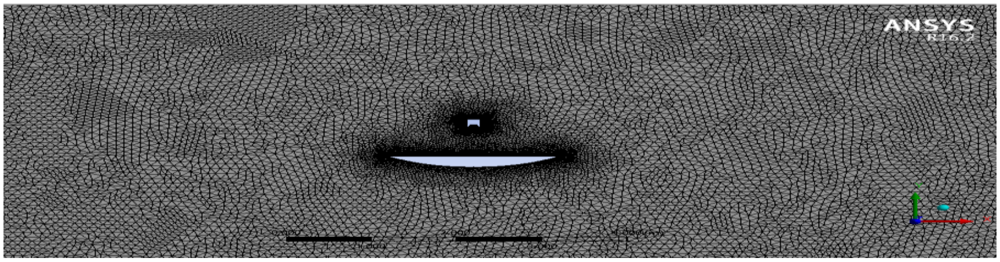

Figure D.1.1: Magnified mesh part of *0*° degree orientation.

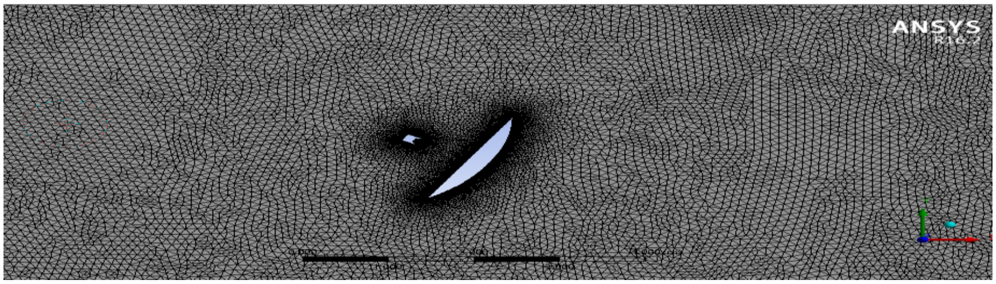

Figure D.1.2: Magnified mesh part of 60° degree orientation.

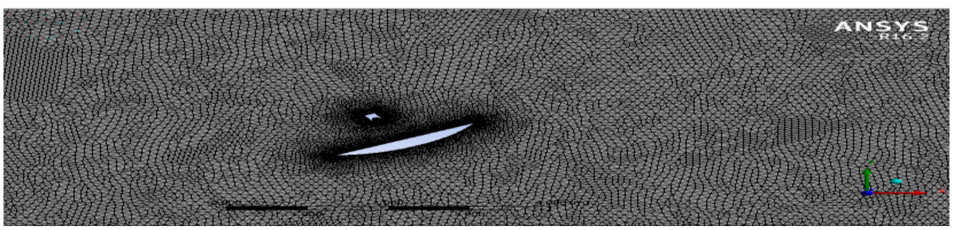

Figure D.1.3: Magnified mesh part of 30° degree orientation.

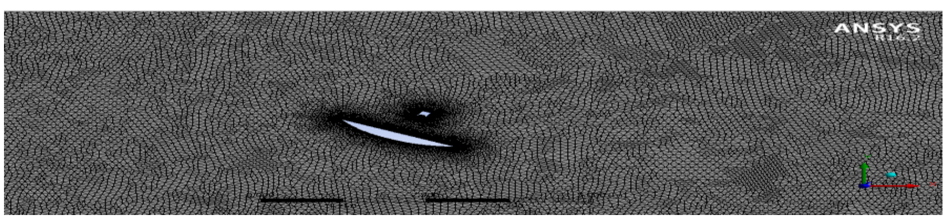

Figure D.1.4: Magnified mesh part of -30° degree orientation.

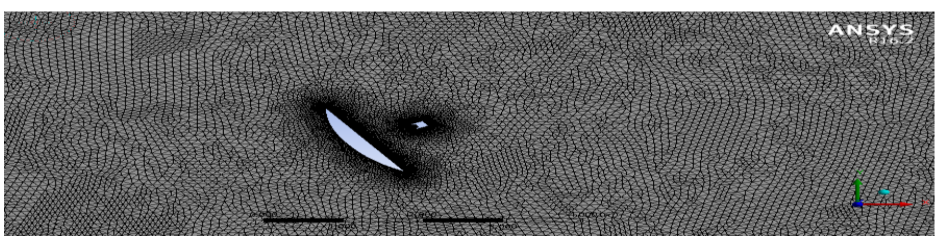

Figure D.1.5: Magnified mesh part of -60° degree orientation.

D.2 Result of Effects of Wind Flow and Dish Orientation on Convective Heat Loss

The local velocity patterns generate recirculation and stagnation zone near and inside the absorber, which ultimately impact the heat loss in the presence of the dish. In the case of 60° flow, the velocity contours (Figure D.2.1) show the low velocity near the cavity zone of the receiver and flow separation from the upper and lower portion of the dish structure. This flow separation generates large recirculation vortices behind the dish, and negative pressure values are obtained in this flow separation region.

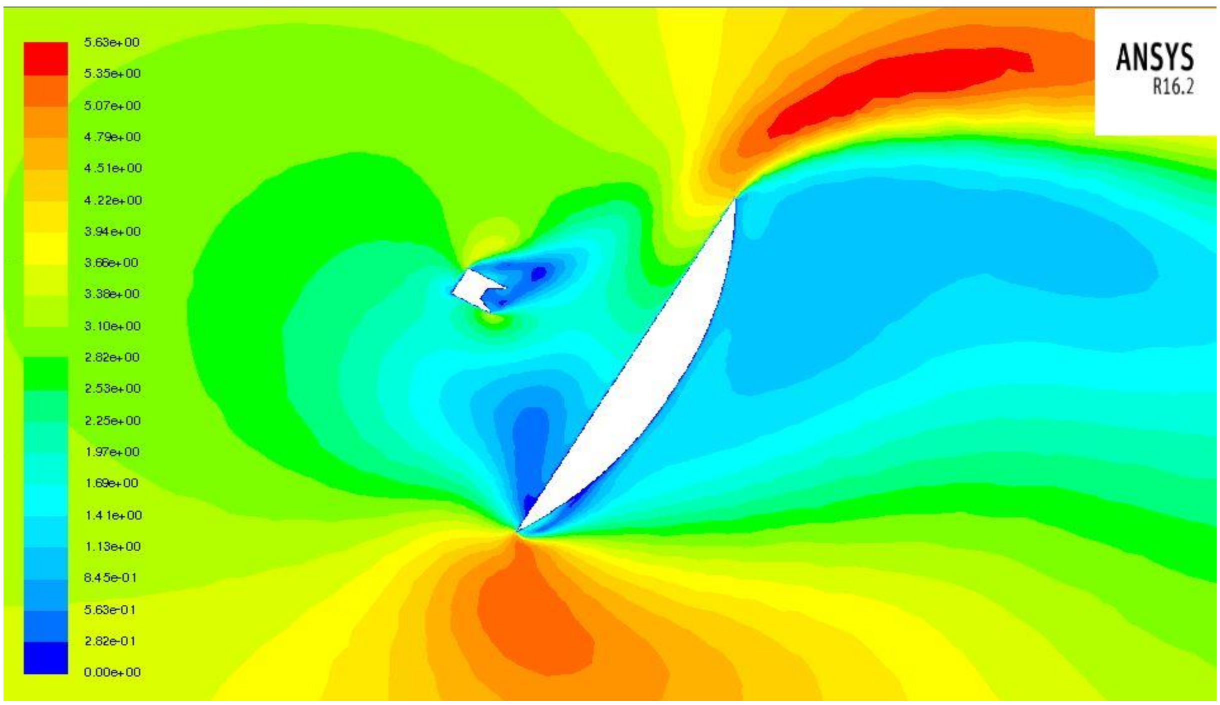

Figure D.2.1: Velocity contours at 60°.

Convective heat transfer coefficient at 60° dish orientation with 0.563 m/s of wind velocity around the receiver obtained as 9.4 W/m^{2}K. As the angle is reduced further, to a tilt angle of 30° (Figure D.2.2) the flow becomes more uniform and there is no major flow separation except a smaller recirculation region near the lower portion of dish. As a result, the flow orientation is mainly upward due to the low pressure generated by the acceleration of the flow over the dish. Convective heat transfer coefficient at 30° dish orientation with 0.503 m/s of wind velocity around the receiver obtained as 8.8 W/m^{2}K.

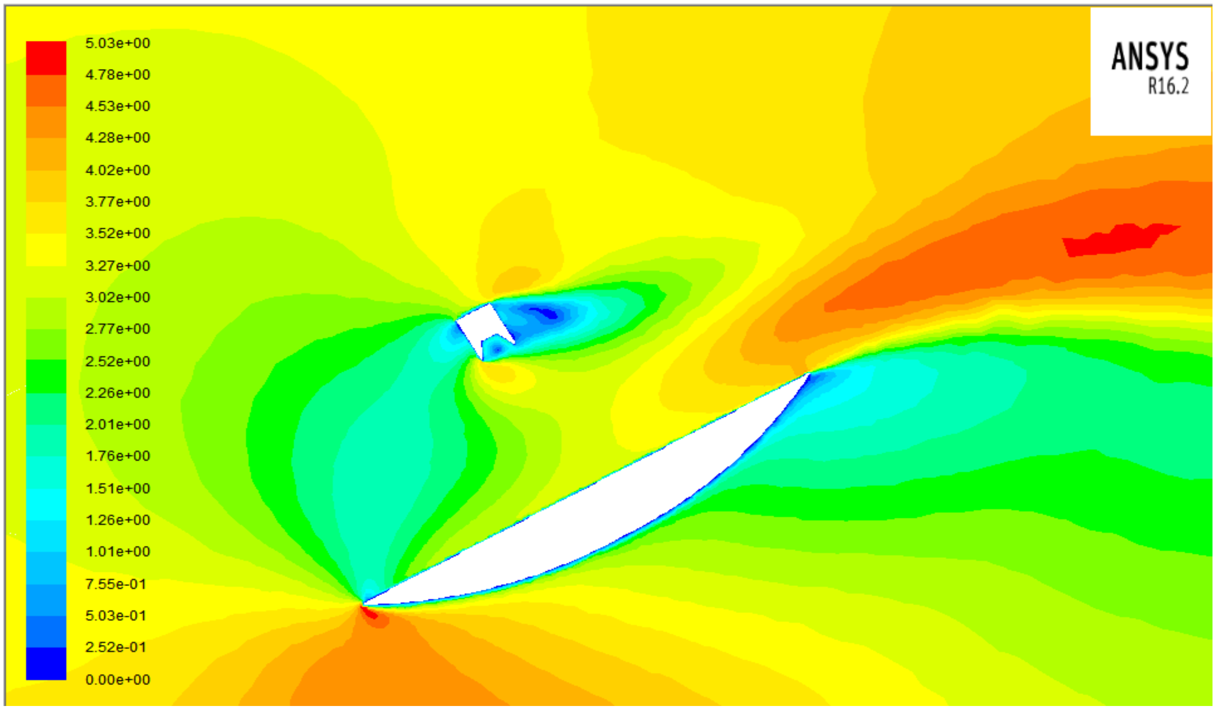

Figure D.2.2: Velocity contours at 30°.

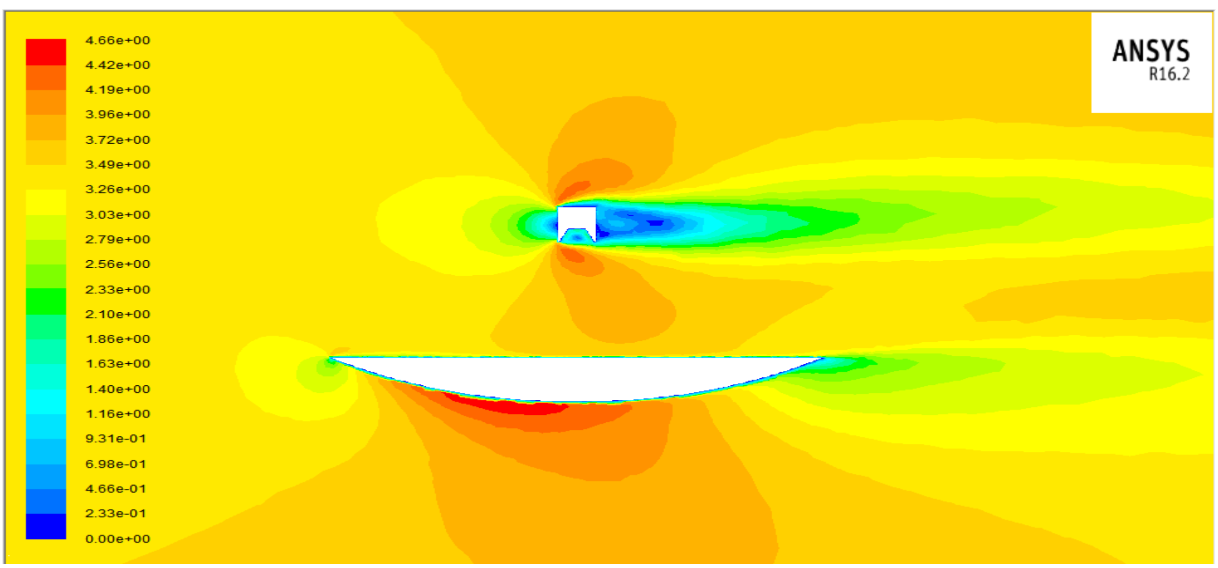

Figure D.2.3: Velocity contours at 0°.

The recirculation regions have effectively vanished as the dish reaches a 0° tilt angle (Figure D.2.3), and it suggests that the dish does not affect the air flow on the top side of dish for orientation. Under this condition, the receiver location would be in such a position that the shape of the dish would not influence the flow near it. Convective heat transfer coefficient at 0° dish orientation with 0.466 m/s of wind velocity around the receiver obtained as 8.4 W/m^{2}K.

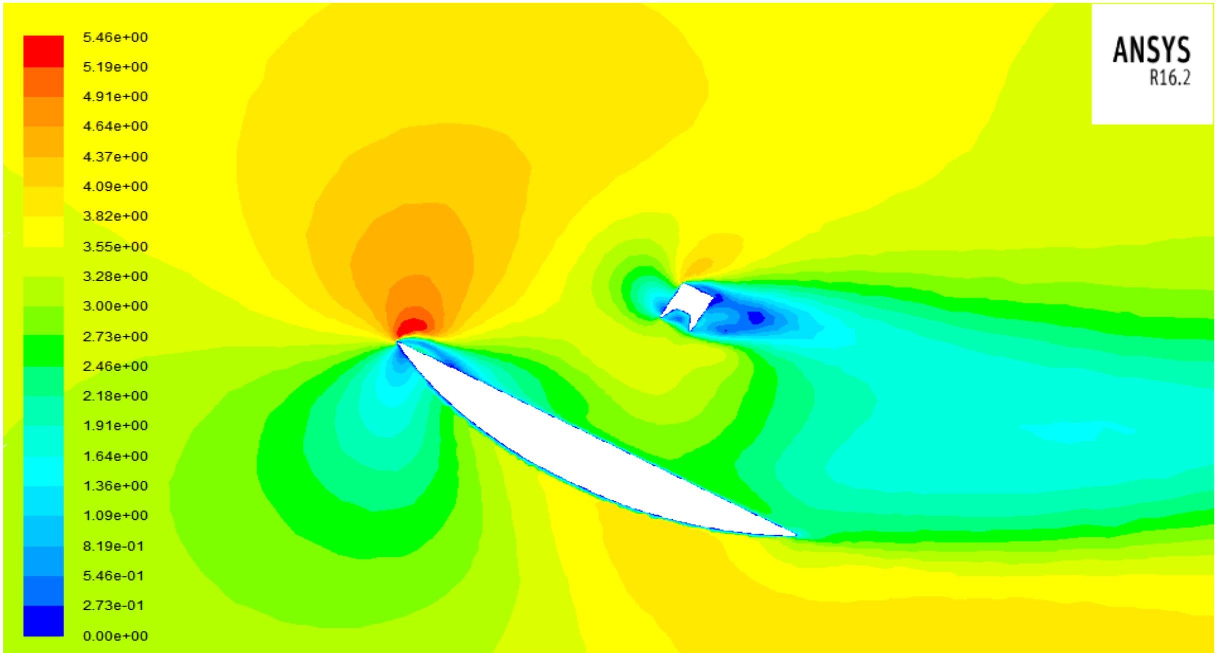

Figure D.2.4: Velocity contours at -30°.

Figure D.2.4 shows the wind flow is from the back side of the dish structure the dish creates a vortex in its wake. Convective heat transfer coefficient at $-30°$ dish orientation with 0.546 m/s of wind velocity around the receiver obtained as 9.22 W/m^{2}K.

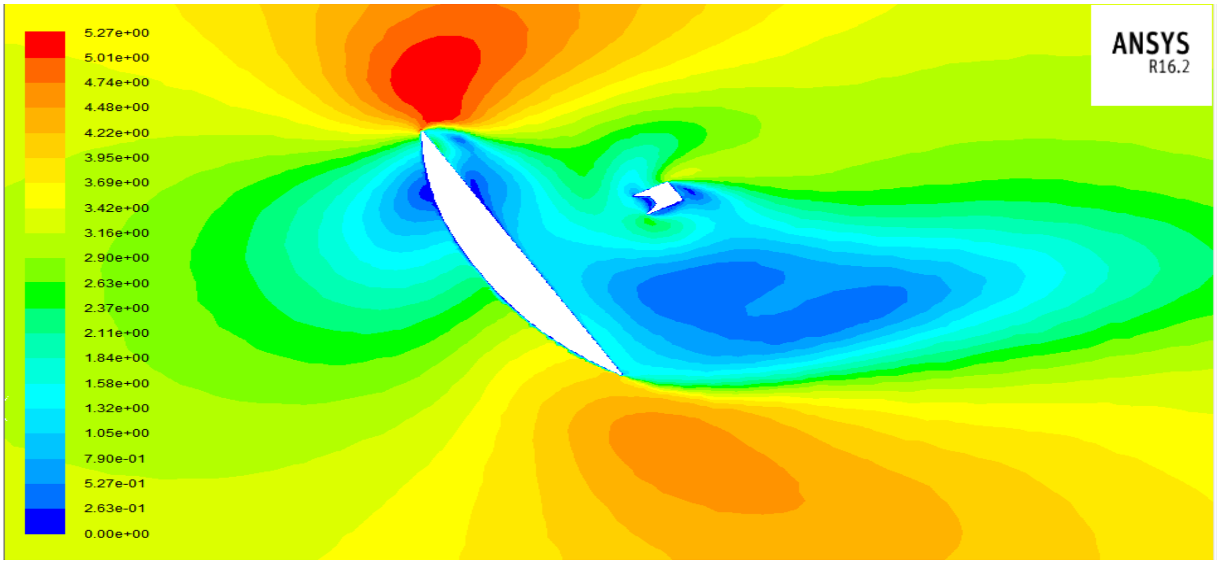

Figure D.2.5: Velocity contours at -60°.

In Figure D.2.5 shows the high velocity at the edge of dish structure producing the negative pressure in the vicinity of the wake region. Convective heat transfer coefficient at $-60°$ dish orientation with 0.527 m/s of wind velocity around the receiver obtained as 9 W/m^{2}K.

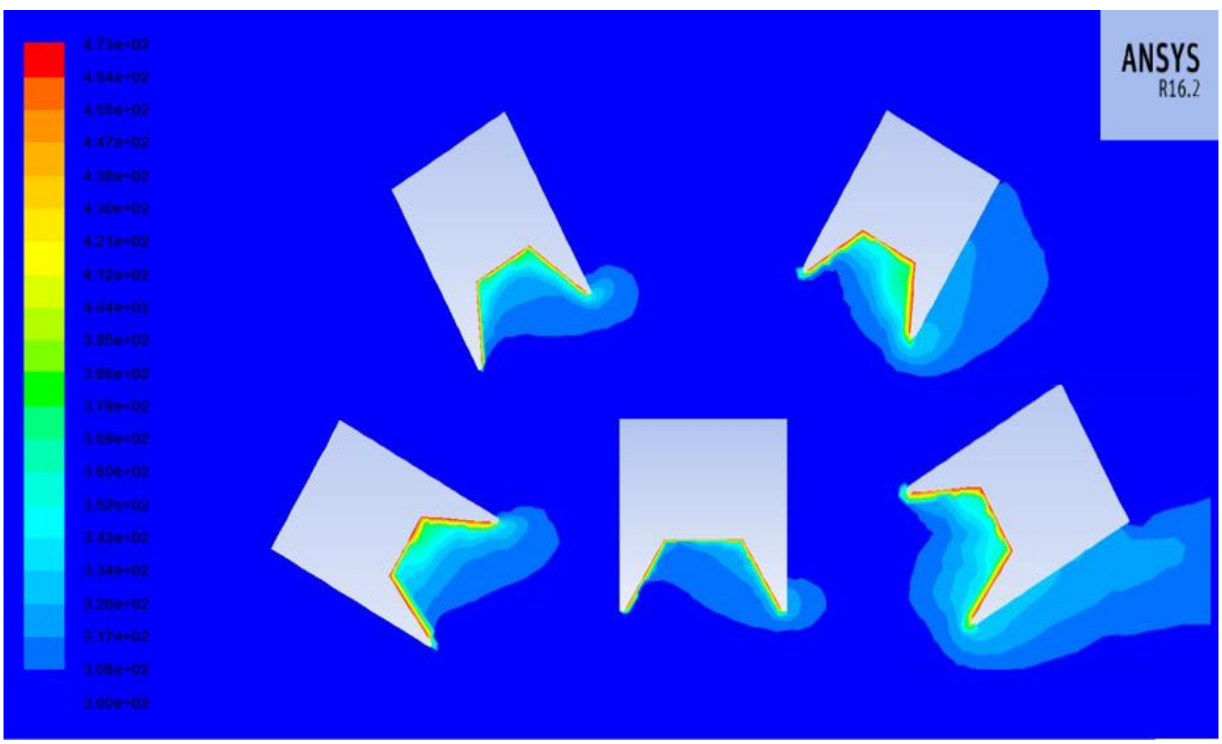

Figure D.2.6: Temperature contour at different dish orientation.

From the results of temperature couture in (Figure D.2.6) it is clear that with the natural convection heat loss is dependent on the tilt angle of the dish. Natural convection heat loss was reduced as the orientation of the receiver was changed from $\pm60°$ to $0°$ tilt angle. The minimum heat loss was observed with $0°$ tilt angle. For tilt angle between $\pm30°$ to $0°$, the receiver was mostly located in the free stream wind and the result demonstrated reduction in convective heat loss from most of the tilt angle. The increasing heat loss with tilt angle results from the strengthening convection caused by the raised lip of the cavity releasing the heated air. On the other hand, by tilting the receiver the stagnation zone starts to decrease with the increase in the tilt angle resulting in some portion of hot air going out of the receiver cavity and cold air flowing into it, producing a rising main air flow and heating up the receiver wall.

APPENDIX E: Grid Independency Test Setup and Residual Graph

Details of "Mesh"	
Sizing	
Use Advanced Size Function	On: Curvature
Relevance Center	Medium
Initial Size Seed	Active Assembly
Smoothing	Medium
Span Angle Center	Fine
Curvature Normal Angle	Default (12.0 °)
Min Size	1.e-005 m
Max Face Size	0.50 m
Max Size	1.0 m
Growth Rate	Default (1.10)
Minimum Edge Length	4.e-003 m
Inflation	
Use Automatic Inflation	None
Inflation Option	Smooth Transition
Transition Ratio	0.272
Maximum Layers	2
Growth Rate	1.2
Inflation Algorithm	Pre
View Advanced Options	No
Assembly Meshing	
Patch Conforming Options	
Patch Independent Options	
Advanced	
Defeaturing	
Statistics	
Nodes	38760
Elements	75920

Details of "Mesh"	
Sizing	
Use Advanced Size Function	On: Curvature
Relevance Center	Medium
Initial Size Seed	Active Assembly
Smoothing	Medium
Span Angle Center	Fine
Curvature Normal Angle	Default (12.0 °)
Min Size	1.e-005 m
Max Face Size	0.30 m
Max Size	1.0 m
Growth Rate	Default (1.10)
Minimum Edge Length	4.e-003 m
Inflation	
Use Automatic Inflation	None
Inflation Option	Smooth Transition
Transition Ratio	0.272
Maximum Layers	2
Growth Rate	1.2
Inflation Algorithm	Pre
View Advanced Options	No
Assembly Meshing	
Patch Conforming Options	
Patch Independent Options	
Advanced	
Defeaturing	
Statistics	
Nodes	90874
Elements	179845

Figure E. 1: Mesh #1and #2 setups.

Details of "Mesh"	
Sizing	
Use Advanced Si...	On: Curvature
Relevance Center	Medium
Initial Size Seed	Active Assembly
Smoothing	Medium
Span Angle Center	Fine
Curvature Nor...	Default (12.0 °)
Min Size	1.e-005 m
Max Face Size	0.10 m
Max Size	1.0 m
Growth Rate	Default (1.10)
Minimum Edge L...	4.e-003 m
Inflation	
Use Automatic In...	None
Inflation Option	Smooth Transition
Transition Ratio	0.272
Maximum Lay...	2
Growth Rate	1.2
Inflation Algorit...	Pre
View Advanced ...	No
Assembly Meshing	
Patch Conforming Options	
Patch Independent Options	
Advanced	
Defeaturing	
Statistics	
Nodes	756356
Elements	1507875

Details of "Mesh"	
Sizing	
Use Advanced Size Function	On: Curvature
Relevance Center	Medium
Initial Size Seed	Active Assembly
Smoothing	Medium
Span Angle Center	Fine
Curvature Normal Angle	Default (12.0 °)
Min Size	1.e-005 m
Max Face Size	9.e-002 m
Max Size	1.0 m
Growth Rate	Default (1.10)
Minimum Edge Length	4.e-003 m
Inflation	
Use Automatic Inflation	None
Inflation Option	Smooth Transition
Transition Ratio	0.272
Maximum Layers	2
Growth Rate	1.2
Inflation Algorithm	Pre
View Advanced Options	No
Assembly Meshing	
Patch Conforming Options	
Patch Independent Options	
Advanced	
Defeaturing	
Statistics	
Nodes	931407
Elements	1857489

Figure E. 2: Mesh #3 and #4 setups.

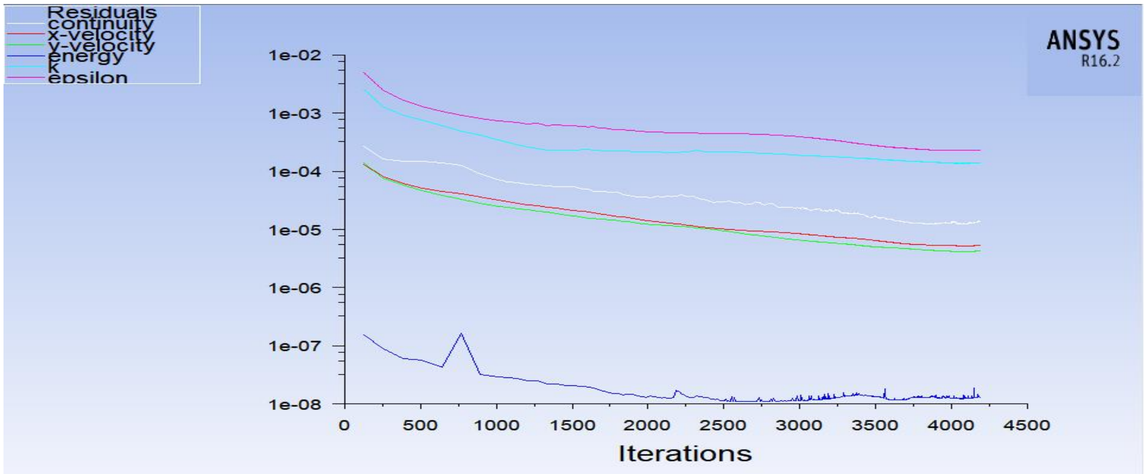

Figure H. 3: Residual graph.